DESIGN, SYNTHESIS AND BIOLOGICAL EVALUATION OF NON-PEPTIDIC SMALL MOLECULAR SMAC MIMETICS AS POTENT IAP INHIBITORS

by

Yuefeng Peng

A dissertation submitted in partial fulfillment
of the requirements for the degree of
Doctor of Philosophy
(Medicinal Chemistry)
in the University of Michigan
2008

Doctoral Committee:

Professor Shaomeng Wang, Chair
Professor Masato Koreeda
Professor Anna K. Mapp
Professor David H. Sherman
Assistant Professor Jason E. Gestwicki

To my family

Acknowledgements

I genuinely appreciate my advisor, Professor Shaomeng Wang for his expert guidance and support. It is a really great honor for me to perform my PhD research under the guidance of Professor Wang, a leading scientist in the area of Medicinal Chemistry.

I would like to thank my committee members, Professor Anna K. Mapp, Professor David H. Sherman, Professor Masato Koreeda, and Professor Jason E. Gestwicki for their time and efforts.

I would like to thank the Chair of Medical Chemistry Department, Professor Ronald W. Woodard for providing me the opportunity to study in one of the top Medicinal Chemistry Programs.

I would like to thank Dr. Haiying Sun for his advice and assistance in the synthesis of Smac mimetics, Dr. Jianfeng Lu for his advice and assistance in the biological studies of Smac mimetics, and Dr. Qian Cai for providing CQ-406 (SM-406) in the biological evaluation experiments.

I would like to thank Dr. Chao-Yie Yang for computational studies, Dr. Zaneta Nikolovska-Coleska for the FP assay and functional assay results. Besides, I would like to thank everyone in the lab for their assistance in my research.

I need to extend a special thank to Dr. George W. A. Milne for his critical reading and editorial assistance of and this dissertation

I appreciate my wife and my parents for their full support.

Table of Contents

List of Figures

List of Tables

Table

List of Abbreviations

A or Ala	Alanine
Ac	Acetyl
Admin.	Administration
Apaf-1	Apoptotic Protease Activating Factor-1
ATP	Adenosine Tri-Phosphate
AUC	Area Under Curve
Bax	Bcl-2 Associated X protein
Bid	BH3 Interacting Domain death agonist
BIR	Baculovirus Inhibitors of Apoptosis Protein Repeat
Bn	Benzyl
Boc	*tert*-Butyloxycarbonyl
BRUCE	Baculoviral IAP Repeat containing Ubiquitin Conjugating Enzyme
Bu	Butyl
C3	Caspase-3
C7	Caspase-7
C8	Caspase-8
C9	Caspase-9
calcd.	Calculated
Cbz	Carbobenzyloxy
Cl.	Clearance
CL C3	Cleaved Caspase-3
CL C7	Cleaved Caspase-7
CARD	Caspase Recruitment Domain
Caspase	Cysteine-dependent Aspartate Protease
Comp.	Compound
Conc.	Concentration
co-IP	co-Immunoprecipitation
c-IAP1	cellular Inhibitors of Apoptosis Protein 1
c-IAP2	cellular Inhibitors of Apoptosis Protein 2
Cyt-*c*	Cytochrome *c*
DCM	Dichloromethane
DIABLO	Direct IAP Binding protein with Low pI
DIEA	N,N-Diisopropylethylamine
DISC	Death-Inducing Signaling Complex
DLB	Double Lysis Buffer
DTT	Dithiothreitol
E or Glu	Glutamic acid

EDC	1-ethyl-3-(3-dimethylaminopropyl) carbodiimide hydrochloride
EDTA	Ethylenediaminetetraacetic Acid 2
equiv.	equivalent
Et	Ethyl
EtOAc	Ethyl estate
F	Bioavailability
F or Ph	Phenylalanine
FADD	Fas Associated Death Domain
FasL	Fas Ligand
FP	Fluorescence Polarization
G or Gly	Glycine
GFP	Green Fluorescent Protein
h.	hour(s)
H or His	Histidine
HOBt	Hydroxybenzotriazole
HPLC	High-performance liquid chromatography
HRMS	High Resolution Mass Spectrometry
I or Ile	Isoleucine
IAC	IAPs Antagonist Compound
IAP	Inhibitors of Apoptosis Protein
IBM	Inhibitors of Apoptosis Protein-Binding Motif
K or Lys	Lysine
K_d	Constant of Dissociation
L or Leu	Leucine
Me	Methyl
min.	minute(s)
ML-IAP	Melanoma Linked Inhibitors of Apoptosis Protein
MRB	Mitochondrial Resuspension Buffer
MRT	Mean Residence Time
MS	Mass Spectrometry
NAIP	Neuronal Apoptosis Inhibitory Protein
NF-κB	Nuclear Factor-κB
NMR	Nuclear magnetic resonance
NIK1	Nim1-like Protein Kinase
NP-40	Nonidet P 40
P or Pro	Proline
PAGE	Polyacrylamide Gel Electrophoresis
PARP	Poly ADP Ribose Polymerase
PBS	Phosphate Buffer Saline
PCD	Programmed Cell Death
Ph	Phenyl
pI	Isoelectric Point
P.I.	Propidium Iodide
PK	Phamacokinetic
PMSF	Phenylmethylsulphonyl Fluoride

Pr	Propyl
PS	Phosphatidylserine
PVDF	Polyvinylidene Difluoride
Q or Gln	Glutamine
R or Arg	Arginine
RING	Really Interesting New Gene
RIP	Receptor-Interacting Protein
R.T.	Room Temperature
S or Ser	Serine
SAR	Structure Activity Relationship
SD	Standard Deviation
SDS	Sodium Dodecyl Sulfate
siRNA	small interfering RNA or silencing RNA or short interfering RNA
Smac	Second Mitochondria-derived Activator of Caspase
STR	Succinate-tetrazolium Reductase
$t_{1/2}$	Half life
T or Thr	Theronine
TBS	*tert*-butyldimethylsilyl
TBS	Tris-Buffered Saline
t-Bu	*tert*-butyl
TFA	Trifluoroacetic acid
THF	Tetrahydrofuran
TMS	Tetramethylsilane
TNFα	Tumor Necrosis Factor α
TRAIL	Tumor Necrosis Factor-Related Apoptosis Inducing Ligand
Ts-IAP	Tesis-specific Inhibitors of Apoptosis Protein
V or Val	Valine
W or Trp	Tryptophan
WST	2-(2-methoxy-4-nitrophenyl)-3-(4-nitrophenyl)-5-(2, 4-isulfophenyl)-2H-tetrazolium, monosodium salt
XIAP	X-chromosome linked Inhibitor of Apoptosis Protein
Y or Tyr	Tyrosine

CHAPTER 1

INTRODUCTION

1.1 Apoptosis and Cancer

Apoptosis, from the Greek, meaning "falling off" petals or leaves from plants or trees,[1-15] is a term used in cellular biology for programmed cell death (PCD). This process, is distinct from necrosis, which is a form of traumatic cell death caused by cellular injury, and follows a series of cellularly controlled steps, resulting ultimately in cell death. Most of the current cancer therapies, such as radiation, chemotherapeutic agents and immunotherapy work by directly or indirectly inducing apoptosis in cancer cells.[16-21] Resistance to apoptosis leaves cancer cells unable to execute apoptosis,[22-24] and is a major problem in current cancer therapy.[25-30] Successful anticancer therapies must include strategies specifically targeting the resistance of cancer cells to apoptosis.[31,32] Hence, targeting the crucial negative regulators which play a role in inhibition of apoptosis of cancer cells can be a promising therapeutic strategy for new anticancer drug design.[33-43]

Apoptosis can be induced by a variety of stimuli, including death ligands such as Tumor Necrosis Factor α (TNFα), TNF-Related Apoptosis Inducing Ligand (TRAIL), or Fas Ligand (FasL) as shown in the extrinsic pathway in Figure 1.1; heat, radiation, hypoxia, viral infection, and nutrient deprivation, in the intrinsic pathway, are also

effective. In the extrinsic pathway, ligation of death ligand with the death receptor leads
to the formation of FADD (Fas-Associated Death Domain), which in turn recruits
procaspase-8 or procaspase-10, forming a Death-Inducing Signaling Complex (DISC),
and inducing auto-activation of the initiator caspase, caspase-8, or caspase-10.[44,45]
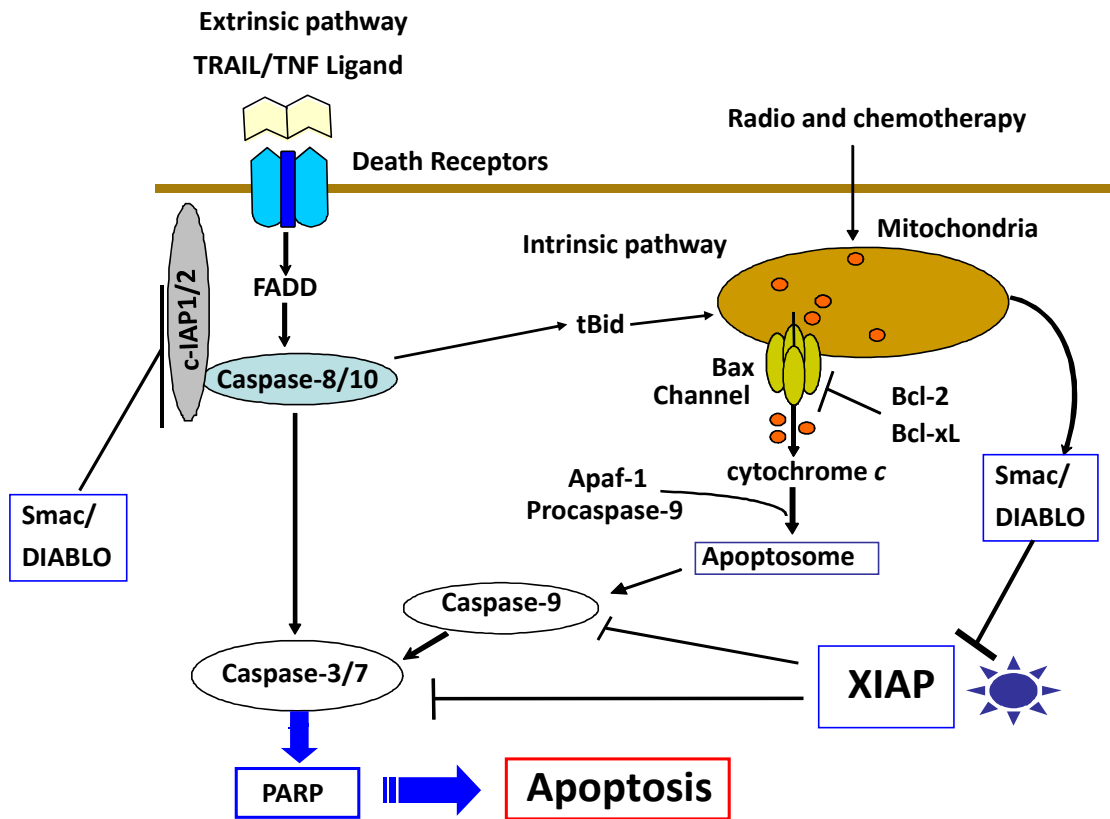
Figure 1.1 Biological pathways of apoptosis.

Initiator caspases cleave procaspase-3 and procaspase-7 to yield the executioners of
apoptosis, caspase-3 and caspase-7.[46-67] In the intrinsic pathway, cellular stress, for
example radiation, induces the translocation of a Bcl-2 family protein such as Bax (Bcl-2
Associated X protein), causing the release of cytochrome c from the mitochondria into
the cytosol.[68] Cytochrome c binds Apaf-1 (Apoptotic Protease Activating Factor-1),
procaspase-9 and ATP (Adenosine Triphosphate) to form the apoptosome complex,

2

which recruits the auto-activation of caspase-9.[69-74] Caspase-9 in turn induces the activation of the effectors, caspase-3 and caspase-7 to effect apoptosis.[75-77]

In some cases, the extrinsic pathway can induce the intrinsic pathway, in which a pro-apoptotic member of Bcl-2 family, Bid (BH3 Interacting Domain death agonist) is cleaved by caspase-8, then interacts with Bax, leading to the release of cytochrome *c* into cytosol from mitochondria.[78-85]

1.2 IAP

IAPs (Inhibitors of Apoptosis Protein) are a class of proteins which can negatively regulate the apoptosis process in cancer cells.[86-93] Eight distinct IAPs are known:

- NAIP (Neuronal Apoptosis Inhibitory Protein)
- XIAP (X-chromosome linked Inhibitor of Apoptosis Protein)
- c-IAP1 (cellular IAP 1)
- c-IAP2 (cellular IAP 2)
- Ts-IAP (Tesis-specific IAP)
- ML-IAP (Melanoma Linked IAP) or Livivn
- BRUCE (Baculoviral IAP Repeat containing Ubiquitin Conjugating Enzyme) or Apollon
- Survivin

The domain structures of XIAP, c-IAP1 and c-IAP2 are shown in Figure 1.2. Most of the IAPs, except NAIP, BRUCE/Apollon, and Survivin, have a carboxy-terminal RING (Really Interesting New Gene) domain which directs self-ubiquitination and

3

protein degradation.[94,95] Of all the IAPs, only c-IAP1 and c-IAP2 have a CARD (CAspase Recruitment Domain) domain, which mediates other CARD-containing proteins.[96,97] The BIR (Baculovirus IAP Repeat) domain, is the functional domain of apoptosis inhibition and is the important characteristic of each IAP member.[98-103] While XIAP, c-IAP1, c-IAP2, ML-IAP, and NAIP can bind caspase-9, caspase-3 and caspase-7 directly to their BIR domains, thus inhibiting caspase activity, Survivin and BRUCE regulate the cytokines and mitotic spindle formation in order to inhibit the apoptosis process.[104-111]
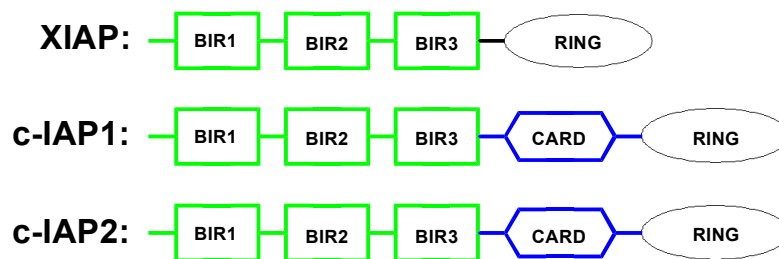
Figure 1.2 Domain structures of XIAP, c-IAP1 and c-IAP2.

XIAP binds both the initiator caspase, caspase-9, with its BIR3 domain and the effector caspase-3 or caspase-7, with BIR2 and the linker before the BIR2 domain.[112,113] By blocking the activity of caspase-3/7, XIAP inhibits apoptosis at the down-stream effector phase, where multiple signal pathways converge. Hence, strategies targeting XIAP can be an effective method to overcome the resistance of cancer cells to the apoptosis.[114-118]

1.3 Smac/DIABLO

4

Smac (Second Mitochondria-derived Activator of Caspase), also known as DIABLO (Direct IAP Binding protein with Low pI), was recently identified as a protein released from mitochondria in response to apoptotic stimuli.[119,120] Smac is a 239 amino-acid protein. Its amino-terminal 55 residues are removed during translocation to yield active Smac.[119,120] As shown in Figure 1.3, the amino-terminal tetrapeptide in Smac, Ala-Val-Pro-Ile (residue 56 to 59) is homologous with the exposed amino-terminal tetrapeptide of caspase-9 (Ala-Thr-Pro-Phe). The amino-terminal tetrapeptides of Smac and caspase-9, also known as IBM (IAP-Binding Motif), bind to a well-defined surface groove in the BIR3 domain of XIAP. By binding with the BIR3 domain of XIAP, Smac inhibits the interaction of XIAP BIR3 domain and caspase-9. This interaction releases caspase-9 and promotes apoptosis.[121]

Smac / DIABLO: A-V-P-I-A-Q-K-S-E-P-H

Caspase-9:   A-T-P-F-Q-E-G-L-R-T-F

Figure 1.3 IAPs-Binding Motif (IBM, in red) of Smac/DIABLO and caspase-9.

The structures of the XIAP BIR3 domain complexed with either Smac protein or Smac amino-terminal peptide have been determined by X-ray crystallography and NMR spectroscopy.[122,123] The amino-terminal tetrapeptide Ala-Val-Pro-Ile binds the XIAP BIR3 domain and is equipotent (K_d = 0.4 μM) with the mature Smac protein (K_d = 0.4 μM). Therefore, it is possible to use small molecule non-peptide Smac mimetics to mimic the interaction between the mature Smac protein and the XIAP BIR3 domain, releasing initiator caspase-9 to promote the apoptosis process.
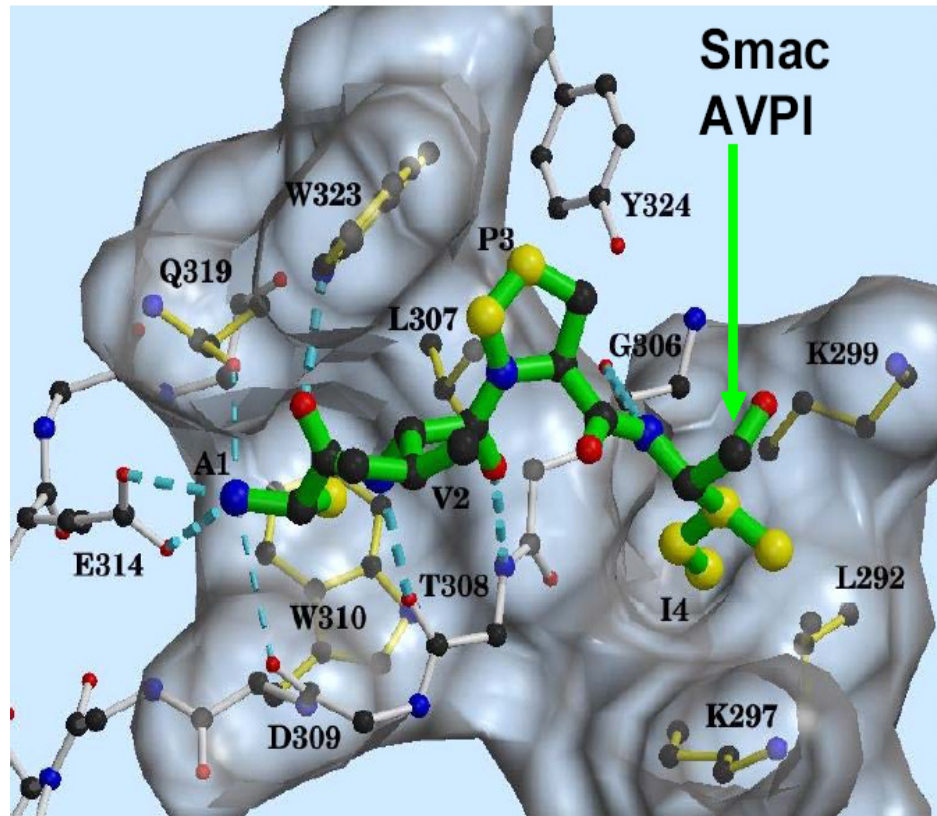
Figure 1.4 X-ray structure of Smac IBM binding with the XIAP BIR3 domain. (Hydrogen bonds are shown in light-blue dashed lines.)

Figure 1.4 shows the interaction of the IAP-binding motif (IBM) of Smac with the XIAP BIR3 domain.[123] The amino group of the amino-terminal alanine (A1 in Figure 1.4) of mature Smac is positively charged and its hydrogen atoms form a total of four hydrogen bonds with the two oxygen atoms in the carboxyl group of XIAP glutamic acid 314 side chain, the carbonyl oxygen of the side chain of glutamine 319, and the backbone carbonyl oxygen of aspartic acid 309. These hydrogen bonds are crucial because mutagenesis experiments show that in the Smac mutant A1M (alanine is replaced with an methionine) the interaction of Smac and the XIAP BIR3 domain is completely disrupted.[124] The methyl side chain of A1 fits tightly in a small hydrophobic pocket formed by the side chains of leucine 307, tryptophan 310, and glutamine 319 of XIAP. The amino hydrogen in the indole ring of tryptophan 323 forms a hydrogen bond with the

6

backbone carbonyl oxygen of A1 and the indole ring participates in a hydrophobic interaction with the five-member ring of proline (P3 in Figure 1.4). The amino hydrogen and the carbonyl oxygen of the valine 2 (V2 in Figure 1.4) form two hydrogen bonds with the backbone carbonyl oxygen and amino hydrogen of threonine 308 respectively, while the methyl side chain of threonine 308 enjoys a hydrophobic interaction with the isopropyl side chain of valine 2. A further hydrogen bond interaction is present between the amino hydrogen of isoleucine 4 (I4 in Figure 1.4) and the backbone carbonyl oxygen of glycine 306. The backbone carbonyl of isoleucine 4 is directed towards the solvent and fails to interact with the XIAP BIR3 domain, while the isobutyl side chain of I4 is inserted into the large hydrophobic pocket formed by lysine 297 and lysine 299 of the XIAP BIR3 domain. V2 and P3 form a reverse turn structure forcing the amino terminal tetrapeptide Ala-Val-Pro-Ile of the mature Smac protein to bind in the Smac binding groove of the XIAP BIR3 domain.[122]

1.4 Structure-Activity Relationships

As discussed in Section 1.3, above, the amino-terminal tetrapeptide Ala-Val-Pro-Ile of Smac binds the XIAP BIR3 domain with potency (K_d = 0.4 μM) similar to that of the mature Smac protein (K_d = 0.4 μM), allowing the design of a small molecule non-peptidic Smac mimetic which can mimic the interaction of the mature Smac protein with the XIAP BIR3 domain. Several groups have been investigating small molecular non-peptidic Smac mimetics as potent inhibitors of XIAP which can overcome apoptosis

resistance in cancer therapy. The Structure Activity Relationships (SAR) of small molecular Smac mimetics have been extensively explored.[125-130]
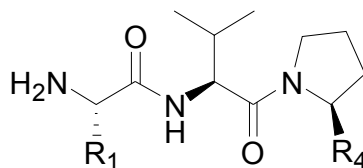
Comp	R_1	R_4	Ki/μM ± SD	Comp	R_1	R_4	Ki/μM ± SD
1	Me	-CONHCH₂-	0.29 ± 0.07	2	Me	-CONHCH₂-	13.40 ± 1.6
3	Me	-CONHCH₂-	2.45 ± 0.7	4	Me	-CONHCH₂-	4.41 ± 1.5
5	Me	-CONHCH₂-	1.27 ± 0.2	6	Me	-CONHCH₂-	0.22 ± 0.07
7	Me	-CONHCH₂-	0.18 ± 0.07	8	Me	-CONH-	4.9 ± 2.1
9	Me	-CONHCH₂CH₂-	0.15 ± 0.09	10	Me	-CONHCH₂-	0.028 ± 0.020
11	Et	-CONHCH₂-	0.024 ± 0.020	12	Me	-CH₂CH₂CH₂-	1.2 ± 0.4
13	H	-CONHCH₂CH₂-	68 ± 7	14	Et	-CONHCH₂-	0.081 ± 0.06
15	i-Pr	-CONHCH₂-	4.15 ± 1.2	16	Pr	-CONHCH₂-	54 ± 7

Table 1.1 Chemical structures of Smac peptide-mimetics and their binding affinities to the XIAP BIR3 protein determined using a fluorescence-polarization-based binding assay.[125]

The SAR of variations in the side chain of alanine 1 and of isoleucine 4 were studied and the results are shown in Table 1.1.[125] The backbone carbonyl of isoleucine 4 is directed towards the solvent and does not interact with the XIAP BIR3 domain while the isobutyl side chain of I4 is in the large hydrophobic pocket formed by lysine 297 and lysine 299 of the XIAP BIR3 domain. Replacement of the backbone carbonyl of isoleucine 4 with a benzyl as in the caspase-9 phenylalanine residue yields compound 1 in Table 1.1. Compound 1, with K_i = 0.29 μM, was as twice as potent as the original

amino terminal tetrapeptide of mature Smac protein (Ala-Val-Pro-Ile; $K_i = 0.58$ μM), determined using the fluorescence-polarization-based assay.[126]

To further explore the SAR concerning R_4, a series of compounds (2-10) with $R_1 =$ CH_3 were synthesized. When the phenyl group in compound 1 was replaced by isopropyl, 2'-ethylbutyl, cyclopropyl or cyclohexyl, the potency of the compounds as Smac mimetics dropped dramatically. When the phenyl group in compound 1 was substituted with another aromatic group however, as in compounds 6 and 7, the potency of Smac mimetics persisted. Hence, an aromatic group in R_4 appears to bind preferentially in the hydrophobic pocket formed by lysine 297 and lysine 299 in the XIAP BIR3 domain. In order to determine the optimum length of the R_4 side chain, compounds 8 and 9, with one more and one less carbon in the R_4 side chain respectively, were tested. As shown in Table 1.1, increase in the chain length was correlated with a slight increase in the potency of the compound but a decrease of the chain length decreased the compound's potency dramatically. Although the backbone carbonyl group of isoleucine 4 is oriented towards the solvent and has no specific interaction with the XIAP BIR3 domain, it plays a role in orientating the isoleucine 4 side chain toward the relative hydrophobic pocket in the XIAP BIR3 domain. Hence, in compound 10, another phenyl ring was added to orientate the other phenyl ring and reduce the conformational flexibility and, as expected, compound 10, a highly potent Smac mimetic, resulted.

The methyl group of R_1 was substituted with an ethyl group to yield compound 11, R_4 remaining unchanged. This change resulted in a slight increase in the Smac mimetic potency as a result of the increased hydrophobic interaction between the R_1 side chain

and hydrophobic pocket formed by leucine 307, tryptophan 310, and glutamine 319 in the XIAP BIR3 domain.

The amino hydrogen of isoleucine 4 and the backbone carbonyl oxygen of glycine 306 interact through a hydrogen bond. In order to test its importance in the binding of Smac mimetics with the XIAP BIR3 domain, the amide bond between these two residues was removed to yield compound 12. The compound potency was dramatically reduced by the removal of this hydrogen bond interaction.

To further explore the SAR of R_1, a series of groups in R_1 (-H, -C_2H_5, -$CH(CH_3)_2$, -$CH_2CH_2CH_3$) were tested as shown in compounds 13-16 in Table 1.1. Evidently, the small hydrophobic pocket formed by leucine 307, tryptophan 310, and glutamine 319 in the XIAP BIR3 domain can accommodate only a small hydrophobic group such as methyl or ethyl, the latter being slightly better than methyl due to enhancement of the hydrophobic interaction. A functional group with more than two carbon atoms appears to be too large for this hydrophobic pocket, witness the dramatic decrease in potency of compound 15 and 16 in Table 1.1.
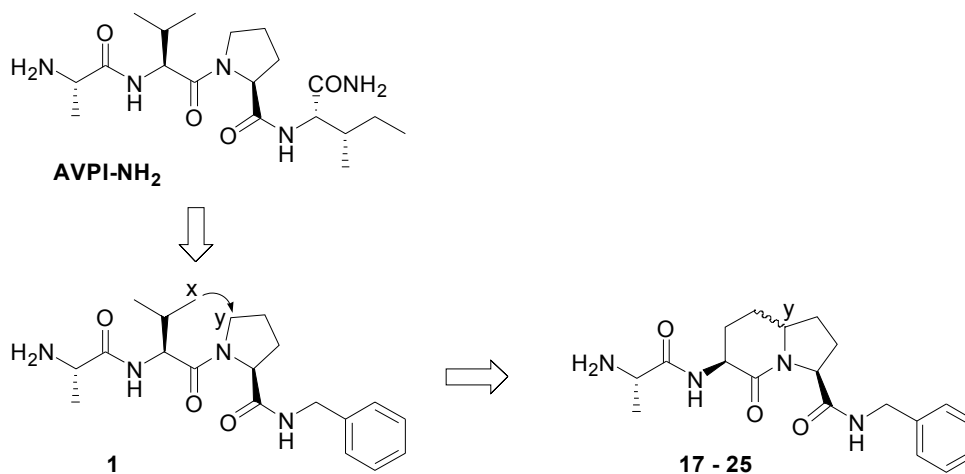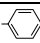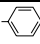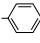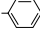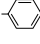
Figure 1.5 Design of conformationally constrained Smac mimetics.

10

Although the Smac mimetic compound 11 is as twenty times as potent as the Smac tetrapeptide Ala-Val-Pro-Ile, it may have limited *in vivo* stability due to its peptide nature. Hence, the small molecule non-peptidic Smac mimetics shown in Figure 1.5 were explored.[127] Compound 1, developed from the original Smac Ala-Val-Pro-Ile tetrapeptide, had double its potency. Computational studies showed that the distance between carbon x in the valine side chain and carbon y in the five-membered proline ring is close to the length of a carbon-carbon single bond. Hence, a strategy to reduce the peptide character of our Smac mimetics was to link the two carbon atoms to form a new fused six-membered ring. The other carbon atom in the isopropyl side chain in valine 2 was removed for ease of synthesis. In this way, Smac mimetic compounds 17 to 25 were prepared, in which the fused 6,5-bicyclic ring mimics the reverse turn structure formed by valine 2 and proline 3 of mature Smac mimetics.
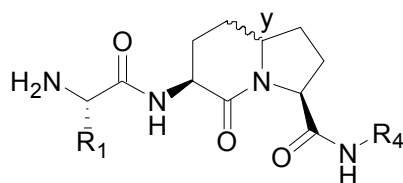
Compound	Stereochemistry of C_y	R_1	R_4	Ki/μM $\pm$ SD
17	R	Me	$-CH_2-\bigcirc$	4.47 $\pm$ 0.65
18	S	Me	$-CH_2-\bigcirc$	>100
19	R	Et	$-CH_2-\bigcirc$	1.41 $\pm$ 0.16
20	R	*n*-Pr	$-CH_2-\bigcirc$	>100
21	R	*i*-Pr	$-CH_2-\bigcirc$	43.11 $\pm$ 1.51
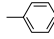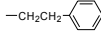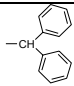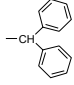
22	R	Me		>100
23	R	Me	—CH₂CH₂—	22.4 ± 1.87
24	R	Me		2.33 ± 0.68
25	R	Et		0.35 ±0.01

Table 1.2 Chemical structures of 6,5-bicyclic Smac mimetics and their binding affinities to the XIAP BIR3 protein determined with a fluorescence-polarization-based binding assay.[127]

Table 1.2 shows the chemical structures of 6,5-bicyclic Smac mimetics and their binding affinities to the XIAP BIR3 domain, determined using a fluorescence-polarization-based binding assay.[127] When carbon x of the isoleucine was linked to carbon y of the proline by a carbon-carbon single bond, a chiral center (carbon y) was created (Figure 1.5). Both of the resulting stereoisomers were tested, and the R isomer was found to be preferred over the S isomer. This was supported by computational modeling study which confirmed that the S isomer of 6,5-bicyclic Smac mimetics was unable to mimic the hydrogen bonding and hydrophobic interactions between Smac amino-terminal Ala-Val-Pro-Ile tetrapeptide and the XIAP BIR3 domain.[127] The R isomer of 6,5-bicyclic Smac mimetic (compound 17) was much more potent than the S isomer but was 10 fold less potent then original Ala-Val-Pro-Ile tetrapeptide. In an effort to increase the potency of these 6,5-bicyclic Smac mimetics, we tested a series of different hydrophobic groups for R_1 (compounds 19-21). An ethyl group was found to be preferred over methyl group for the R_1 substituent due to its increase in the hydrophobic interaction with the hydrophobic pocket formed by leucine 307, tryptophan 310, and glutamine 319 in the XIAP BIR3 domain. However, propyl and isopropyl may seem too large for this small hydrophobic binding pocket, as can be seen the decrease in binding

potency of compound 20 and 21. While the R_1 substituent remained as methyl, a series of different aromatic groups were tested for the R_4 substituent. Diphenylmethyl was found to be preferred for the R_4 substituent, as a consequence of the increase of both the interaction with the hydrophobic pocket formed by leucine 307, tryptophan 310, and glutamine 319 in the XIAP BIR3 domain and the reduction in the conformational flexibility of the compound. When R_1 substituent was substituted with an ethyl and R_4 substituent was substituted with a diphenylmethyl, as in compound 25, the most potent 6,5-bicyclic Smac mimetic was produced. This compound was slightly more potent than the original Smac amino-terminal Ala-Val-Pro-Ile tetrapeptide.
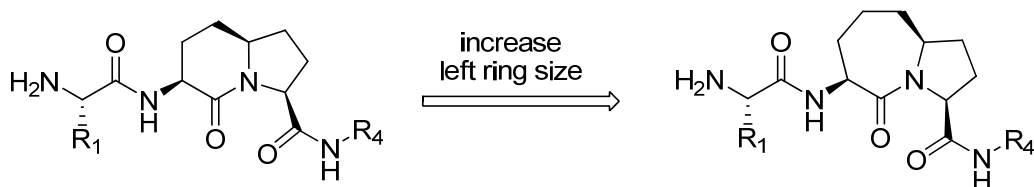
Figure 1.6 Design of conformationally constrained Smac mimetics with higher potency.

Our computational modeling studies showed that the 6,5-bicyclic system was more constrained than the reverse turn formed by valine 2 and proline 3 in the amino-terminus of mature Smac protein. Relaxation of the 6-membered ring in the 6,5-bicyclic system may generate a conformation better able to mimic the conformation of the original N-terminal Ala-Val-Pro-Ile tetrapeptide of mature Smac. To probe this, one more carbon atom was inserted in the 6-membered ring to increase the conformational flexibility of the bicyclic Smac mimetics.[128]
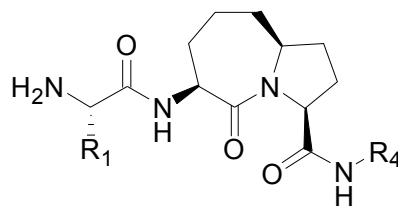
Compound	R_1	R_4	$K_i \pm$ SD (μM)
26	Me	—CH₂— (phenyl)	0.15 ± 0.02
27	Me	—CH (diphenyl)	0.060 ± 0.02
28	Et	—CH (diphenyl)	0.025 ± 0.004

Table 1.3 Chemical structures of 7,5-bicyclic Smac mimetics and their binding affinities to the XIAP BIR3 protein as determined using a fluorescence-polarization-based binding assay.[128]

While both R_1 and R_4 remained the same, increasing the size of the 6-membered ring by insertion of a single carbon atom improves the potency of bicyclic Smac mimetics binding with the XIAP BIR3 domain by a factor of 30, as can be seen from a comparison of the binding potency of compound 26 with that of 17. As expected, when R_4 was substituted with a diphenylmethyl group or R_1 was substituted with an ethyl group, the potency of these 7,5-bicyclic Smac mimetics binding with the XIAP BIR3 domain was improved. In this way, a 7,5-bicyclic Smac mimetic, compound 28, with an excellent potency in binding with the XIAP BIR3 domain ($K_i = 25$ nM), was obtained.
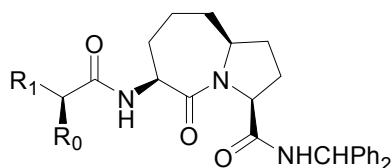
Compound	R_0	R_1	$K_i \pm$ SD (μM)
28	NH_2	C_2H_5	0.025 ± 0.004
29	$NHCH_3$	C_2H_5	0.061 ± 0.006
30	$N(CH_3)_2$	C_2H_5	14.4 ± 0.6
31	OH	CH_3	29.0 ± 1.4

Table 1.4 Design of cell-permeable Smac mimetics and their binding affinities to the XIAP BIR3 protein as determined using a fluorescence-polarization-based binding assay.[129]

The Smac mimetic compound 28 has however very weak activity in cell-based assays. It was recently reported that methylation of amino-terminal nitrogen atom could increase the cellular potency of Smac mimetics[130] and so the Smac mimetic compounds 29 and 30 were developed, with single and double methylations of the amino-terminal nitrogen atoms respectively. As expected, Smac mimetic compound 29 was as 150 times as potent as the unmethylated Smac mimetic compound 28 in tumor cell growth inhibition in human breast cancer MDA-MB-231 cell lines (Figure 1.7). The doubly methylated Smac mimetic compound 30 was 60 times less potent in binding with the XIAP BIR3 domain compound 28 due to the disruption of the hydrogen bonding interaction between the amino terminal of Smac mimetic and aspartic acid 309, glycine 314, and glutamine 319 in the XIAP BIR3 domain. Compound 30 was however 4 times more potent than compound 28 in a cell growth inhibition activity in human breast cancer MDA-MB-231 cells, and this was attributed to its superior cell-permeability. Compound 31, in which the amino-terminal group of is substituted by a hydroxyl group, was weaker than compound 28 both in binding with the XIAP BIR3 domain and in a cell growth inhibition activity measured in human breast cancer MDA-MB-231 cells and this was

assumed to be a result of the complete disruption of its amino-terminal hydrogen bonding interaction with the XIAP BIR3 domain. In this way, a potent, cell-permeable, small-molecular and non-peptidic Smac mimetic, compound 29 (IC_{50} = 0.1 µM), was obtained.[129]
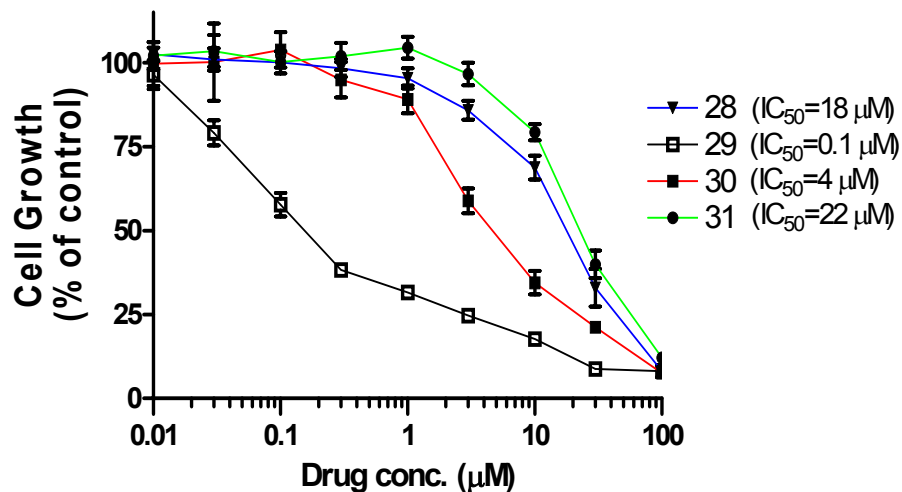
Figure 1.7 Inhibition of cell growth by Smac mimetics in human breast cancer MDA-MB-231 cell lines. Cells were treated for 4 days, and cell growth inhibition was determined using the WST-based assay[129].

Mature wild-type Smac can form an elongated dimer which binds to both the BIR2 and BIR3 domains of XIAP.[131-133] Hence, it is possible to develop a bivalent small-molecular non-peptidic Smac mimetic to mimic this Smac dimer in binding with XIAP. Such a bivalent, bidentate Smac mimetic should be a more effective promoter of apoptosis in cancer cells because it can release both the initiator caspase-9 and the effector caspase-3 and caspase-7, by binding to both the BIR2 and BIR3 domains of XIAP.
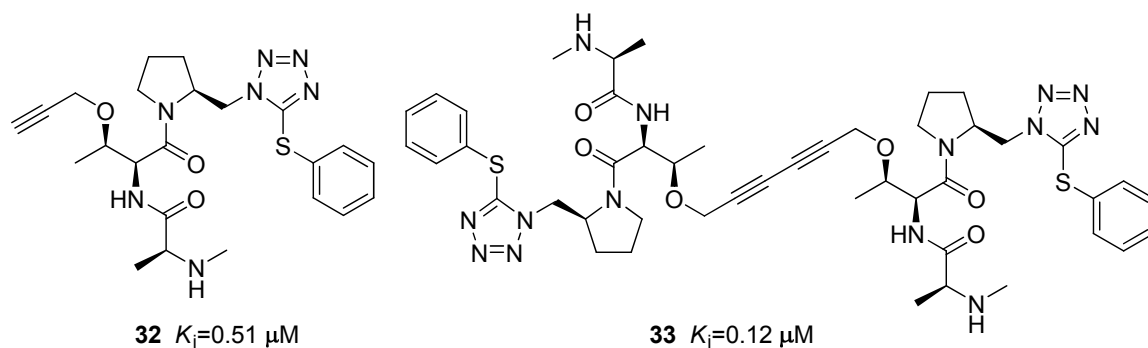
Figure 1.8 Chemical structures of the monovalent and bivalent Smac mimetics.[134]

Recently, a bivalent Smac mimetic was developed (compound 33 in Figure 1.8) from a monovalent Smac mimetic (compound 32).[134] As expected, bivalent Smac mimetic compound 33 was slightly more potent than its relative monovalent Smac mimetic compound 32. However, compound 33 was dramatically more potent than compound 32 in inducing apoptosis in combination with TRAIL or TNF-α in human glioblastoma T98G cell lines.[134] The potency of the bivalent Smac mimetic could be a consequence of its ability to bind both the BIR2 and BIR3 domains of XIAP, releasing both initiator and effector caspases.
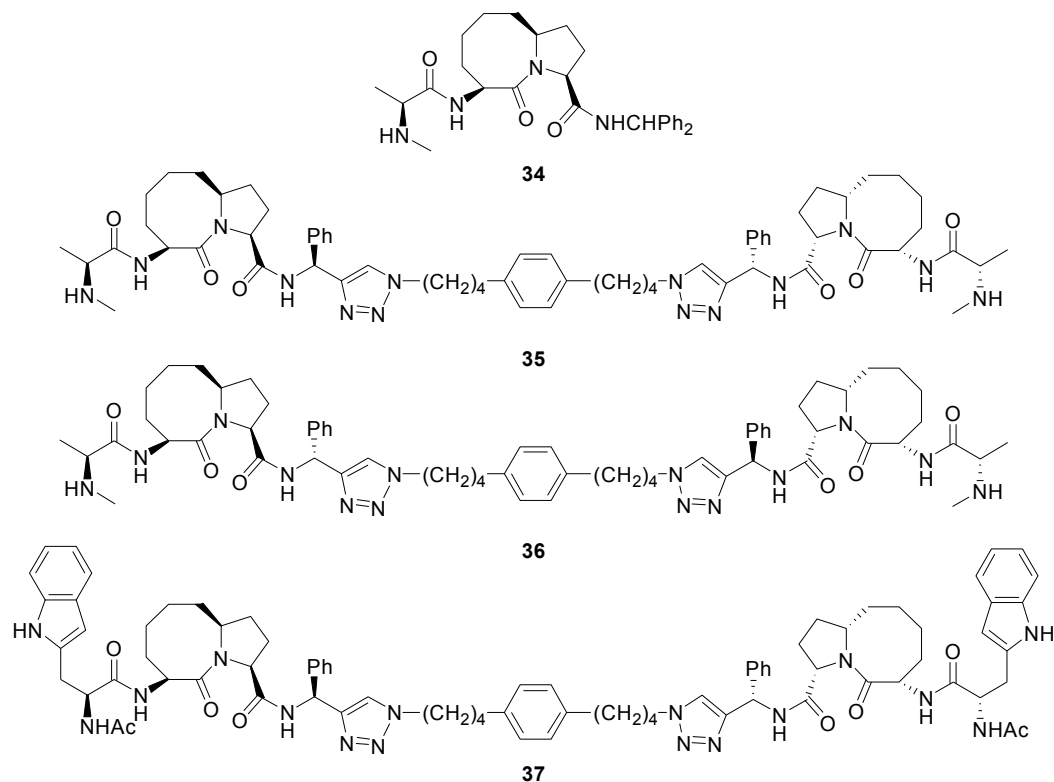
Compound	$K_i \pm$ SD (nM) (BIR3)	$K_i \pm$ SD (nM) (BIR2-BIR3)
34	26 ± 5.0	438 ± 137
35	N/A	1.39 ± 0.17
36	N/A	71.5 ± 34.9
37	N/A	> 100,000

Table 1.5 Chemical structures of monovalent and bivalent 8,5-bicyclic Smac mimetic compounds and their binding affinities with the XIAP BIR3 domain (residue 240-356) and XIAP BIR2-BIR3 domains (residue 120-356) determined in a competitive fluorescence-polarization-based assay.[135]

A potent, non-peptidic, cell-permeable, bivalent Smac mimetic, compound 35, was developed recently.[135] Computational modeling studies showed that the 7-membered fused ring of the 7,5-bicyclic Smac mimetic compounds 26, 27 and 28 could be further relaxed by increasing the ring size. The 8,5-bicyclic Smac mimetic compound 34 was developed and found to be slightly more potent (Table 1.5) than the related 7,5-bicyclic

Smac mimetic compound 27 (Table 1.3). Modeling studies also showed that the phenyl ring of the Smac mimetic compound 34 in the pro-(*S*) configuration is directed towards the solvent and has no interaction with the XIAP protein, making it a suitable anchoring site at which to tether another monovalent Smac mimetic unit. The pro-(*S*) phenyl ring was substituted with a [1,2,3]-triazole ring using "click chemistry",[136-142] yielding the bivalent Smac mimetic compound 35. Another bivalent Smac mimetic, compound 37, in which pro-(*R*) phenyl ring was used to tether another monovalent Smac mimetic unit, was also developed. As expected, both these bivalent Smac mimetic compounds (35 and 36) were dramatically more potent than the monovalent Smac mimetic compound 34 in binding with the XIAP protein containing both BIR2 and BIR3 domains (residues 120-356). The bivalent Smac mimetic compound 35 was 50 times more potent than the bivalent Smac mimetic compound 36 in binding to the XIAP BIR2-BIR3 protein, and is the most potent Smac mimetic reported to date. Compound 37 in which both the important hydrogen bonding interaction between the Smac mimetic amino terminal and glutamic acid 314, glutamine 319 and aspartic acid 309, and the hydrophobic interaction of Smac amino-terminal methyl group with the hydrophobic pocket formed by leucine 307, tryptophan 310, and glutamine 319 in the XIAP are disrupted, was designed as an inactive control for the bivalent Smac mimetics,. As shown in Table 1.5, the bivalent Smac mimetic inactive control, compound 37, essentially fails to bind with the XIAP BIR2-BIR3 protein.[135]
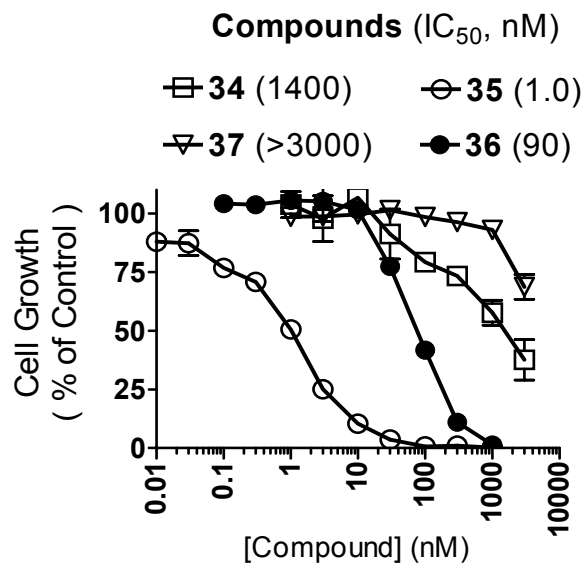
Figure 1.9 Inhibition of cell growth by Smac mimetics in the HL-60 leukemia cancer cell line. HL-60 cells were treated with the Smac mimetics for 4 days and cell growth was analyzed by WST-8 assay.[135]

As shown in Figure 1.9, bivalent Smac mimetic compound 35 is dramatically more potent in inhibition of cell growth in HL-60 leukemia cancer cell lines than the related monovalent Smac mimetic compound 34. Further studies showed that bivalent Smac mimetic compound 35 can induce the dimerization of the XIAP BIR3-only proteins by forming a 1:2 complex with them. In contrast, the bivalent Smac mimetic compound 35 can bind both the XIAP BIR2 and BIR3 domains simultaneously when the recombinant XIAP protein contains both the BIR2 and BIR3 domains. This result confirms the hypothesis that bivalent Smac mimetics can release both the initiator and effector caspases to promote apoptosis in cancer cells by binding the XIAP BIR3 and BIR2 domains simultaneously.[135]

38: K_i = 34±5.0 nM (XIAP BIR3)
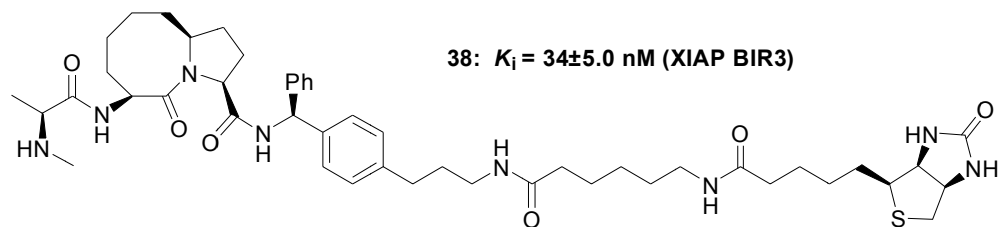
Compound 38 (μM)	-	1	3	10	10	10	10	10
Compound 35 (nM)	-	-	-	-	1	10	100	1000
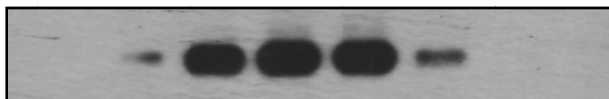
Figure 1.10 Probing the interaction of Smac mimetics to cellular XIAP in the HL-60 leukemia cell line by a competitive, co-immunoprecipitation pull-down assay using biotinylated Smac mimetic (compound 38). HL-60 whole cell lysates were incubated with compound 38 alone, or preincubated with compound 38, followed by coincubation with compound 35. Complexes formed between compound 38 and its targeted proteins were recovered by incubation with Streptavidin-argarose beads. XIAP protein associated with beads was eluted by heating and detected by western blotting using a monoclonal XIAP antibody.

In order to further probe the cellular molecular targets of designed Smac mimetics, biotinylated 7,5- and 8,5-bicyclic Smac mimetics were developed.[125,135] Using the same strategy as in the development of the bivalent Smac mimetics, the biotin molecule was tethered to the pro-(*S*) ring, which lies outside the XIAP BIR3 binding site and has no specific interaction with the XIAP protein. In binding with the XIAP BIR3 domain, the designed biotinylated 8,5-bicyclic Smac mimetic compound 38 and the unlabeled Smac mimetic compound 34 were equipotent. A co-immunoprecipitation assay was performed to verify that the XIAP protein is the intracellular target of designed Smac mimetics. As shown in Figure 1.10, the biotinylated Smac mimetic compound 38 pulled down the XIAP protein in the HL-60 leukemia cell lines dose-dependently, and the bivalent Smac mimetic compound 35 competed off the binding between the biotinylated Smac mimetic compound 38 and XIAP protein in a dose-dependent manner, verifying XIAP as the cellular target of designed Smac mimetics.[135]

CHAPTER 2

DESIGN AND SYNTHESIS OF NON-PEPTIDIC SMALL MOLECULE SMAC MIMETICS

2.1 Design Rationale

2.1.1 Design of monovalent Smac mimetics

Figure 2.1 Chemical structures of SM-122 and designed new monovalent Smac mimetics.

The 7,5-bicyclic system in Smac mimetic compound 28 (Table 1.4) and the 8,5-bicylic system in compound 34 (Table 1.5) are the core structures of previously published Smac mimetics.[125,135] The bicyclic core structure mimics the original

conformation formed by Smac AVPI tetrapeptide, ensuring the methyl or ethyl in the head part and the terminal R_1 group of the compounds have the appropriate orientation to penetrate deeply into the relatively hydrophobic binding pockets of the XIAP BIR3 domain.[122,123] The 8,5-bicyclic Smac mimetics are more potent than the 7,5-bicyclic Smac mimetics, and our recently developed 9,5-bicyclic Smac mimetics have the same potency binding with the XIAP BIR3 domain. Therefore, we regard the 8,5-bicyclic structure as the optimal bicyclic system in the development of future Smac mimetics.
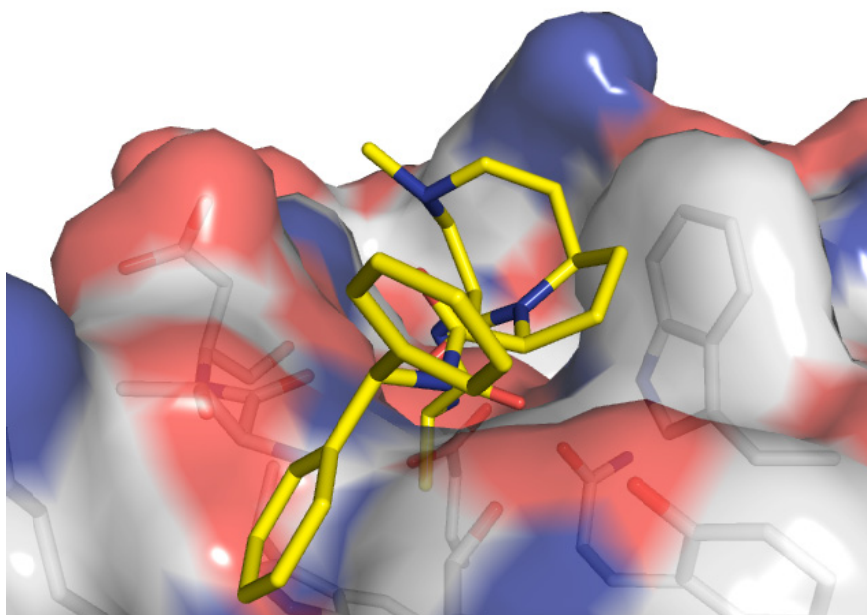
Figure 2.2 Computational modeling structure of Smac mimetic compound YP-245P3 binding with the XIAP BIR3 domain.

Our modeling studies showed that while the 8-membered ring in compound 34 (SM-122) has van der Waals contacts with Trp323 of the XIAP BIR3 domain, the middle portion (carbon X) is largely exposed to solvent. Based upon this model, we predicted that replacement of carbon X by a nitrogen atom will not be detrimental to the binding of XIAP. Two types of functional groups can then be tethered to this newly introduced nitrogen atom, as shown in compounds 39 and 40 respectively in Figure 2.1. Compounds 39 and 40 will have two slightly different conformations compared to compound 34, and it is hoped that one of them may bind more effectively than compound 34. Meanwhile, modification of the R_x or R_y group in the new Smac mimetics (Figure 2.1) having no detrimental effect on the binding potency with XIAP, it is hoped that through this modification new Smac mimetics can be developed with improved pharmacokinetic (PK) properties compared to the previously studied Smac mimetics.

2.1.2 Design of Bivalent Smac mimetics
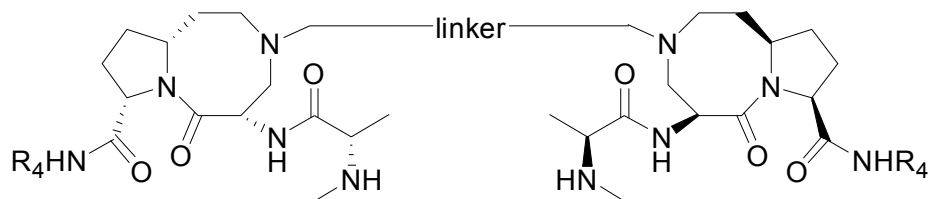
Figure 2.3 Chemical structure of designed bivalent Smac mimetics.

As shown in Figure 2.2, the methyl group tethered to the nitrogen atom in the 8-membered ring is oriented towards the solvent and has no specific interaction with the XIAP BIR3 domain. This nitrogen atom is therefore a suitable site at which to chemically tether a second monovalent Smac mimetic moiety, forming a bidentate Smac mimetic. Similarly, both the carbon-nitrogen single bond and the amide bond were tested as sites at which to link the two monovalent Smac mimetic moieties. As can be seen in Figure 2.3, the newly developed bivalent Smac mimetics are structurally different from those previously published, in which monovalent Smac mimetic moieties were linked via their aromatic tails (R_4).[135]

2.2 Retrosynthetic Analysis
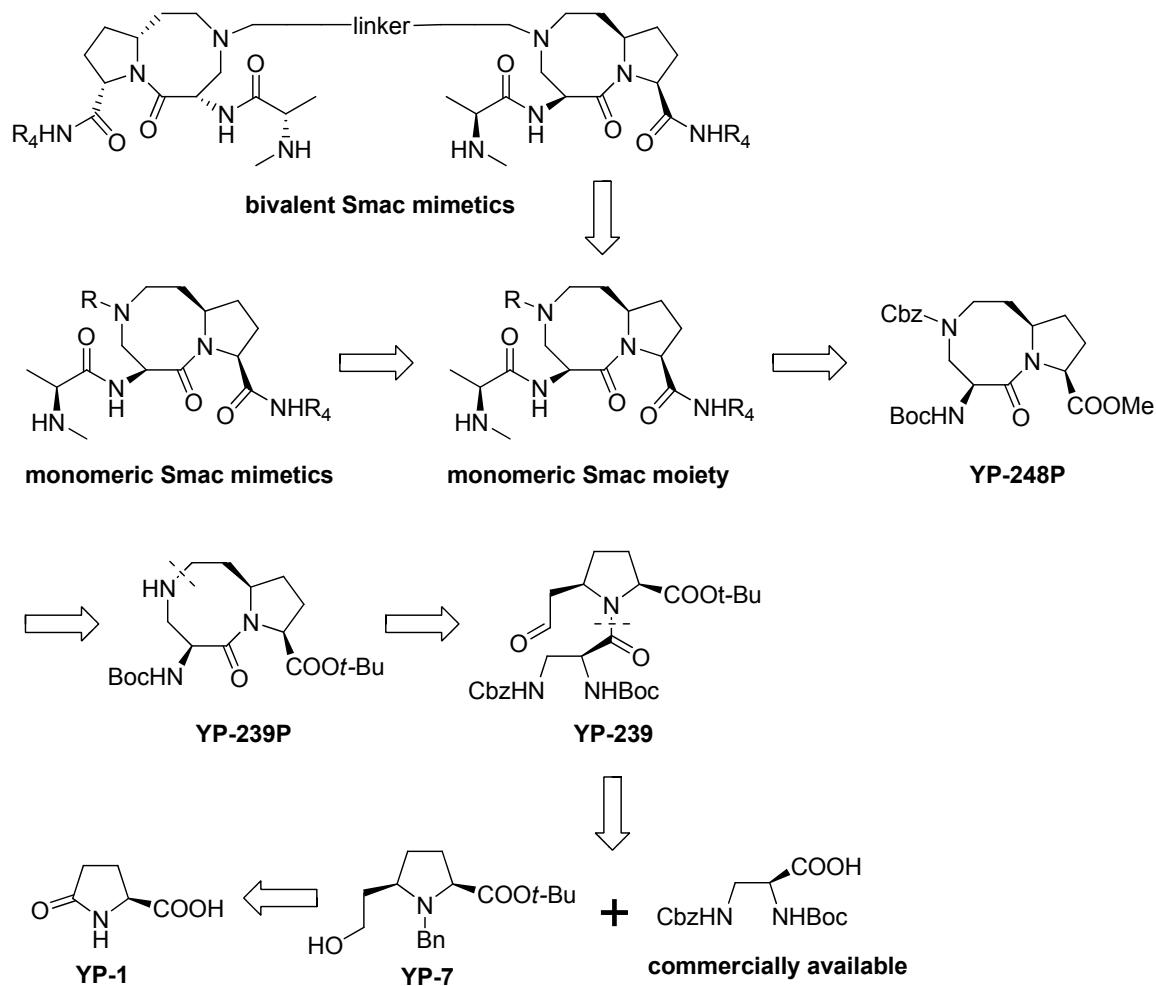
Figure 2.4 Retro-synthetic analysis of designed Smac mimetics.

A retrosynthetic analysis of designed Smac mimetics is shown in Figure 2.4. Both

bivalent Smac mimetics and monovalent Smac mimetics can be prepared from the related

monovalent moieties which bear the common core structure, a nitrogen-containing 8,5-

bicyclic fused ring system. Compound YP-248P which, with the common core structure,

is the most important intermediate in the synthetic route can be prepared from YP-239P

by protection of the secondary amine as its carbobenzyloxy derivative followed by

transesterification. The cyclic amine YP-239P can be obtained from the aldehyde YP-239

by catalytic hydrogenation and the aldehyde YP-239 can be prepared by the condensation

26

of the commercially available N-α-t-butyloxycarbonyl-N-β-benzyloxycarbonyl-L-2,3-diaminopropionic acid with the deprotected free secondary amine of compound YP-7. Compound YP-7 is a known compound which can be obtained in six steps from (*S*)-(-)-2-pyrrolidone-5-carboxylic acid (compound YP-1 in Figure 2.4).[143,144]
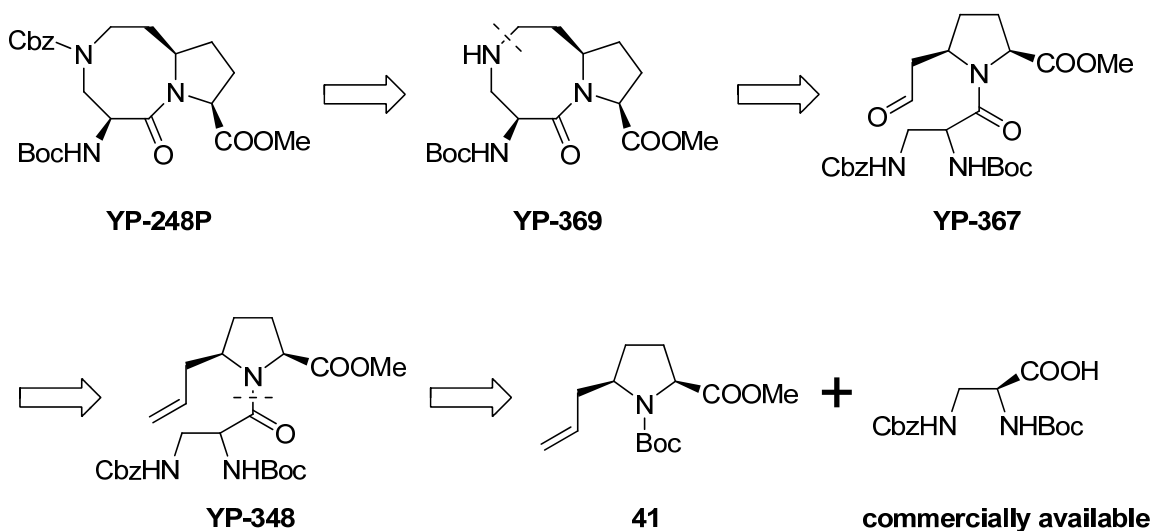
Figure 2.5 Retro-synthetic analysis of the new route.

Subsequently, a new concise synthetic route for the core structure YP-248P was developed based on the retrosynthetic analysis of compound YP-248P shown in Figure 2.5. In the newly developed route, the transesterification reaction following the cyclization of YP-367 was avoided, increasing the overall yield. The key intermediate YP-248P can be directly prepared from its relative cyclic amine YP-369, which can be obtained using the same catalytic hydrogenation condition as in synthesis of YP-239P. The aldehyde YP-367 can be prepared from the terminal alkene YP-348 by ozonolysis.

The amide YP-348 is prepared by condensation of the commercially available N-α-t-butyloxycarbonyl-N-β-benzyloxycarbonyl-L-2,3-diaminopropionic acid and the deprotected secondary amine derived from compound 41. Compound 41 is a known compound and can be synthesized by published methods.[145-148]

2.3 Results and Discussion

Comp.	Structure	BIR3 $K_i \pm SD$ (nM)
YP-245P3 (SM-245)	CONHCHPh₂ structure	340 ± 65.9
YP-246P (SM-246)	Bn–N ... CONHCHPh₂ structure	91.8 ± 30.4
YP-330 (SM-330)	acetyl ... CONHCHPh₂ structure	5.4 ± 3.0
YP-337 (SM-337)	Bn ... CONHCHPh₂ structure	8.4 ± 1.6
YP-350 (SM-350)	F-phenyl ... CONHCHPh₂ structure	6.0 ± 1.5
YP-356 (SM-356)	F,F-phenyl ... CONHCHPh₂ structure	6.8 ± 0.8
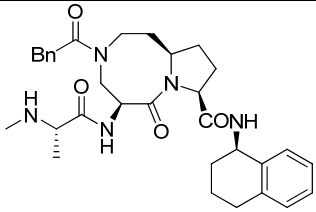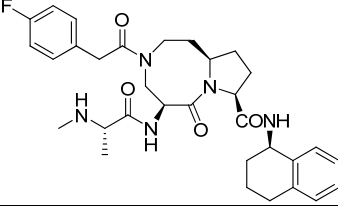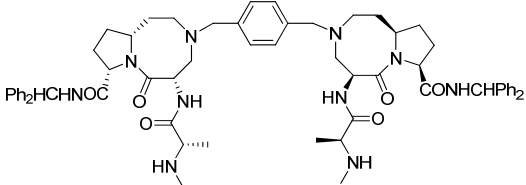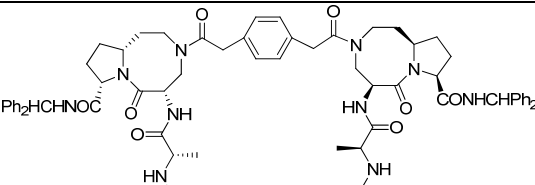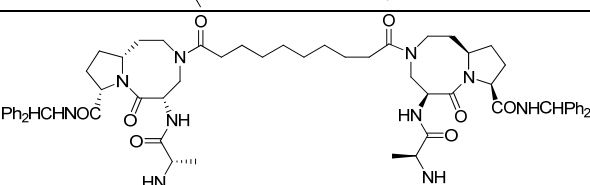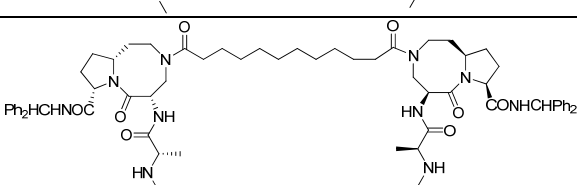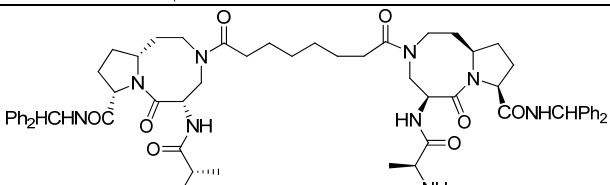
Comp.	Structure	BIR3 $K_i \pm$SD (nM)	L-BIR2-BIR3 $K_i \pm$SD (nM)
YP-376 (SM-376)		2.0 ± 1.0	
YP-377 (SM-377)		1.4 ± 0.7	
YP-317 (SM-317)		185 ± 5.7	43 ± 0.8
YP-343 (SM-343)		21 ± 7.0	2.7 ± 0.5
YP-381 (SM-381)		27.5 ± 6.2	1.8 ± 0.6
YP-383 (SM-383)		43.1 ± 3.6	1.8 ± 0.5
YP-385 (SM-385)		12.7 ± 3.9	1.0 ± 0.5

Table 2.1 Chemical structures of synthesized monovalent and bivalent Smac mimetics and their binding affinities to the XIAP BIR3 or XIAP linker-BIR2-BIR3 determined using a fluorescence-polarization-based binding assay.[126] XIAP BIR3 binding was tested for both monovalent and bivalent Smac mimetics, while additionally, XIAP linker-BIR2-BIR3 binding was tested for bivalent Smac mimetics.

A series of monovalent and bivalent Smac mimetics was designed and synthesized, and their binding affinities were determined using the fluorescence-polarization(FP)-based binding assay.[126] The results are shown in Table 2.1. In the monovalent Smac mimetics YP-245P3 (SM-245) and YP-246P (SM-246), a methyl group and a benzyl group are directly tethered to the newly introduced nitrogen atom in the 8-membered ring respectively; these two Smac mimetics, with binding affinities of 340 nM and 92 nM respectively, have less potency than the original lead compound SM-122 (compound 34 in Chapter 1) in binding with the XIAP BIR3 domain.

Our computational modeling studies showed that both the tethered phenyl group in SM-246 and the newly introduced methyl group in SM-245 have no specific interactions with the XIAP BIR3 domain. However, SM-246 is 5 times more potent than SM-245 in binding with the XIAP BIR3 domain. This increase in potency could be caused by the increased rigidity of the fused 8-membered ring, while the decrease in potency of both SM-245 and SM-246 compared with lead compound SM-122 could be caused by the decreased rigidity of that ring.

The monovalent Smac mimetic compounds SM-330 and SM-337 have a carbonyl group inserted between the alkyl group and the nitrogen atom in the 8-membered ring of SM-245 and SM-246, respectively. This carbonyl group forms an amide bond with the adjacent nitrogen atom and increases the rigidity of the ring. Both new Smac mimetics are much more potent than the related SM-245 and SM-246 in binding with the XIAP

BIR3 domain as shown in Table 2.1 and they are 3-4 times more potent than the lead compound SM-122 in binding affinity with the XIAP BIR3 domain.

Consequently, SM-337 was used as a new lead compound in the development of nitrogen-containing 8,5-bicyclic Smac mimetics. The *para* and *ortho* sites of the benzyl group tethered to the nitrogen atom in the 8-membered ring can be metabolized by cytochrome P450 *in vivo*, and with this in mind, we designed SM-350 and SM-356 with a view to improving the pharmacokinetic properties. In SM-350, the *para* site of the phenyl ring was blocked with a fluorine atom while in SM-356 the *para* site and one of the *ortho* sites of the phenyl ring were both blocked with fluorine atoms. Both SM-350 and SM-356 were found to have similar potency compared with the lead compound SM-337 in binding with the XIAP BIR3 domain.

Previous studies showed that an (*R*)-tetrahydronaphthyl group can be well accommodated in the large hydrophobic pocket formed by lysine 297 and lysine 299 of the XIAP BIR3 domain. These compounds might be expected to have superior potency than the corresponding diphenylmethyl compounds, for example, 245P3, in binding to the XIAP BIR3 domain.[130,149] Compound SM-376 in which the terminal diphenylmethyl group was replaced by a (*R*)-tetrahydronaphthyl group was designed and synthesized. This compound was found to be the most potent monovalent Smac mimetic to date both in binding with the XIAP BIR3 domain and in inhibition of tumor cell growth. The Smac mimetic SM-377, in which the *para* site of the phenyl ring is blocked with a fluorine

atom, was also designed and synthesized in the hope that it would demonstrate improved pharmacokinetic properties.

Using Smac mimetic SM-246 as the monovalent moiety and 1,4-dimethylenephenyl as the linker, the bivalent Smac mimetic SM-317 was synthesized and another bivalent Smac mimetic, SM-343, was also developed using the more potent Smac mimetic SM-337 as the monovalent moiety. As expected, SM-343 is much more potent than SM-317 in binding with the XIAP BIR3 domain and it is dramatically more potent than SM-317 in binding with the XIAP linked-BIR2-BIR3 protein.

Using the monovalent Smac mimetic compound SM-330 as the template, we designed and synthesized SM-381, SM-383 and SM-385, bivalent Smac mimetic compounds with dicarboxylic acid linkers of different lengths as shown in Table 2.1. The linkers in SM-381, SM-383 and SM-385 have 8, 10, and 6 methylene groups respectively. The binding affinities of these bivalent Smac mimetics against XIAP BIR3 domain increase as the lengths of the linker decrease, but they have similar potency in binding with the XIAP linker-BIR2-BIR3 protein, as shown in Table 2.1.

The activities in tumor cells of these synthetic monovalent and bivalent Smac mimetics were determined and analyzed in detail in Chapters 3-5, below.

2.4 Conclusion

Various monovalent and bivalent small-molecular non-peptidic Smac mimetics were successfully designed and synthesized. SM-337 has a dramatically improved potency in binding to XIAP BIR 3 compared with our original lead compound SM-122. Using this compound, SM-337, as our new design template, several potent monovalent and bivalent Smac mimetics were developed.

SM-376 and SM-377 are the most potent monovalent Smac mimetics reported to date, with a binding affinity (K_i) to XIAP BIR3 domain as 2.0 and 1.4 nM respectively. The cell-permeable Smac mimetics, SM-376 and SM-377, are as potent as the bivalent Smac mimetic lead compound SM-164 in tumor cell growth inhibition in human breast cancer MDA-MB-231 cells. SM-406 (Chapter 5), a derivative of SM-376 and SM-377, shows excellent pharmacokinetic properties and is a promising drug candidate.

The bivalent Smac mimetics SM-381, SM-383 and SM-385 are as potent as the bivalent Smac mimetic lead compound SM-164 in both binding the XIAP BIR3 protein and the XIAP linker-BIR2-BIR3 protein. These three newly developed bivalent Smac mimetics have a linker that differs from the triazole linker in SM-164. This has advantages in terms of ease of synthesis and further optimization of the aromatic binding in the hydrophobic pocket formed by lysine 297 and lysine 299 of the XIAP BIR3 domain. Further optimization of this aromatic fragment and the length of the linker may yield bivalent Smac mimetics that are even better than the original lead compound SM-164.

2.5 Synthesis of Smac Mimetics
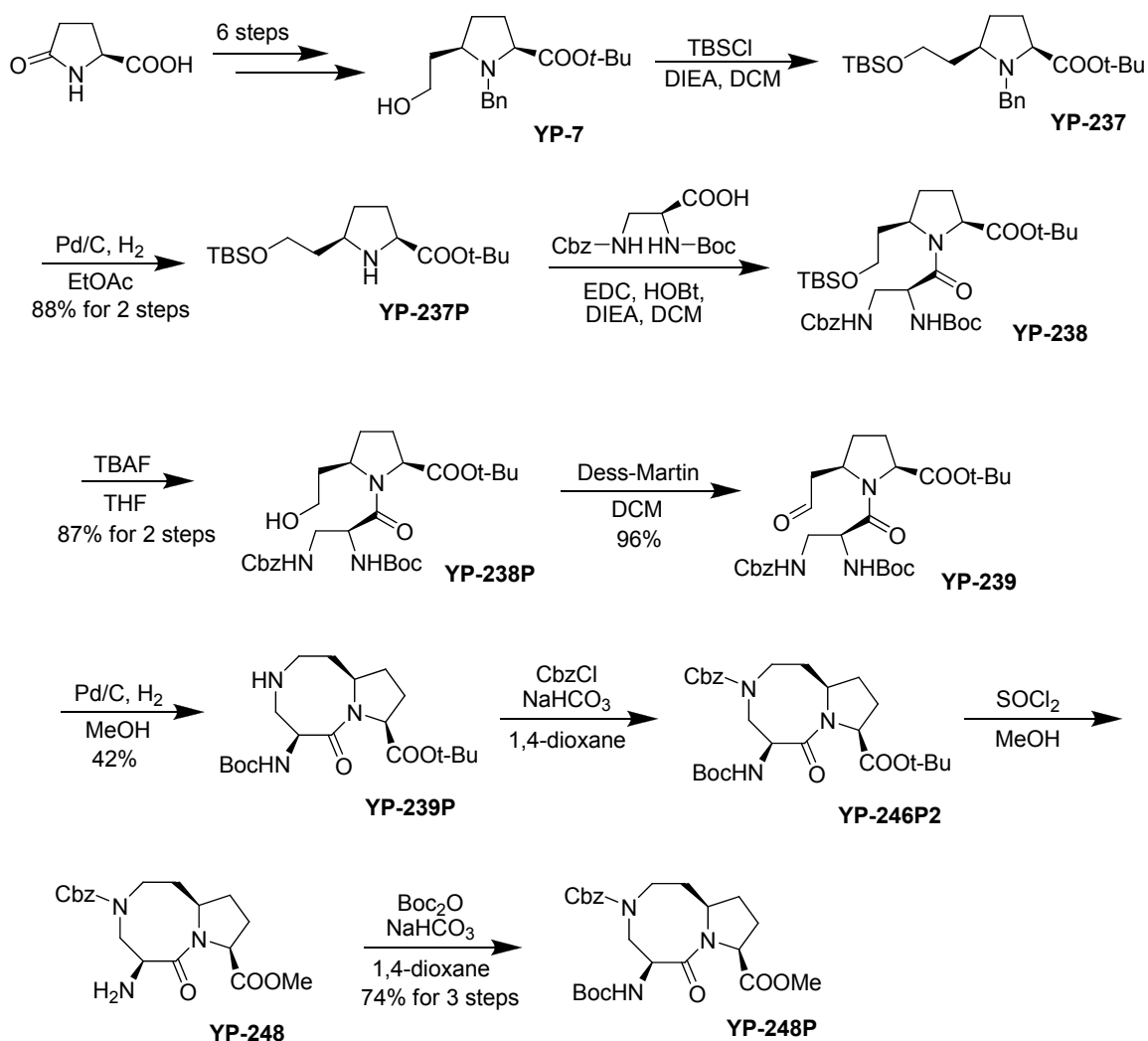
Figure 2.6 Synthetic route to key intermediate YP-248P.

Figure 2.6 shows the synthetic route to compound YP-248P, the key intermediate

for the synthesis of both monovalent and bivalent Smac mimetics. Commercially

available (*S*)-(-)-2-pyrrolidone-5-carboxylic acid was used as the starting material and

known compound YP-7 was obtained after 6 published steps.[143,144] The free hydroxyl

group in compound YP-7 was first protected with a *tert*-butyldimethylsilyl (TBS) group

to yield compound YP-237, whose benzyl protecting group was then removed by catalytic hydrogenation. The free secondary amine YP-237P was obtained after these two steps of reactions with an overall yield from YP-7 of 88%.

The pyrrolidine YP-237P was coupled with commercially available N-α-t-butyloxycarbonyl-N-β-benzyloxycarbonyl-L-2,3-diaminopropionic acid to yield the amide YP-238. The TBS protective group in compound YP-238 was then removed with tetra-*n*-butylammonium fluoride (TBAF) in tetrahydrofuran to give the free alcohol YP-238 with an 87% overall yield for the two reactions. The alcohol YP-238 was oxidized with Dess-Martin reagent to yield the aldehyde YP-239 in a yield of 96%. Upon catalytic hydrogenation, the desired nitrogen-containing 8,5-bicyclic structure was formed. Three chemical reactions occur in this single step: first, the carbobenzyloxy (Cbz) protective group is removed to yield a free terminal amine; then the terminal amine reacts intramolecularly with the aldehyde group forming the cyclic imine and finally, this cyclic imine is reduced to the desired cyclic amine. This step was performed at low concentrations so as to encourage the intramolecular reaction, and gave a yield of 42%. The free cyclic amine was then protected with a carbobenzyloxy group to yield compound YP-246P2. The *tert*-butyl ester YP-246P2 was allowed to react with $SOCl_2$, added dropwise in methanol at 0°C to yield the methyl ester YP-248. In this step, the *tert*-butyloxycarbonyl (t-Boc) group was also removed and so in a final step, the free amino group was protected with a t-Boc protective group to yield the key intermediate YP-248P. These three reaction steps gave an overall yield of 74%.[150]
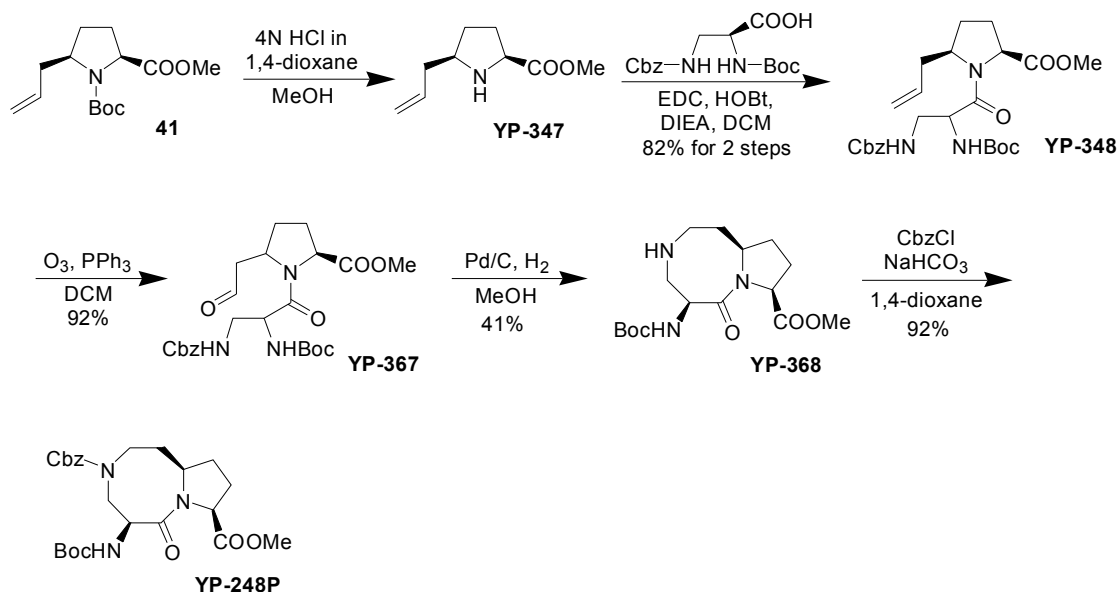
Figure 2.7 New synthetic route to the key intermediate YP-248P.

The synthesis route of key intermediate YP-248P in Figure 2.6 is lengthy and has a low overall yield from YP-7 of only 23%. Subsequently, we developed a new and concise route to this same intermediate and this synthetic route is shown in Figure 2.7. Compound 41, which can be prepared using published methods,[145-148] was the starting material in this new synthetic route. The t-Boc protecting group was first removed to yield the free amine YP-347, which was then coupled with the commercially available N-α-t-butyloxycarbonyl-N-β-benzyloxycarbonyl-L-2,3-diaminopropionic acid to form the amide YP-348. The overall yield for these two steps was 82%. YP-348 was oxidized to the aldehyde YP-367 in a yield of 92% by ozonolysis. Under conditions of catalytic hydrogenation, the aldehyde YP-367 was deprotected, cyclized, and finally reduced to the desired cyclic amine YP-368. This step showed the yield of 41%, similar to that obtained

36

in the previous route. Finally, the key intermediate YP-248P was obtained by protection

of the secondary amino group in compound YP-368. The yield for this step was 92%.
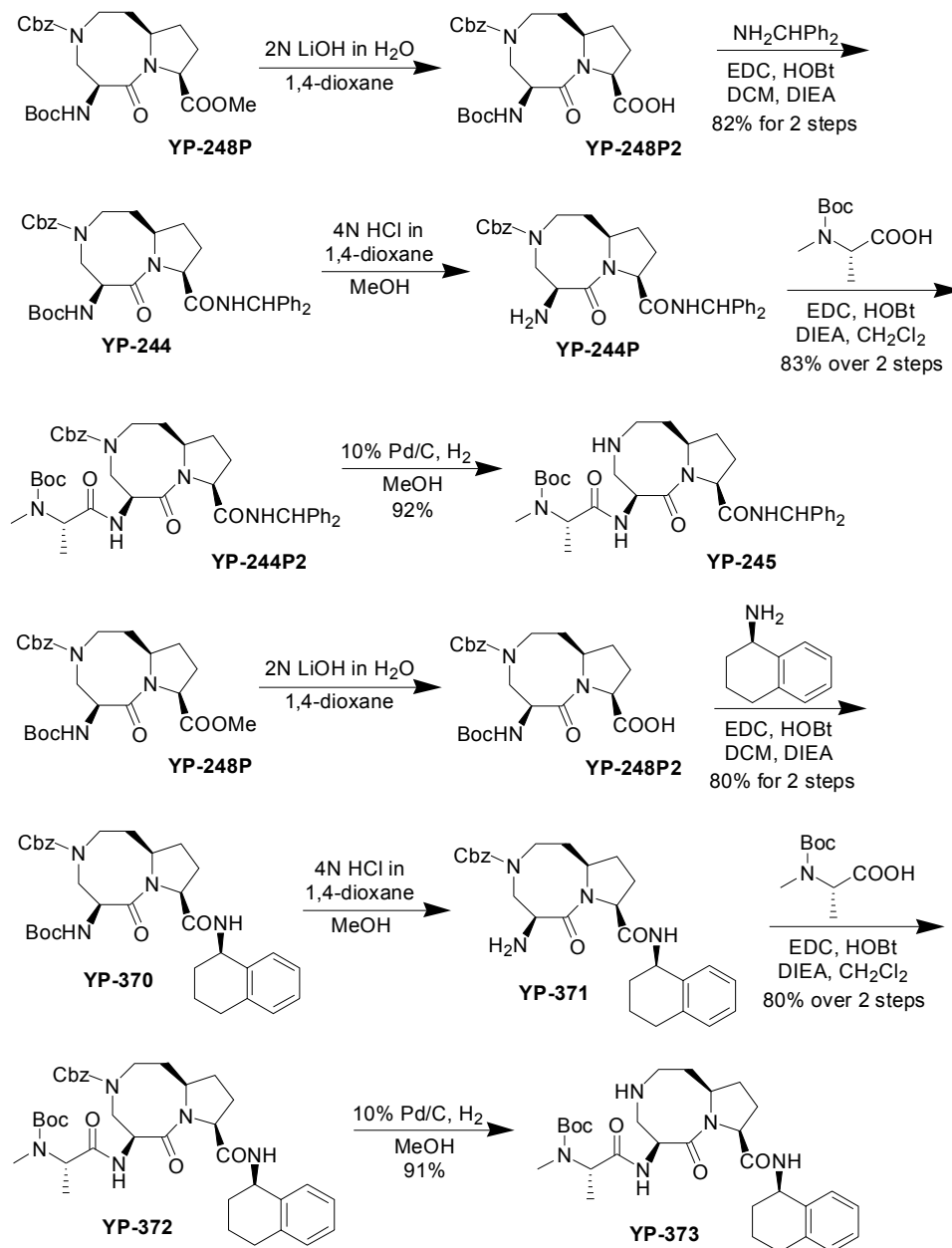
Figure 2.8 Synthesis of key components YP-245 and YP-373.

Figure 2.8 shows the synthetic route to compounds YP-245 and YP-373, which are the key intermediates in the syntheses of the monovalent and bivalent Smac mimetic compounds. The methyl ester YP-248P was first converted to the free carboxylic acid YP-248P2, which was then coupled with the commercially available diphenylmethyl amine to form the amide YP-244. The overall yield for these two steps was 82%.

Removal of the t-Boc protective group from compound YP-244 gave the free amine YP-244P, which was coupled with the commercially t-Boc-N-methylalanine to form the amide YP-244P with an overall yield of 83% for these two steps. The carbobenzyloxy protecting group was removed by catalytic hydrogenation to yield the free cyclic amine YP-245 with a yield of 92%.

Similarly, the methyl ester YP-248P was first converted to the free carboxylic acid YP-248P2, which was then coupled with the commercially available (*R*)-1,2,3,4-tetrahydro-1-naphthylamine to form the amide YP-370 with an overall yield of 80% for these two steps. Then the t-Boc protecting group in compound YP-370 was removed to yield the free amine YP-371, which was coupled with the commercially available t-Boc-N-methylalanine to form the amide YP-372 with an overall yield of 80% for the two steps. The carbobenzyloxy protecting group was finally removed by catalytic hydrogenation to yield the free cyclic amine YP-373 with a yield of 91%.
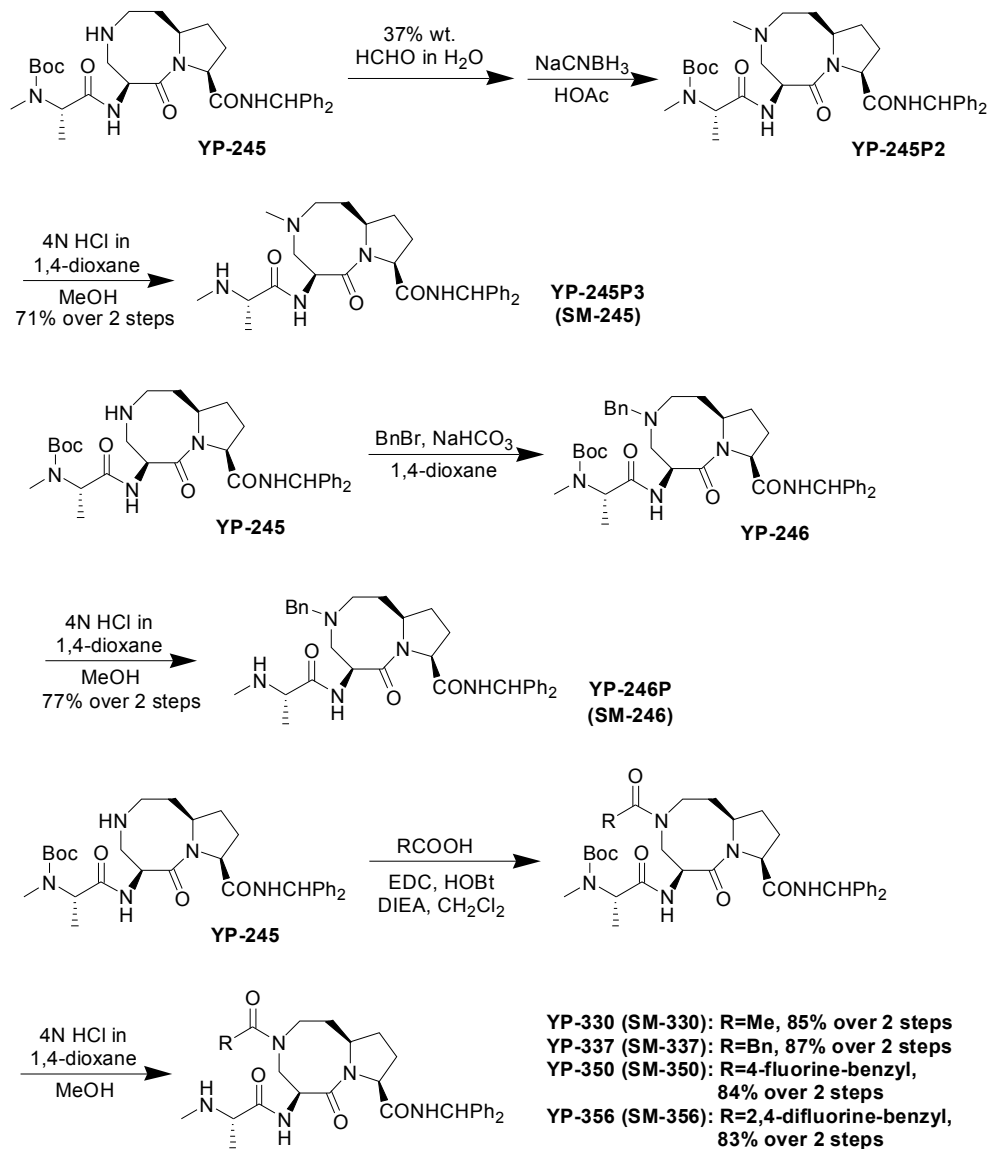
Figure 2.9 Synthesis of monovalent Smac mimetics.

The synthesis of monovalent Smac mimetics is shown in Figure 2.9. A methyl group was attached to the nitrogen atom in the 8-membered ring via a reductive amination reaction forming compound YP-245P2, whose t-Boc protecting group was subsequently removed to yield the monovalent Smac mimetic compound YP-245P3 (SM-245) with an overall yield of 71% for the two steps. A benzyl group was attached to the

nitrogen atom in the 8-membered ring via an S_N2 reaction, in which the cyclic amine YP-245 was treated with benzyl bromide to form YP-246, whose t-Boc protecting group was removed to yield the monovalent Smac mimetic compound YP-246P (SM-246) with an overall yield of 77% for the two steps. Condensation reactions between the cyclic amine YP-245 and the appropriate carboxylic acid, followed by the removal of the t-Boc groups, were performed to obtain the relative monovalent Smac mimetic compounds YP-330 (SM-330), YP-337 (SM-337), YP-350 (SM-350), and YP-356 (SM-356). The yield, reagents and conditions for these two reactions are shown in Figure 2.9.
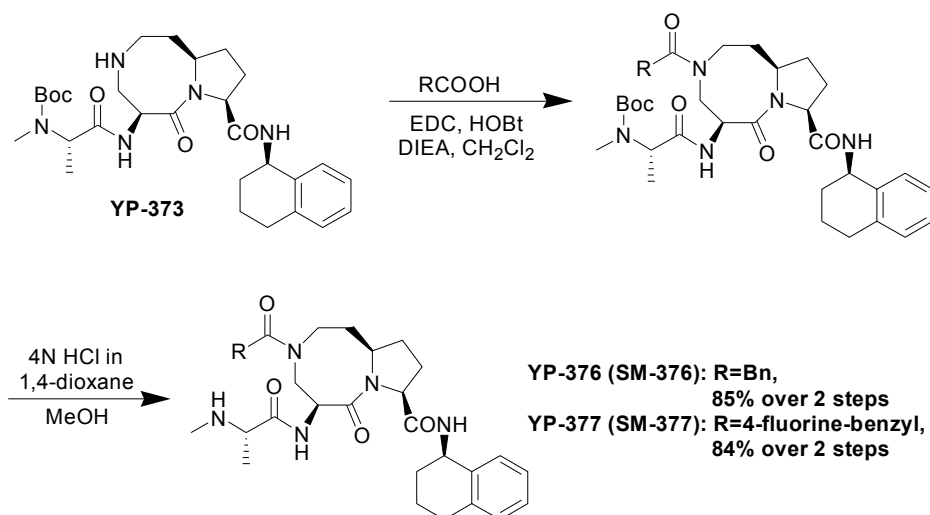
Figure 2.10 Synthesis of monovalent Smac mimetics SM-376 and SM-377.

Syntheses of the monovalent Smac mimetic compounds SM-376 and SM-377 are shown in Figure 2.10. Condensation of the cyclic amine YP-373 with phenylacetic acid or 4-fluorophenylacetic acid, followed by the deprotection of the t-Boc protecting groups,

was performed to yield the monovalent Smac mimetic compounds YP-376 (SM-376) and

YP-377 (SM-377) with overall yields of 85% and 84% respectively.
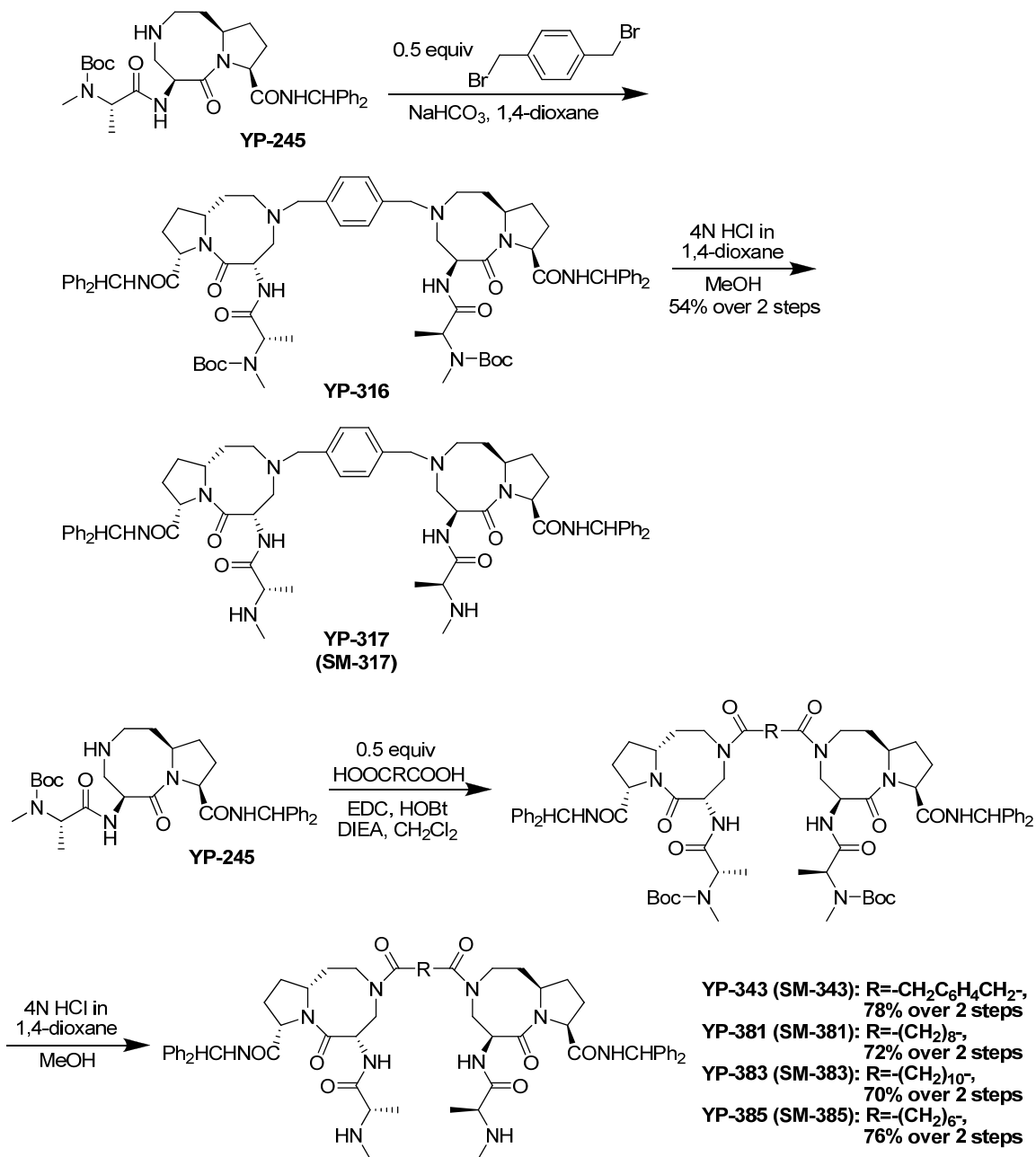
Figure 2.11 Synthesis of bivalent Smac mimetics.

The syntheses of bivalent Smac mimetic compounds are shown in Figure 2.17. Cyclic amine YP-245 underwent an S_N2 reaction with a half equivalent of *p*-xylylene dibromide to form the bivalent compound YP-316, whose t-Boc protective groups were then removed to obtain the bivalent Smac mimetic compound YP-317 (SM-317) with an overall yield of 54% for the two steps. Condensation of the cyclic amine YP-245 and the appropriate dicarboxylic acid, followed by removal of the t-Boc groups, was performed to obtain the bivalent Smac mimetic compounds YP-343 (SM-343), YP-381 (SM-381), YP-383 (SM-383), and YP-385 (SM-385) respectively. The yields, reagents and conditions for these steps are shown in Figure 2.11.

2.6 Methods and Materials

General methods: NMR spectra were measured at a proton frequency of 300 MHz. [1]H chemical shifts are reported relative to tetramethylsilane (0.00 ppm) or DHO (4.70 ppm) as internal standards. [13]C chemical shifts are reported relative to $CDCl_3$ (77.00 ppm) or CD_3OD (49.00 ppm) as internal standards. The final products were purified by C18 reverse phase semi-preparative HPLC column with solvent A (0.1% of TFA in water) and solvent B (0.1% of TFA in CH_3CN) as eluents.
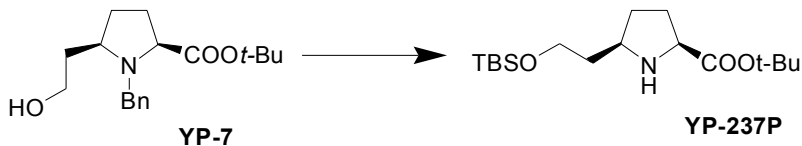
Synthesis of compound YP-237P: To a solution of compound **YP-7** (1.26 g, 4.1 mmol) of in dichloromethane (20 mL) was added *tert*-butyldimethylsilyl chloride (930 mg, 6.2 mmol) and N,N-diisopropylethylamine (1.5 mL).[143,144,151] The mixture was stirred at room temperature overnight and then evaporated to dryness. The residue was purified by chromatography to afford 1.61 g of silyl ether to a solution of which (1.50 g, 3.58 mmol) in methanol (20 mL) was added 10% Pd/C (0.2 g). The mixture was stirred at room temperature under H_2 overnight. The catalyst was removed and the filtrate was evaporated to dryness. The crude product was purified by chromatography to afford compound **YP-237** (1.1 g, 88% over two steps). $[\alpha]^{20}_D$ -21.5° (c = 1.0, CHCl$_3$); ^{1}HNMR (300 MHz, CDCl$_3$, TMS) δ 3.71 (t, *J* = 6.5 Hz, 3H), 3.60 (dd, *J* = 9.0, 5.4 Hz, 1H), 3.11 (m, 1H), 2.05 (m, 1H), 1.95-1.63 (m, 3H), 1.46 (s, 9H), 1.25 (m, 1H), 0.89 (s, 9H), 0.05 (s, 6H); ^{13}CNMR (75 MHz, CDCl$_3$) δ 174.5, 80.8, 61.5, 60.6, 57.5, 38.8, 31.8, 30.4, 28.0, 25.9, 18.2, -5.4; HRMS: calcd. m/z for [M+H]$^+$ 330.2464; found 330.2466.
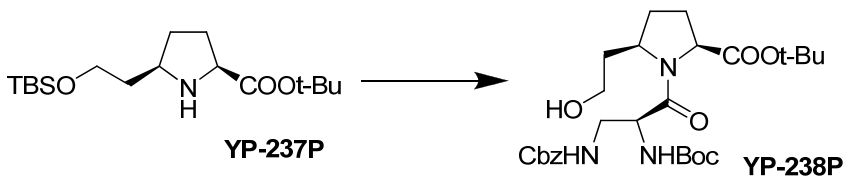
Synthesis of compound YP-238P: To a solution of compound **YP-237P** (1.05 g, 3.19 mmol) in dichloromethane (15 mL) was added t-Boc-Dap(Z)-OH·DCHA (2.32 g, 1.4

equiv.), EDC (1-ethyl-3-(3-dimethylaminopropyl) carbodiimide hydrochloride) (978 mg, 1.6 equiv.), HOBt (Hydroxybenzotriazole) (690 mg, 1.6 equiv.), and N,N-diisopropylethylamine (3 mL). The mixture was stirred at room temperature overnight and then concentrated to give a residue which was purified by chromatography to afford an amide (1.86 g). To a solution of the above amide (860 mg, 1.32 mmol) in THF (10 mL) was added tetrabutylammonium fluoride solution (1M, 1.6 mL, 1.2 equiv.) in THF and the solution was stirred at room temperature for 3 h.[152-154] After adding dichloromethane (50 mL), the solution was washed with brine, dried over Na_2SO_4 and then condensed. The crude product was purified by chromatography to yield compound **YP-238P** (690 mg, 87% over two steps). $[\alpha]^{20}_D$ -90.0° (c = 1.67, $CHCl_3$); ^1H NMR shows this compound is a 1:1 mixture of two rotamers. ^1HNMR (300 MHz, $CDCl_3$, TMS) δ 7.28 (m, 5H), 5.59 (m,1H), 5.35 (m, 1H), 5.20-5.05 (m, 2H), 4.85 (m, ½ H), 4.65 (m, ½ H), 4.46 (m, 1H), 4.35 (m, 1H), 3.80 (m, ½ H), 3.70-3.50 (m, 2H), 3.40 (m, 1H), 3.25 (m, ½ H), 2.32 (m, 1H), 2.20-1.50 (m, 4H), 1.46 (s, 4.5H), 1.44 (s, 4.5H), 1.43 (s, 4.5H), 1.41 (s, 4.5H); HRMS: calcd m/z 558.2791 for $[M+Na]^+$; found 558.2794.
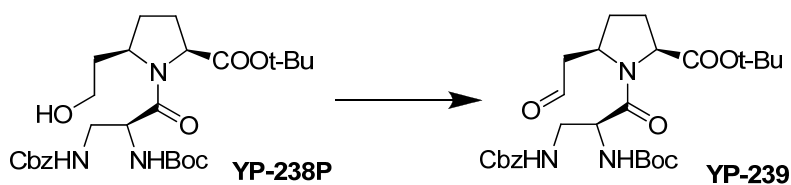
Synthesis of compound YP-239: To a solution of compound **YP-238P** (667 mg, 1.25 mmol) in dichloromethane (10 mL) was added Dess-Martin periodinane (636 mg, 1.5

mmol, 1.2 equiv.) at room temperature. The mixture was stirred for 3 h, filtered through celite and then evaporated. The residue was purified by chromatography to give **YP-239** (639 mg, 96%). $[\alpha]^{20}_{D}$ -51.6° (c = 1.67, CHCl$_3$); ^{1}HNMR shows that this compound has two rotamers with a ratio of 2:1. ^{1}HNMR (300 MHz, CDCl$_3$, TMS) δ 9.76 (s, 2/3 H), 9.71 (s, 1/3 H), 7.40-7.28 (m, 5H), 5.72-5.30 (m, 2H), 5.20-4.95 (m, 2H), 4.90-4.25 (m, 3H), 3.52-3.05 (m, 3H), 2.90-1.60 (m, 4H), 1.50-1.35 (m, 18H); HRMS: calcd m/z 556.2635 for [M+Na]$^+$; found 556.2629.
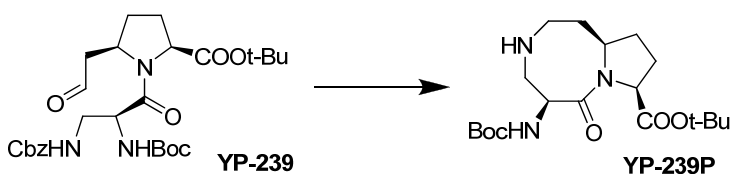
Synthesis of compound YP-239P: To a solution of compound **YP-239** (380 mg, 0.713 mmol) in methanol (20 mL) was added 10% Pd/C (0.2 g). The mixture was stirred at room temperature under H$_2$ overnight, filtered through celite and then condensed. The residue was purified by chromatography to give compound **YP-239P** (114 mg, 42%).[150] $[\alpha]^{20}_{D}$ -8.4° (c = 0.65, CHCl$_3$); ^{1}HNMR (300 MHz, CDCl$_3$, TMS) δ 5.49 (brd, J = 8.1 Hz, 1H), 4.70 (m, 1H), 4.41 (t, J = 9.3 Hz, 1H), 4.30 (m, 1H), 3.25-3.18 (m, 2H), 2.89 (m, 1H), 2.75 (dd, J = 13.5, 11.1 Hz, 1H), 2.34 (m, 1H), 2.18-1.60 (m, 6H), 1.49 (s, 9H), 1.44 (s, 9H); ^{13}CNMR(75 MHz, CDCl$_3$) δ 171.8, 170.4, 155.2, 81.7, 79.5, 60.6, 58.5, 54.9, 52.3, 46.9, 37.5, 32.1, 28.3, 28.0, 27.0; HRMS: calcd m/z 406.2318 for [M+Na]$^+$; found 406.2317.
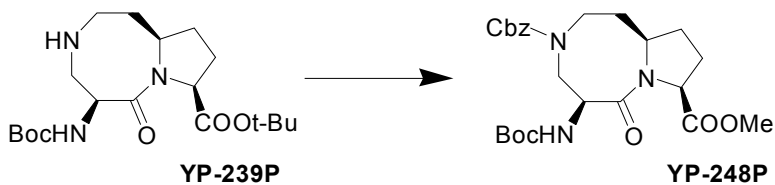
YP-239P → **YP-248P**

Synthesis of compound YP-248P: To a solution of compound **YP-239P** (1.5 g, 3.9 mmol) in 1,4-dioxane (15 ml) were added CbzCl (0.66 mL, 1.2 equiv.) and NaHCO$_3$ (820 mg, 2.5 equiv.).[155] The mixture was stirred overnight at room temperature, filtered and concentrated under vacuum. The residue was purified by chromatography to give 1.9 g of Cbz-protected compound (R_f = 0.5 when EtOAc/Hexane = 1/1). To a well-stirred solution of this Cbz-protected compound (0.9 g, 1.7 mmol) in MeOH (5 mL) at 0°C, SOCl$_2$ (1 mL, 14 mmol) was added dropwise. The mixture was stirred at room temperature for 1 h, then was quenched with saturated NaHCO$_3$ solution and the pH adjusted to 8. The aqueous layer was extracted with CH$_2$Cl$_2$, and combined organic phases were dried over Na$_2$SO$_4$, filtered, and concentrated under vacuum. The crude amine was dissolved in 1,4-dioxane (10 mL), then t-Boc$_2$O (0.44 g, 1.2 equiv.) and NaHCO$_3$ (0.35 g, 2.5 equiv.) were added. The mixture was stirred overnight at room temperature and then filtered and concentrated under vacuum. The residue was purified by chromatography to give 0.6 g of compound **YP-248P** (R_f = 0.4 when EtOAc/Hexane= 2/1) (74% over 3 steps). ^{1}H NMR shows that this compound has two rotamers with a ratio of 2:1. ^{1}H NMR (300 MHz, CDCl$_3$, TMS) δ 7.47-7.25 (m, 5H), 5.63 (brd, J=8Hz, 1H), 5.31-5.16 (m, 2H), 4.64-4.60 (m, 1H), 4.51-

4.46 (t, J=8Hz, 1H), 4.30-3.98 (m, 2H), 3.74 (brs, 3H), 3.63 (m, 1H), 3.50 (m, 1H), 3.30 (m, 1H), 2.38 (m, 1H), 2.28-1.76 (m, 5H), 1.44-1.45 (s, 9H). ESI MS: m/z 476.2 [M+H]$^+$.
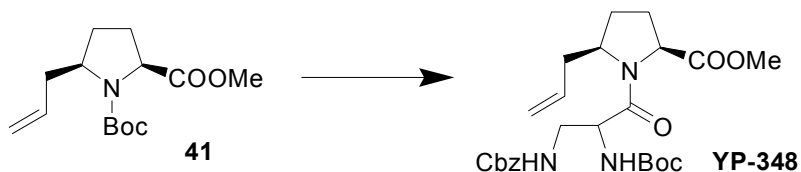
Synthesis of compound YP-348: To a solution of compound **41** (3.2 g, 12 mmol) in MeOH (20 mL) was added a solution of 4N HCl in 1,4-dioxane (6 mL, 2 equiv.).[145-148,156] The mixture was stirred overnight at room temperature, and then concentrated to yield 2.2 g of crude amine to a solution of which in DCM (20 mL) was added t-Boc-Dap(Z)-OH·DCHA (6.6 g, 1.1 equiv.), EDC (2.9 g, 1.2 equiv.), HOBt (2.0 g, 1.2 equiv.), and DIEA (5.5 mL, 2.5 equiv.). The mixture was stirred overnight at room temperature, and then concentrated and purified by chromatography to give compound **YP-348** (R$_f$= 0.3 EtOAc/Hexane= 1/1) (5.8 g, 82% over two steps). ^{1}HNMR shows that this compound has two rotamers with a ratio of 2:1. ^{1}HNMR (300 MHz, CDCl$_3$, TMS) δ 7.34-7.28 (m, 5H), 5.80-5.77 (m, 1H), 5.59 (m, 1H), 5.36-5.33 (d, J=10 Hz, 2H), 5.19-5.01 (m, 4H), 4.67-4.62 (m, 1H), 4.47-4.44 (m, 1H), 3.76-3.74 (s, 1H), 3.74-3.71 (s, 2H), 2.32-2.30 (m, 1H), 2.16-2.12 (m, 1H), 1.99-1.95 (m, 2H), 1.42 (s, 9H). ^{13}CNMR (75 MHz, CDCl$_3$) δ 172.4, 170.5, 156.5, 155.2, 136.4, 134.6, 133.8, 128.3, 127.9, 118.5, 117.1, 80.0, 66.6, 59.7, 58.2, 52.6, 43.4, 29.2, 28.1, 26.6.
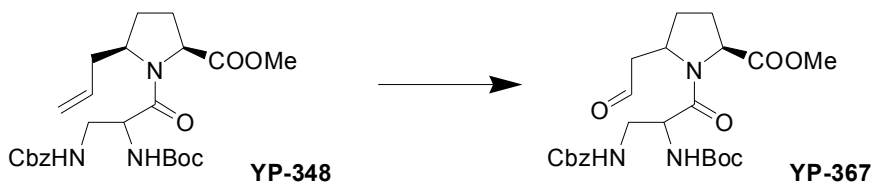
Synthesis of compound YP-367: A solution of compound **YP-348** (0.75 g, 1.5 mmol) in DCM (10 mL) was cooled to -78 °C. Ozone was passed through the solution until a blue color persisted, then air was passed through until the blue color disappeared. PPh$_3$ (0.8 g, 2 equiv.) was added and the mixture was stirred for 30 min at room temperature. The mixture was condensed and purified by chromatography to give compound **YP-367** (R$_f$= 0.3 EtOAc/Hexane= 1/1) (0.68 g, 92%). ^{1}HNMR shows that this compound has two rotamers with a ratio of 1:1. ^{1}HNMR (300 MHz, CDCl$_3$, TMS) δ 9.78-9.67 (m, 1H), 7.53-7.32 (m, 5H), 5.44 (s, 1/2 H), 5.32 (s, 1/2 H), 5.15-5.06 (m, 2H), 4.64 (m, 1H), 4.40-4.39 (m, 1H), 3.78-3.76 (s, 3/2 H), 3.76-3.74 (s, 3/2H), 3.48-3.42 (m, 3H), 2.78-2.52 (m, 1H), 2.40-2.20 (m, 1H), 2.16 (m, 2H), 2.06-1.89 (m, 1H), 1.44-1.43 (m, 9H). ^{13}CNMR (75 MHz, CDCl$_3$) δ 200.3, 199.5, 172.6, 172.2, 170.3, 156.5, 136.4, 128.4, 128.0, 66.7, 59.7, 59.1, 54.3, 52.4, 52.3, 48.4, 43.3, 29.6, 28.2, 21.0.
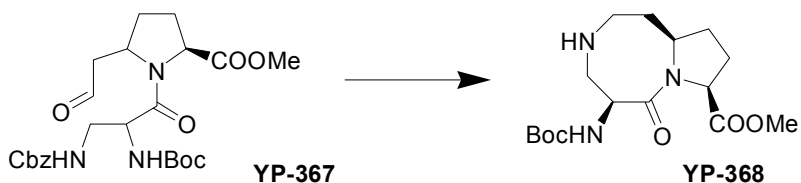
Synthesis of compound YP-368: To a solution of compound **YP-367** (0.6 g, 1.2 mmol) in MeOH (40 mL) was added 10% Pd/C (0.4 g). The mixture was stirred at room temperature under H$_2$ overnight, filtered through celite and then evaporated. The residue

48

was purified by chromatography to give compound **YP-368** (0.25 g, 41%). ^{1}HNMR (300 MHz, CDCl$_3$, TMS) δ 5.45-5.42 (d, J=8.0 Hz, 1H), 4.72-4.71 (m, 1H), 4.57-4.51 (t, J=9.1 Hz, 1H), 4.38-4.28 (m, 1H), 3.77 (s, 3H), 3.25-3.18 (m, 1H), 2.80-2.70 (m, 1H), 2.35 (m, 1H), 2.18-1.60 (m, 6H), 1.46 (s, 9H). ^{13}CNMR (75 MHz, CDCl$_3$) δ 173.4, 170.6, 155.1, 131.9, 79.6, 59.4, 58.3, 54.9, 52.4, 46.7, 37.4, 32.1, 29.6, 28.4, 26.9, 22.6.
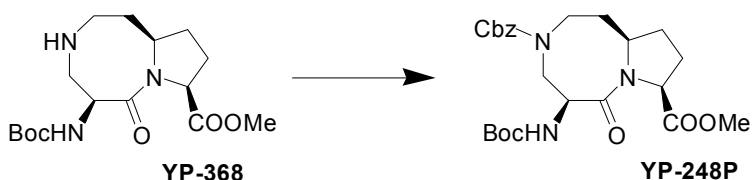
YP-368   **YP-248P**

Synthesis of compound YP-248P: To a solution of compound **YP-368** (1.6 g, 4.5 mmol) in 1,4-dioxane (20 ml) were added CbzCl (0.8 mL, 1.2 equiv.) and NaHCO$_3$ (0.9 g, 2.5 equiv.). The mixture was stirred overnight at room temperature and then filtered and concentrated under vacuum.[157,158] The residue was purified by chromatography to give compound **YP-248P** (*R$_f$*= 0.5 when EtOAc/Hexane= 1/1) (2.0 g, 92%). ^{1}H NMR shows that this compound has two rotamers with a ratio of 2:1. ^{1}H NMR (300 MHz, CDCl$_3$, TMS) δ 7.47-7.25 (m, 5H), 5.63 (brd, J=8Hz, 1H), 5.31-5.16 (m, 2H), 4.64-4.60 (m, 1H), 4.51-4.46 (t, J=8Hz, 1H), 4.30-3.98 (m, 2H), 3.74 (brs, 3H), 3.63 (m, 1H), 3.50 (m, 1H), 3.30 (m, 1H), 2.38 (m, 1H), 2.28-1.76 (m, 5H), 1.44-1.45 (s, 9H). ESI MS: m/z 476.2 [M+H][+].
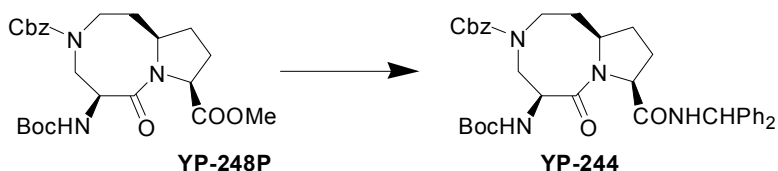
YP-248P → **YP-244**

Synthesis of compound YP-244: To a solution of compound **YP-248P** (0.3 g, 0.6 mmol) in 1,4-dioxane (5 mL) was added 2N LiOH/H_2O (0.8 mL, 2.5 equiv.). The mixture was stirred 1h at room temperature, then 1N HCl was added to adjust the pH to 3. The aqueous layer was extracted with CH_2Cl_2, and combined organic phases were dried (Na_2SO_4), filtered, and concentrated under vacuum. The crude acid was dissolved in CH_2Cl_2 (15 mL), and then NH_2CHPh_2 (0.1 mL, 1.1 equiv.), EDC (0.14 g, 1.2 equiv.), HOBt (0.1 g, 1.2 equiv.) and DIEA (diisopropylethylamine, 0.26 mL, 2.5 equiv.) were added. The mixture was stirred at overnight room temperature and then concentrated. The residue was purified by chromatography to give compound **YP-244** (R_f = 0.3 when EtOAc/Hexane= 1/1) (0.3 g, 82% over 2 steps). ^{1}HNMR (300 MHz, CDCl$_3$, TMS) δ 7.92-7.75 (m, 1H), 7.48-7.24 (m, 15H), 6.20 (m, 1H), 5.72 (m, 1H), 5.15 (brs, 2H), 4.68 (m, 1H), 4.56 (m, 1H), 4.35-4.05 (m, 2H), 3.55 (m, 1H), 2.73-2.58 (m, 2H), 2.34 (m, 1H), 2.20-1.65 (m, 5H), 1.48 (brs, 9H). ESI MS: m/z 627.3 [M+H]$^+$.
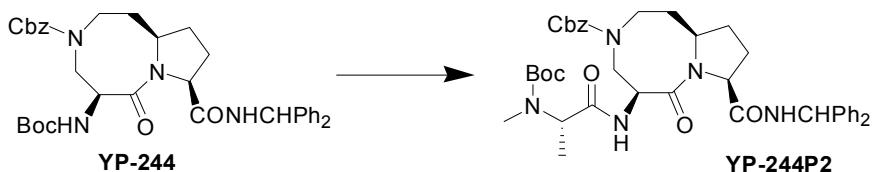
YP-244 → **YP-244P2**

Synthesis of compound YP-244P2: To a solution of compound **YP-244** (0.3 g, 0.5 mmol) in MeOH (5 mL), was added 0.5 mL of a solution of 4N HCl in 1,4-dioxane.[159,160]

The mixture was stirred overnight at room temperature and then condensed and quenched with saturated NaHCO₃ solution and adjusted to pH = 8. The aqueous layer was extracted with CH$_2$Cl$_2$, and combined organic phases were dried over Na$_2$SO$_4$, filtered, and concentrated under vacuum. The crude amine was dissolved in CH$_2$Cl$_2$ (15 mL), and then Boc-N-methyl-alanine (0.1 g, 1.1 equiv.), EDC (0.11 g, 1.2 equiv.), HOBt (0.08 g, 1.2 equiv.) and DIEA (0.2 mL, 2.5 equiv.) were added. The mixture was stirred overnight at room temperature and then condensed and purified by chromatography to give compound **YP-244P2** (R_f= 0.3 when EtOAc/Hexane= 3/1) (0.28 g, 83% over two steps). ^{1}H NMR shows that this compound has two rotamers with a ratio of 1:1. ^{1}H NMR (300 MHz, CDCl$_3$, TMS) δ 7.83-4.69 (m, 1H), 7.47-7.45 (m, 1H), 7.36-7.26 (m, 15H), 6.24-6.18 (t, J= 8.2 Hz, 1H), 5.15 (s, 2H), 4.89-4.79 (m, 1H), 4.70-4.62 (q, J=6.9 Hz, 1H), 4.23-4.07 (m, 2H), 3.60-3.47 (1H), 2.82 (s, 3/2 H), 2.79 (s, 3/2 H), 2.62-2.59 (m, 2H), 2.48-2.30 (m, 1H), 2.13-2.03 (m, 2H), 1.86-1.79 (m, 2H), 1.51 (s, 9/2 H), 1.49 (s, 9/2 H), 1.38-1.35 (d, J= 7.0 Hz, 3H).
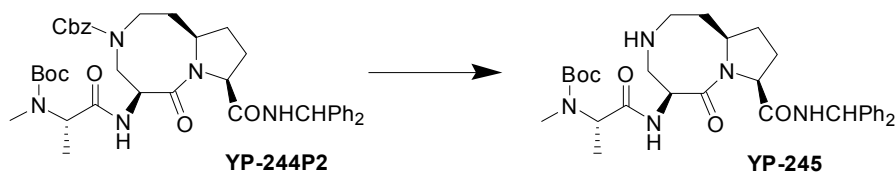
Synthesis of compound YP-245: To a solution of compound **YP-244P2** (0.28 g, 0.4 mmol) in MeOH (20 mL) was added 10% Pd/C (0.1 g). The mixture was stirred at room temperature under H$_2$ overnight.[161] The catalyst was removed and the filtrate was evaporated. The crude product was purified by chromatography to afford compound **YP-**

245 (R$_f$ = 0.3 when MeOH/EtOAc = 1/9) (0.2 g, 92%). ^{1}HNMR (300 MHz, CDCl$_3$, TMS) δ 7.32-7.18 (m, 11H), 6.90 (brs, 1H), 6.22 (d, J = 7.3 Hz, 1H), 5.05 (m, 1H), 4.70 (t, J = 8.5 Hz, 1H), 4.50 (brm, 1H), 4.25 (m, 1H), 2.99 (m, 1H), 2.83 (m, 1H), 2.81 (s, 3H), 2.65 (m, 1H), 2.45 (m, 1H), 2.28 (t, J = 11 Hz, 1H), 2.18-2.05 (m, 2H), 1.80-1.65 (m, 2H), 1.53 (s, 9H), 1.45 (m, 1H), 1.30 (d, J = 7.1 Hz, 3H). ESI MS: m/z 600.4 [M+Na]$^+$
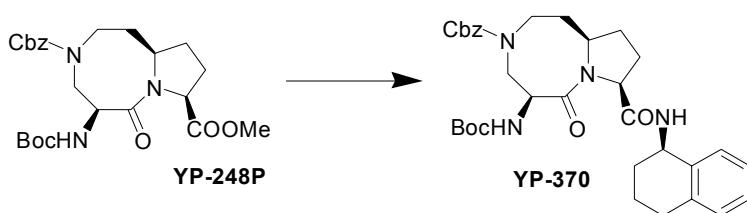
Synthesis of compound YP-370: To a solution of compound **YP-248P** (0.3 g, 0.6 mmol) in 1,4-dioxane (5 mL) was added 2N LiOH/H$_2$O (0.8 mL, 2.5 equiv.). The mixture was stirred 1h at room temperature, then 1N HCl was added to adjust pH to 3. The aqueous layer was extracted with CH$_2$Cl$_2$, and combined organic phases were dried (Na$_2$SO$_4$), filtered, and concentrated under vacuum. The crude acid was dissolved in CH$_2$Cl$_2$ (15 mL), and then (R)-1,2,3,4-tetrahydro1-naphthylamine (0.1 g, 1.1 equiv.), EDC (0.14 g, 1.2 equiv.), HOBt (0.1 g, 1.2 equiv.) and DIEA (diisopropylethyl amine, 0.26 mL, 2.5 equiv.) were added. The mixture was stirred at overnight room temperature and then condensed. The residue was purified by chromatography to give compound **YP-370** (R$_f$ = 0.3 when CH$_3$COOEt/Hexane= 1/1) (0.28 g, 80% over 2 steps). ^{1}H NMR (300 MHz, CDCl$_3$, TMS) δ 7.60-7.05 (m, 9H), 5.78-5.50 (m, 1H), 5.20-5.11 (m, 2H), 4.65-4.30 (m,

2H), 4.28-4.22 (m, 1H), 3.60-3.48 (m, 1H), 3.42-3.38 (m, 1H), 2.93-2.68 (m, 2H), 2.58-2.40 (m, 1H), 2.28-1.98 (m, 4H), 1.98-1.70 (m, 6H), 1.44 (s, 9H).

YP-370 → YP-372
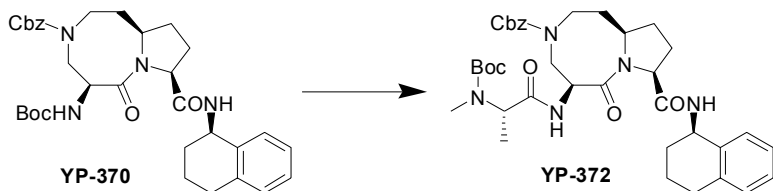
Synthesis of compound YP-372: To a solution of compound **YP-370** (0.28 g, 0.48 mmol) in MeOH (5 mL), was added a solution of 4N HCl in 1,4-dioxane (0.5 mL). The mixture was stirred overnight at room temperature and then condensed and quenched with saturated NaHCO$_3$ solution and adjusted to pH = 8. The aqueous layer was extracted with CH$_2$Cl$_2$, and combined organic phases were dried over Na$_2$SO$_4$, filtered, and concentrated under vacuum. The crude amine was dissolved in CH$_2$Cl$_2$ (15 mL), and then t-Boc-N-methylalanine (0.1 g, 1.1 equiv.), EDC (0.11 g, 1.2 equiv.), HOBt (0.08 g, 1.2 equiv.) and DIEA (0.2 mL, 2.5 equiv.) were added. The mixture was stirred overnight at room temperature and then condensed and purified by chromatography to give compound **YP-372** (R$_f$ = 0.3 when EtOAc/Hexane= 3/1) (0.25 g, 80% over two steps). ^{1}H NMR shows that this compound has two rotamers with a ratio of 1:1. ^{1}H NMR (300 MHz, CDCl$_3$, TMS) δ 7.45 (m, 1H), 7.36-7.10 (m, 9H), 6.72-6.58 (m, 1H), 5.21-5.14 (t, J= 9.9 Hz, 2H), 4.82 (m, 1H), 4.48-4.41 (m, 1H), 4.14-4.09 (m, 2H), 3.82-3.60 (m, 1H), 3.20-2.90 (m, 2H), 2.79 (s, 3/2 H), 2.77 (s, 3/2 H), 2.50-2.36 (m, 1H), 2.18-2.01 (m, 4H), 1.89-1.82 (m,

6H), 1.49 (s, 9/2 H), 1.46 (s, 9/2 H), 1.37-1.33 (m, 3H). HRMS: calcd m/z 698.3530 for [M+Na]$^+$; found 698.3541.


YP-372　　　　　　**YP-373**
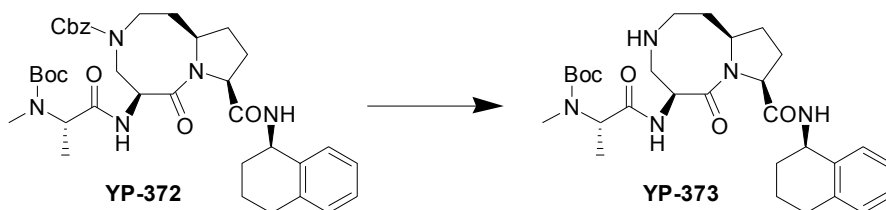
Synthesis of compound YP-373: To a solution of compound **YP-372** (0.25 g, 0.37 mmol) in MeOH (20 mL) was added 10% Pd/C (0.1 g).[162,163] The mixture was stirred at room temperature under H$_2$ overnight, then the catalyst was removed and the filtrate was evaporated to dryness. The crude product was purified by chromatography to afford compound **YP-373** (R$_f$ = 0.3 when MeOH/EtOAc = 1/4) (0.18 g, 91%). ^{1}H NMR (300 MHz, CDCl$_3$, TMS) δ 8.77-8.75 (d, J= 7.1 Hz, 1H), 7.21-7.05 (m, 4H), 6.90-6.73 (br, 1H), 5.06-4.98 (m, 2H), 4.65-4.59 (t, J= 8.1 Hz, 1H), 4.23-4.17 (m, 1H), 3.02-3.01 (m, 1H), 2.76 (s, 3H), 2.70-2.68 (m, 2H), 2.60-2.48 (m, 2H), 2.38 (m, 1H), 2.12-2.03 (m, 4H), 1.82-1.72 (m, 6H), 1.47 (s, 9H), 1.32-1.29 (d, J= 7.1 Hz, 3H). ^{13}C NMR (75 MHz, CDCl$_3$) δ 170.6, 168.4, 137.6, 136.4, 129.3, 128.9, 127.2, 125.8, 60.3, 58.2 54.4, 49.3, 47.4, 46.8, 34.9, 31.8, 29.0, 28.2, 27.6, 18.7, 14.1; HRMS: calcd m/z 564.3162 for [M+Na]$^+$; found 564.3163.
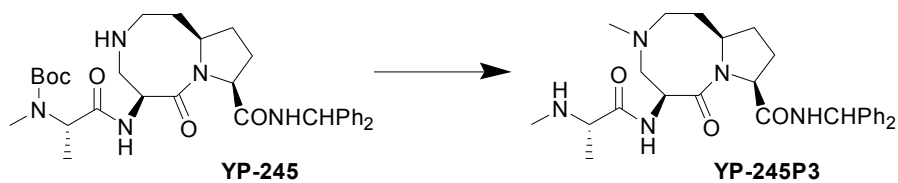
YP-245 → YP-245P3

Synthesis of compound YP-245P3: To a solution of compound **YP-245** (40 mg, 0.07 mmol) in MeOH (5 mL) was added a solution of HCHO 37% w.t. in H_2O (0.025 mL, 5 equiv.). The mixture was stirred for 30 min at room temperature, and then $NaCNBH_3$ (26 mg, 6 equiv.) and a catalytic amount of acetic acid were added. The mixture was stirred for 1 h at room temperature, and then quenched with 10 mL of water. The aqueous layer was extracted with CH_2Cl_2, and combined organic phases were dried over Na_2SO_4, filtered, and concentrated under vacuum. The crude amine was dissolved in MeOH (5 mL), and then a solution of 4N HCl in 1,4-dioxane (0.2 mL) was added. The mixture was stirred overnight at room temperature, concentrated and purified by chromatography on a C18 reverse phase semi-preparative HPLC column and then lyophilized to give compound **YP-245P3** (24 mg, 71% over 2 steps). The gradient ran from 90% of solvent A and 10% solvent B to 60% solvent A and 40% solvent B in 30 min. The purity of YP-245P3 was confirmed by analytical HPLC to be over 98%. ^{1}HNMR (300 MHz, D_2O) δ 7.42-7.25 (m, 10H), 6.07 (d, J = 6.8 Hz, 1H), 5.35 (m, 1H), 4.70 (m, 1H), 4.61 (m, 1H), 3.99 (dd, J = 14.0, 7.0 Hz, 1H), 3.86 (m, 1H), 3.65 (m, 1H), 3.56 (m, 1H), 3.30 (m, 1H), 3.00 (s, 3H), 2.68 (s, 3H), 2.49 (m, 1H), 2.32-1.82 (m, 5H), 1.51 (d, J = 7.1 Hz, 3H). HRMS: calcd. m/z for $[M+H]^+$ 492.2975; found 492.2971. Anal. ($C_{28}H_{37}N_5O_3 \cdot 3.1CF_3COOH$): C, H, N.
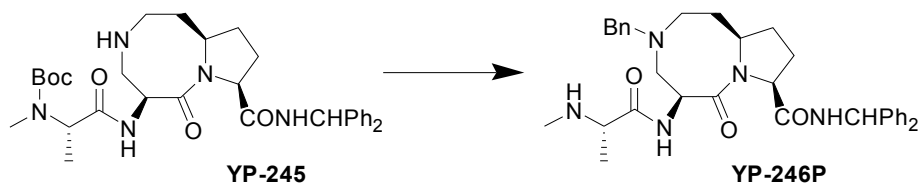
YP-245   →   **YP-246P**

Synthesis of compound YP-246P: To a solution of compound **YP-245** (40 mg, 0.069 mmol) in 1,4-dioxane (10 mL) were added BnBr (0.01 mL, 1.2 equiv.) and NaHCO$_3$ (15 mg, 2.5 equiv.).[164,165] The mixture was stirred overnight at room temperature, and then filtered, concentrated, and purified by chromatography to afford the desired amine (R$_f$ = 0.3 when EtOAc/Hexane = 3/1). This amine was dissolved in MeOH (5 mL) and then a solution of 4N HCl in 1,4-dioxane (0.2 mL) was added. The mixture was stirred overnight at room temperature, evaporated and purified by chromatography on a C18 reverse phase semi-preparative HPLC column then lyophilized to give compound **YP-246P** (30 mg, 77% over 2 steps). The gradient ran from 90% of solvent A and 10% solvent B to 60% solvent A and 40% solvent B in 30 min. The purity was confirmed by analytical HPLC to be over 98%. ^{1}HNMR (300 MHz, D$_2$O) δ 7.34 (m, 2H), 7.28-7.02 (m, 13H), 6.05 (d, J = 6.9 Hz, 1H), 5.38 (m, 1H), 4.72 (m, 1H), 4.52 (m, 1H), 4.25 (ABq, J = 8.4 Hz, 2H), 3.97 (dd, J = 13.5, 6.8 Hz, 1H), 3.82-3.56 (m, 2H), 3.49 (m, 1H), 3.18 (m, 1H), 2.67 (s, 3H), 2.35 (m, 1H), 2.08 (m, 1H), 1.75-1.52 (m, 4H), 1.47 (d, J = 7.0 Hz, 3H). HRMS: calcd. m/z for [M+H]$^+$ 568.3288; found 568.3284. Anal. (C$_{34}$H$_{41}$N$_5$O$_3$· 2.5CF$_3$COOH): C, H, N.
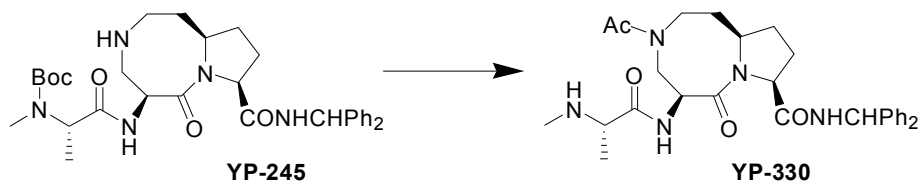
Synthesis of compound YP-330: To a solution of compound **YP-245** (20 mg, 0.035 mmol) in CH_2Cl_2 (10 mL) were added Ac_2O (0.004 mL, 1.2 equiv.) and DIEA (0.015 mL, 2.5 equiv.). The mixture was stirred 4h at room temperature, and then concentrated and purified by chromatography to give the desired amide (R_f = 0.3 in EtOAc). The desired amide was dissolved in MeOH (5 mL), and then a solution of 4N HCl in 1,4-dioxane (0.2 mL) was added. The mixture was stirred overnight at room temperature, condensed and purified by chromatography on a C18 reverse phase semi-preparative HPLC column and then lyophilized to give compound **YP-330** (15 mg, 85% over 2 steps). The gradient ran from 80% of solvent A and 20% solvent B to 50% solvent A and 50% solvent B in 30 min. The purity was confirmed by analytical HPLC to be over 98%. ^{1}HNMR (300 MHz, D_2O) δ 7.38-7.19 (m, 10H), 5.95 (brs, 1H), 4.96 (m, 1H), 4.40 (m, 1H), 4.25 (m, 1H), 3.94 (m, 1H), 3.66 (m, 1H), 3.60-3.35 (m, 3H), 2.63 (s, 3H), 2.25 (m, 1H), 2.15-1.65 (m, 8H), 1.47 (d, J = 7.1Hz, 3H). ^{13}C NMR (75 MHz, D_2O) δ 175.3, 173.3, 172.9, 170.2, 141.2, 129.2, 128.1, 127.7, 62.3, 62.1 58.5, 57.8, 57.3, 52.6, 51.8, 32.2, 31.3, 27.5 21.5, 20.7, 15.5. HRMS: calcd. m/z for $[M+H]^+$ 520.2924; found 520.2924. Anal. ($C_{29}H_{37}N_5O_4\cdot$ 1.0HCl·1.5CF$_3$COOH): C, H, N.

YP-245 → YP-337
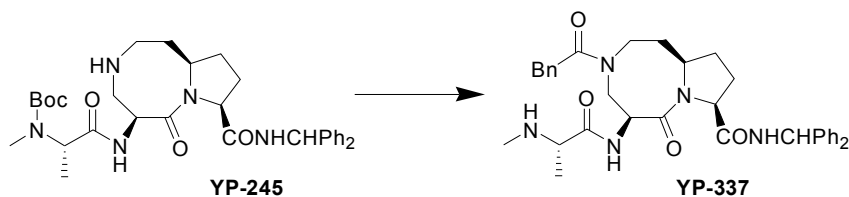
Synthesis of compound YP-337: To a solution of compound **YP-245** (20 mg, 0.035 mmol) in CH_2Cl_2 (10 mL) was added BnCOOH (6 mg, 1.2 equiv.), EDC (9 mg, 1.4 equiv.), HOBt (6.5 mg, 1.4 equiv.) and DIEA (0.015 mL, 2.5 equiv.). The mixture was stirred overnight at room temperature, and then condensed and purified by chromatography to give the desired amide (R_f = 0.3 when EtOAc/Hexane= 4/1). The desired amide was dissolved in MeOH (5 mL), and a solution of 4N HCl in 1,4-dioxane (0.2 mL) was added. The mixture was stirred overnight at room temperature, condensed and purified by chromatography on a C18 reverse phase semi-preparative HPLC column and then lyophilized to give compound **YP-337** (18 mg, 87% over 2 steps). The gradient ran from 80% of solvent A and 20% solvent B to 50% solvent A and 50% solvent B in 30 min. The purity was confirmed by analytical HPLC to be over 98%. ^{1}HNMR (300 MHz, D_2O) δ 7.27-6.90 (m, 15H), 5.95 (brs, 1H), 4.65 (m, 1H), 4.38 (m, 1H), 4.06 (m, 1H), 3.85 (m, 1H), 3.78-3.30 (m, 6H), 2.55 (brs, 3H), 2.08 (m, 1H), 1.98-1.30 (m, 8H). ^{13}C NMR (75 MHz, CD_3OD) δ 174.6, 174.0, 169.6, 169.4, 143.1, 136.4, 130.3, 129.5, 128.6, 128.2, 127.8, 62.7, 58.3, 54.2, 41.6, 33.3, 31.9, 28.2, 16.3. HRMS: calcd. m/z for $[M+H]^+$ 596.3237, found 596.3250. Anal. ($C_{35}H_{41}N_5O_4 \cdot 1.0HCl \cdot 1.2CF_3COOH$): C, H, N.

YP-245 → **YP-350**
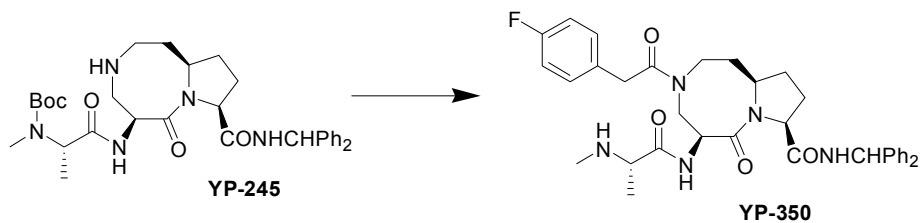
Synthesis of compound YP-350: To a solution of compound **YP-245** (20 mg, 0.035 mmol) in CH_2Cl_2 (10 mL) were added 4-fluorophenylacetic acid (6.5 mg, 1.2 equiv.), EDC (9 mg, 1.4 equiv.), HOBt (6.5 mg, 1.4 equiv.) and DIEA (0.015 mL, 2.5 equiv.). The mixture was stirred overnight at room temperature, and then condensed and purified by chromatography to give the desired amide (R_f = 0.3 when EtOAc/Hexane= 3/1). This product was dissolved in MeOH (5 mL), and then a solution of 4N HCl in 1,4-dioxane (0.2 mL) was added. The mixture was stirred at overnight room temperature, condensed and purified by chromatography on a C18 reverse phase semi-preparative HPLC column and then lyophilized to give compound **YP-350** (18 mg, 84% over 2 steps). The gradient ran from 80% of solvent A and 20% solvent B to 50% solvent A and 50% solvent B in 30 min. The purity was confirmed by analytical HPLC to be over 98%. ^{1}H NMR (300 MHz, CD₃OD, TMS) δ 8.94-8.92 (d, J = 7.9 Hz, 1H), 7.34-7.26 (m, 12H), 7.04-6.98 (m, 2H), 6.18-6.15 (d, J = 7.9 Hz, 1H), 4.60-4.57 (m, 1H), 4.31 (br, 1H), 4.02-3.76 (m, 4H), 3.50 (m, 1H), 2.68 (s, 3H), 2.34 (m, 1H), 2.11-1.82 (m, 5H), 1.55-1.53 (d, J = 7.0 Hz, 3H). ^{13}CNMR (75 MHz, CD₃OD) δ 173.2, 170.2, 169.7, 164.8, 161.5, 143.1, 132.5, 131.9, 129.6, 128.6, 128.1, 116.2, 62.7, 58.4, 53.9, 40.5, 33.3, 32.3, 31.8, 28.3, 16.3. HRMS: calcd. m/z for [M+Na][+] 636.2962; found 636.2974.

Synthesis of compound YP-356: To a solution of compound **YP-245** (20 mg, 0.035 mmol) in CH₂Cl₂ (10 mL) was added 2,4-difluorophenylacetic acid (7.2 mg, 1.2 equiv.), EDC (9 mg, 1.4 equiv.), HOBt (6.5 mg, 1.4 equiv.) and DIEA (0.015 mL, 2.5 equiv.). The mixture was stirred overnight at room temperature, and then evaporated and purified by chromatography to give the desired amide (R_f = 0.3 when EtOAc/Hexane= 2/1). The desired amide was dissolved in MeOH (5 mL), and a solution of 4N HCl in 1,4-dioxane (0.2 mL) was added. The mixture was stirred overnight at room temperature, condensed and purified by chromatography on a C18 reverse phase semi-preparative HPLC column and then lyophilized to give compound **YP-356** (18.4 mg, 83% over 2 steps). The gradient ran from 80% of solvent A and 20% solvent B to 50% solvent A and 50% solvent B in 30 min. The purity was confirmed by analytical HPLC to be over 98%. ^{1}H NMR (300 MHz, CD₃OD, TMS) δ 8.93-8.91 (d, *J* = 8.0 Hz, 1H), 7.38-7.26 (m, 11H), 6.90-6.86 (m, 2H), 6.18-6.16 (d, *J* = 7.9 Hz, 1H), 5.10-5.00 (m, 1H), 4.61-4.58 (m, 1H), 4.40-4.28 (m, 1H), 4.15-3.91 (m, 4H), 3.36 (m, 2H), 2.69 (s, 2H), 2.67 (s, 1H), 2.42-2.28 (m, 1H), 2.02-1.95 (m, 5H), 1.55-1.53 (d, *J* = 7.0 Hz, 3H). ^{13}CNMR (75 MHz, CD₃OD) δ 173.2, 172.4, 170.2, 169.7, 169.4, 143.2, 134.1, 129.6, 128.4, 128.1, 120.1, 112.0, 104.1, 62.7, 58.4, 53.9, 34.2, 33.3, 32.3, 31.7, 28.3, 16.2. HRMS: calcd. m/z for [M+Na]⁺ 654.2868; found 654.2866.
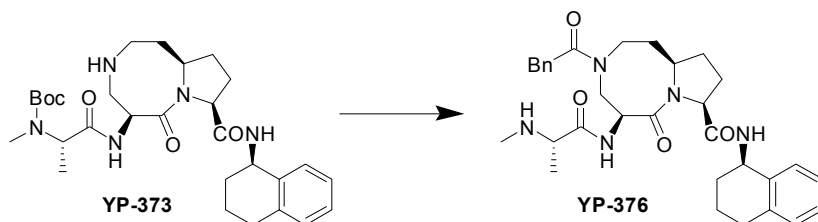
Synthesis of compound YP-376: To a solution of compound **YP-373** (80 mg, 0.15 mmol) in CH$_2$Cl$_2$ (20 mL) were added phenylacetic acid (24 mg, 1.2 equiv.), EDC (40 mg, 1.4 equiv.), HOBt (28 mg, 1.4 equiv.) and DIEA (0.06 mL, 2.5 equiv.). The mixture was stirred overnight at room temperature, and then condensed and purified by chromatography to give the desired amide (R$_f$ = 0.3 in EtOAc). The desired amide was dissolved in MeOH (10 mL), and then a solution of 4N HCl in 1,4-dioxane (0.3 mL) was added. The mixture was stirred overnight at room temperature, concentrated and purified by chromatography on a C18 reverse phase semi-preparative HPLC column and then lyophilized to give compound **YP-376** (70 mg, 85% over 2 steps). The gradient ran from 80% of solvent A and 20% solvent B to 50% solvent A and 50% solvent B in 30 min. The purity was confirmed by analytical HPLC to be over 98%. ^{1}H NMR (300 MHz, CD$_3$OD, TMS) δ 8.50-8.43 (m, 1H), 7.46-7.44 (m, 1H), 7.32-7.31 (m, 4H), 7.26-7.24 (m, 1H), 7.15-7.11 (m, 3H), 5.09 (m, 2H), 4.43 (m, 1H), 4.20(m, 1H), 4.01-3.92 (m, 4H), 3.58-3.42 (m, 1H), 2.83-2.81 (m, 2H), 2.70 (s, 1H), 2.68 (s, 2H), 2.38-2.25 (m, 1H), 2.09-1.82 (m, 8H), 1.27-1.53 (d, J = 7.0 Hz, 3H). ^{13}C NMR (75 MHz, CD$_3$OD) δ 174.1, 173.6, 169.6, 169.3, 138.5, 137.9, 136.5, 130.2, 129.8, 128.0, 127.0, 62.9, 58.3, 54.4, 41.6, 32.1,

31.9, 31.4, 30.2, 28.4, 21.7, 16.4. HRMS: calcd. m/z for [M+Na]$^+$ 582.3056; found 582.3080.
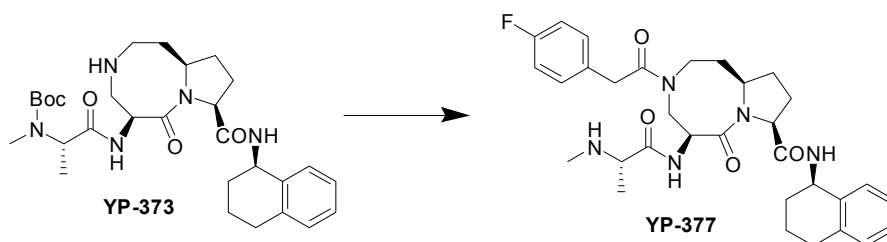
Synthesis of compound YP-377: To a solution of compound **YP-373** (80 mg, 0.15 mmol) in CH$_2$Cl$_2$ (20 mL) were added 4-fluorophenylacetic acid (28 mg, 1.2 equiv.), EDC (40 mg, 1.4 equiv.), HOBt (28 mg, 1.4 equiv.) and DIEA (0.06 mL, 2.5 equiv.). The mixture was stirred overnight at room temperature, and then concentrated and purified by chromatography to give the desired amide (R_f= 0.3 in EtOAc). The desired amide was dissolved in MeOH (10 mL), and a solution of 4N HCl in 1,4-dioxane (0.3 mL) was added. The mixture was stirred overnight at room temperature, concentrated and purified by chromatography on a C18 reverse phase semi-preparative HPLC column and then lyophilized to give compound **YP-377** (73 mg, 84% over 2 steps). Gradient ran from 80% of solvent A and 20% solvent B to 50% solvent A and 50% solvent B in 30 min. The purity was confirmed by analytical HPLC to be over 98%. ^{1}H NMR (300 MHz, CD$_3$OD, TMS) δ 8.50-8.40 (m, 1H), 7.47-7.44 (m, 1H), 7.36-7.31 (m, 2H), 7.15-7.01 (m, 5H), 5.09 (m, 2H), 4.43 (m, 1H), 4.38-4.28 (m, 1H), 4.12 (m, 1H), 4.02-3.93 (m, 4H), 2.83-2.81 (m, 2H), 2.70 (s, 3H), 2.38-2.28 (m, 1H), 2.12-1.82 (m, 8H), 1.56-1.53 (d, J = 7.0 Hz, 3H). ^{13}CNMR (75 MHz, CD$_3$OD) δ 173.8, 173.5, 169.7, 169.3, 138.5, 132.5, 131.8,

129.9, 126.9, 116.3, 62.9, 58.3, 57.8, 54.1, 40.6, 33.4, 32.2, 31.7, 30.2, 28.4, 21.7, 16.3.

HRMS: calcd. m/z for $[M+H]^+$ 578.3143; found 578.3147.
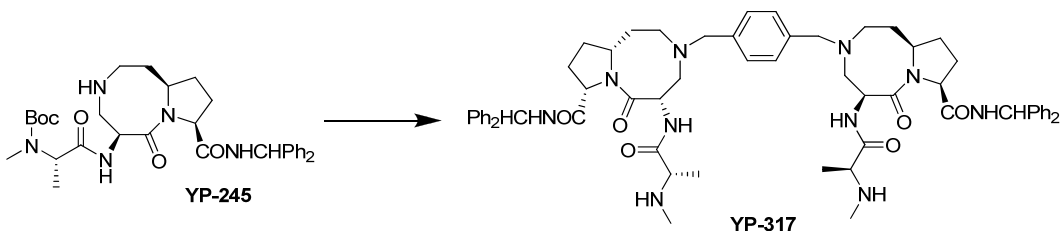
YP-245

YP-317

Synthesis of compound YP-317: To a solution of compound **YP-245P** (20 mg, 0.035 mmol) in 1,4-dioxane (10 mL) were added p-xylylene dibromide (10 mg, 1.1 equiv.) and NaHCO$_3$ (7 mg, 1.2 equiv.). The mixture was stirred overnight at room temperature, and then . **YP-245P** (20 mg, 0.035 mmol, 1 equiv.) and NaHCO$_3$ (7 mg, 1.2 equiv.) were added. The mixture was stirred overnight at room temperature, and then filtered, condensed, and purified by chromatography to afford the desired amine (R$_f$ = 0.3 when EtOAc/MeOH= 9/1). This amine was dissolved in MeOH (5 mL) and a solution of 4N HCl in 1,4-dioxane (0.2 mL) was added. The mixture was stirred overnight at room temperature, concentrated and purified by chromatography on a C18 reverse phase semi-preparative HPLC column and then lyophilized to give compound **YP-317** (24 mg, 54% over 2 steps). The gradient ran from 90% of solvent A and 10% solvent B to 60% solvent A and 40% solvent B in 30 min. The purity was confirmed by analytical HPLC to be over 98%. ^{1}H NMR (300 MHz, D$_2$O, TMS) δ 9.26-9.23 (d, J = 7.6 Hz, 1H), 7.22-6.09 (m, 12H), 6.05-6.02 (d, J = 7.2 Hz, 1H), 5.36-5.30 (m, 1H), 4.52 (m, 1H), 3.86-3.78 (m, 2H), 3.58-3.53 (m, 2H), 2.99 (t, J = 12 Hz, 1H), 2.56 (s, 3H), 2.32 (m, 1H), 2.11-2.00 (m, 1H),

1.75-1.67 (m, 4H), 1.37-1.35 (d, J = 7.1 Hz, 3H). ^{13}CNMR (75 MHz, D$_2$O) δ 173.9, 170.1, 167.9, 140.7, 132.3, 130.5, 128.4, 114.7, 62.9, 61.0, 59.0, 58.2, 57.1, 56.4, 55.2, 54.1, 47.9, 31.6, 31.2, 27.0, 15.4. HRMS: calcd. m/z for [M+H]$^+$ 1057.6028; found 1057.6057.
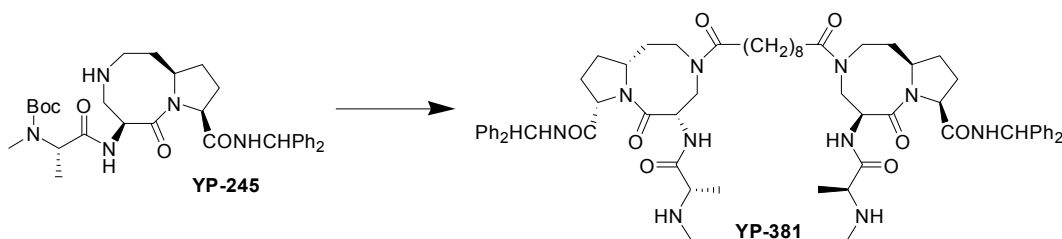
Synthesis of compound YP-381: To a solution of compound **YP-245** (20 mg, 0.035 mmol) in CH$_2$Cl$_2$ (10 mL) was added 1,8-octanedicarboxylic acid (4 mg, 0.55 equiv.), EDC (9 mg, 1.4 equiv.), HOBt (6.5 mg, 1.4 equiv.) and DIEA (0.015 mL, 2.5 equiv.). The mixture was stirred overnight at room temperature, and then condensed and purified by chromatography to give the desired amide (R$_f$ = 0.3 with EtOAc). The desired amide was dissolved in MeOH (5 mL), and then a solution of 4N HCl in 1,4-dioxane (0.2 mL) was added. The mixture was stirred overnight at room temperature, concentrated and purified by chromatography on a C18 reverse phase semi-preparative HPLC column and then lyophilized to give compound **YP-381** (14 mg, 72% over 2 steps). The gradient ran from 80% of solvent A and 20% solvent B to 50% solvent A and 50% solvent B in 30 min. The purity was confirmed by analytical HPLC to be over 98%. ^{1}H NMR (300 MHz, CD$_3$OD, TMS) δ 8.94-8.91 (d, J = 7.9 Hz, 1H), 7.37- 7.24 (m, 10H), 6.17-6.14 (d, J = 8.2 Hz, 1H), 4.58-4.55 (m, 1H), 4.24 (br, 1H), 3.99-3.90 (m, 2H), 3.50-3.38 (m, 1H), 2.70 (s, 3H), 2.65-2.40 (m, 2H), 2.31 (m, 1H), 2.09-1.78 (m, 6H), 1.61 (m, 2H), 1.56-1.53 (d, J =

7.0 Hz, 3H), 1.32 (s, 4H). ^{13}CNMR (75 MHz, CD$_3$OD) δ 176.5, 175.9, 173.2, 169.6, 143.0, 129.6, 128.8, 128.2, 62.7, 58.2, 53.7, 34.4, 33.4, 32.3, 31.8, 30.3, 28.3, 26.1, 16.2. HRMS: calcd. m/z for [M+Na]$^+$ 1143.6371; found 1143.6387. Anal. (C$_{64}$H$_{84}$N$_{10}$O$_8$·2HCl· 2CF$_3$COOH·3.5H$_2$O): C, H, N.

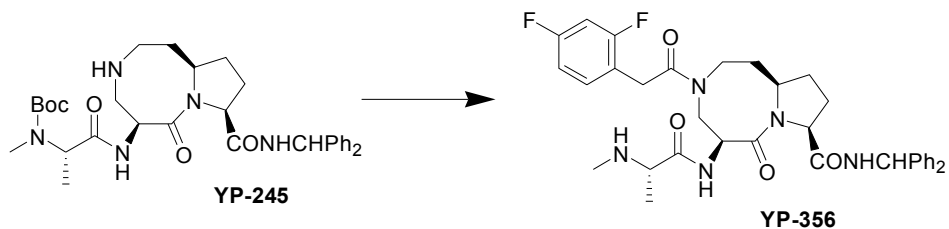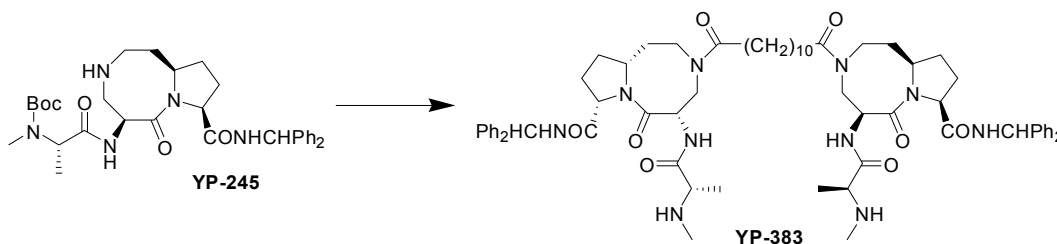**Synthesis of compound YP-383:** To a solution of compound **YP-245** (20 mg, 0.035 mmol) in CH$_2$Cl$_2$ (10 mL) were added 1,12-dodecanedioic acid (4.4 mg, 0.55 equiv.), EDC (9 mg, 1.4 equiv.), HOBt (6.5 mg, 1.4 equiv.) and DIEA (0.015 mL, 2.5 equiv.). The mixture was stirred overnight at room temperature, then condensed and purified by chromatography to give the desired amide (R$_f$ = 0.3 with EtOAc). The desired amide was dissolved in MeOH (5 mL), and then a solution of 4N HCl in 1,4-dioxane (0.2 mL) was added. The mixture was stirred overnight at room temperature, concentrated and purified by chromatography on a C18 reverse phase semi-preparative HPLC column and then lyophilized to give compound **YP-383** (14 mg, 70% over 2 steps). The gradient ran from 80% of solvent A and 20% solvent B to 50% solvent A and 50% solvent B in 30 min. The purity was confirmed by analytical HPLC to be over 98%. ^{1}H NMR (300 MHz, CD$_3$OD, TMS) δ 7.35-7.27 (m, 10H), 6.16 (s, 1H), 4.59-4.52 (m, 1H), 4.24 (br, 1H), 4.02-3.99 (m, 1H), 3.97-3.92 (m, 1H), 3.90-3.87 (m, 1H), 3.58-3.48 (m, 2H), 2.70 (s, 3H),

2.56-2.34 (m, 2H), 2.34-2.32 (m, 1H), 2.06-1.19 (m, 6H), 1.56-1.53 (d, J = 7.0 Hz, 3H), 1.30 (s, 6H). ^{13}CNMR (75 MHz, CD$_3$OD) δ 176.5, 175.9, 173.2, 169.6, 143.0, 129.6, 128.8, 128.2, 62.7, 58.2, 53.7, 34.4, 33.4, 31.7, 30.6, 30.4, 28.3, 26.3, 16.1. HRMS: calcd. m/z for [M+Na]$^+$ 1171.6684; found 1171.6680.
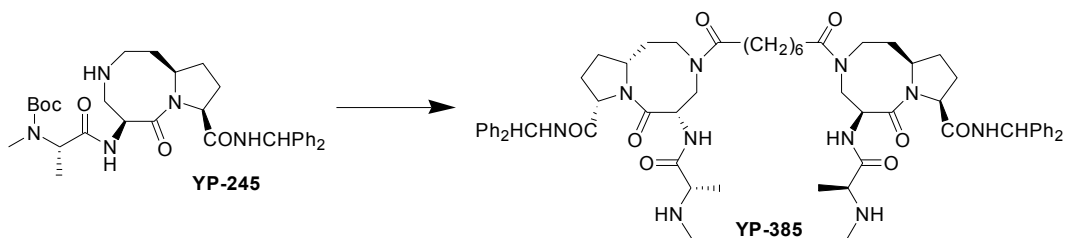
Synthesis of compound YP-385: To a solution of compound **YP-245** (20 mg, 0.035 mmol) in CH$_2$Cl$_2$ (10 mL) was added 1,6-hexanedicarboxylic acid (3.4 mg, 0.55 equiv.), EDC (9 mg, 1.4 equiv.), HOBt (6.5 mg, 1.4 equiv.) and DIEA (0.015 mL, 2.5 equiv.). The mixture was stirred overnight at room temperature, and then condensed and purified by chromatography to give the desired amide (R$_f$ = 0.3 EtOAc/MeOH= 99/1). The desired amide was dissolved in MeOH (5 mL), and a solution of 4N HCl in 1,4-dioxane (0.2 mL) was added. The mixture was stirred overnight at room temperature, concentrated and purified by chromatography on a C18 reverse phase semi-preparative HPLC column and then lyophilized to give compound **YP-385** (14 mg, 76% over 2 steps). The gradient ran from 80% of solvent A and 20% solvent B to 50% solvent A and 50% solvent B in 30 min. The purity was confirmed by analytical HPLC to be over 98%. ^{1}H NMR (300 MHz, CD$_3$OD, TMS) δ 8.95-8.93 (d, J = 8.1 Hz, 1H), 7.37-7.24 (m, 10H), 6.17-6.14 (d, J = 8.0 Hz, 1H), 4.58-4.56 (m, 1H), 4.24 (br, 1H), 3.99-3.92 (m, 2H), 3.82-

3.70 (m, 1H), 2.70 (s, 3H), 2.62-2.40 (m, 2H), 2.33 (m, 1H), 2.04-1.75 (m, 6H), 1.60-1.56 (m, 2H), 1.55-1.52 (d, J = 7.0 Hz, 3H), 1.34-1.30 (m, 2H). ^{13}CNMR (75 MHz, CD$_3$OD) δ 176.5, 175.8, 173.3, 169.7, 143.0, 129.6, 128.8, 128.2, 62.7, 58.2, 53.7, 34.5, 33.4, 31.7, 30.2, 28.3, 26.2, 16.1. HRMS: calcd. m/z for [M+H]$^+$ 1093.6239; found 1093.6252. Anal. (C$_{62}$H$_{80}$N$_{10}$O$_8$·2HCl·2CF$_3$COOH·2H$_2$O): C, H, N.

CHAPTER 3

BIOLOGICAL EVALUATION OF MONOVALENT SMAC
MIMETICS

3.1 Binding Potency of Monovalent Smac Mimetics
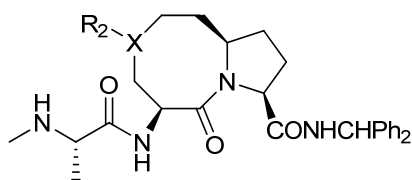
Smac mimetics

Compound	X	R_2	XIAP (nM)	c-IAP1 (nM)	c-IAP2 (nM)
SM-122	CH_2	N/A	26 ± 4	1.0 ± 0.3	1.8 ± 0.6
SM-227	N	H-	20.0 ± 14.5	1.2 ± 0.1	4.6 ± 1.5
SM-245	N	CH_3-	341 ± 65.9	3.3 ± 1.3	17.5 ± 4.3
SM-246	N	$PhCH_2$-	91.8 ± 30.4	3.7 ± 1.4	9.8 ± 4.1
SM-330	N	CH_3CO-	5.4 ± 3.0	1.3 ± 0.3	1.9 ± 0.8
SM-337	N	$PhCH_2CO$-	8.4 ± 1.6	1.5 ± 0.5	4.2 ± 0.6

Table 3.1 Binding affinities of Smac mimetics to XIAP, c-IAP1/2, as determined by competitive, fluorescence-polarization based assays. Data are shown in the form of $K_i \pm SD$ (nM).

To further explore the SAR of monovalent Smac mimetics, SM-227 was recently

developed in our laboratory. In SM-227, no additional functional group is tethered to the

nitrogen atom in the 8-membered ring of the 8,5-bicyclic system. The binding affinities of monovalent Smac mimetics with XIAP and c-IAP1/2 are shown in Table 3.1.[166] Binding affinities of SM-245, SM-246, SM-330, and SM-337 for XIAP and c-IAP1/2 have the same trend as the binding with the XIAP BIR3 domain, as discussed in the previous chapter. As expected, in the absence of major differences from the original lead compound SM-122, SM-227 has the same binding potency against XIAP, c-IAP1/2 with SM-122.
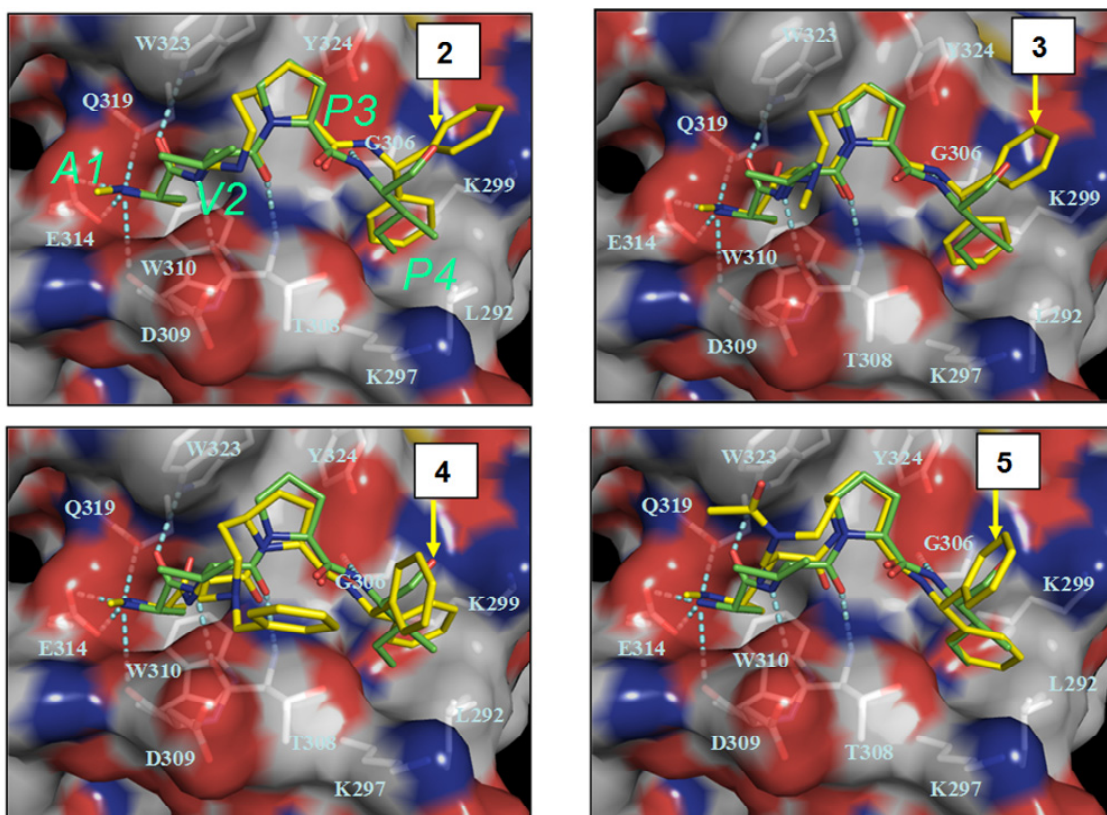
Figure 3.1 Predicted binding models of SM-227 (2), SM-245 (3), SM-246 (4), and SM-330 (5) to XIAP BIR3 domain, in superposition with Smac AVPI peptide. Smac mimetics are colored in green and the AVPI peptide in yellow. Binding pockets are shown in transparent surface. Oxygen, nitrogen, sulfur atoms are colored in red, blue, and yellow respectively, while hydrogen bonds are depicted in light blue dash lines.

Predicted models of binding to the XIAP BIR3 domain of the monovalent Smac mimetics SM-227, SM-245, SM-246 and SM-330 in superposition with the Smac AVPI

peptide are shown in Figure 3.1. As expected, SM-227, SM-245, SM-246 and SM-330 can mimic the reverse turn conformation of Smac AVPI tetrapeptide, while the functional groups tethered to the nitrogen atom in the 8,5-bicyclic system in SM-245, SM-246, and SM-330 are directed towards the solvent, and have no specific interaction with the XIAP BIR3 domain.

3.2 Tumor Cell Growth Inhibition Activity of Monovalent Smac Mimetics
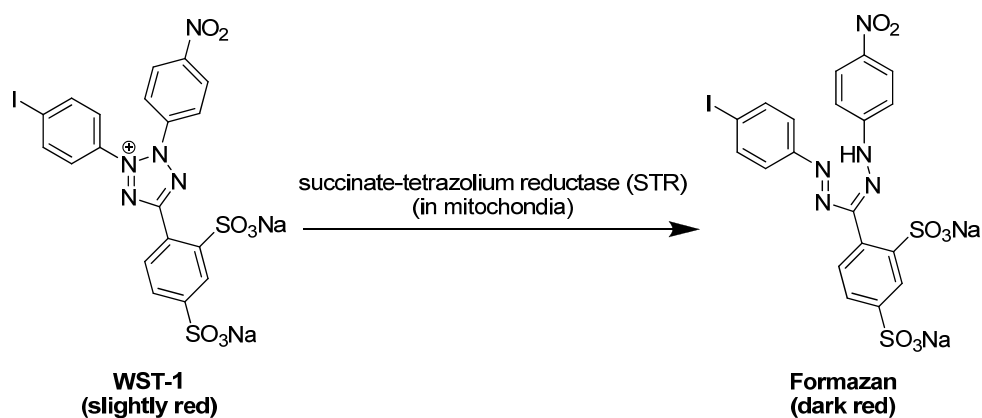
Figure 3.2 Principles of WST-based cell proliferation assay.

WST (Water Soluble Tetrazolium)-based cell proliferation assays were preformed to test the capability of Smac mimetics in tumor cell growth inhibition.[167] The principles of WST assays are shown in Figure 3.2. STR (Succinate Tetrazolium Reductase) is active in the mitochondrial respiratory chain, transforming slightly red WST-1 to dark red formazan only in viable cells. Therefore, the formation of formazan is in proportion to the number of viable cells.[168,169] By measuring the relative light absorbance at 450 nm, the

ratio of viable cells in the measured group to the untreated group (cell viability percentage) can be obtained, as shown in Figure 3.3.

Human ovarian cancer SK-OV-3 cells   **Human breast cancer MDA-MB-231 cells**

		IC_{50}=Aver.+SD (nM)
⊟	SM-122	325.6±76.6
■	SM-227	484.6±111.7
▼	SM-245	892.6±19.5
▲	SM-246	720.3±94.3
●	SM-330	59.6±25.5
◆	SM-337	27.3±3.0
△	SM-376	6.7±3.8

		IC_{50}=Aver.+SD (nM)
⊟	SM-122	259.2±66.8
■	SM-227	890.0±383.3
▼	SM-245	1326.0±4.3
▲	SM-246	1011.6±206.3
●	SM-330	68.5±36.5
◆	SM-337	31.4±7.6
△	SM-376	23.1±15.5
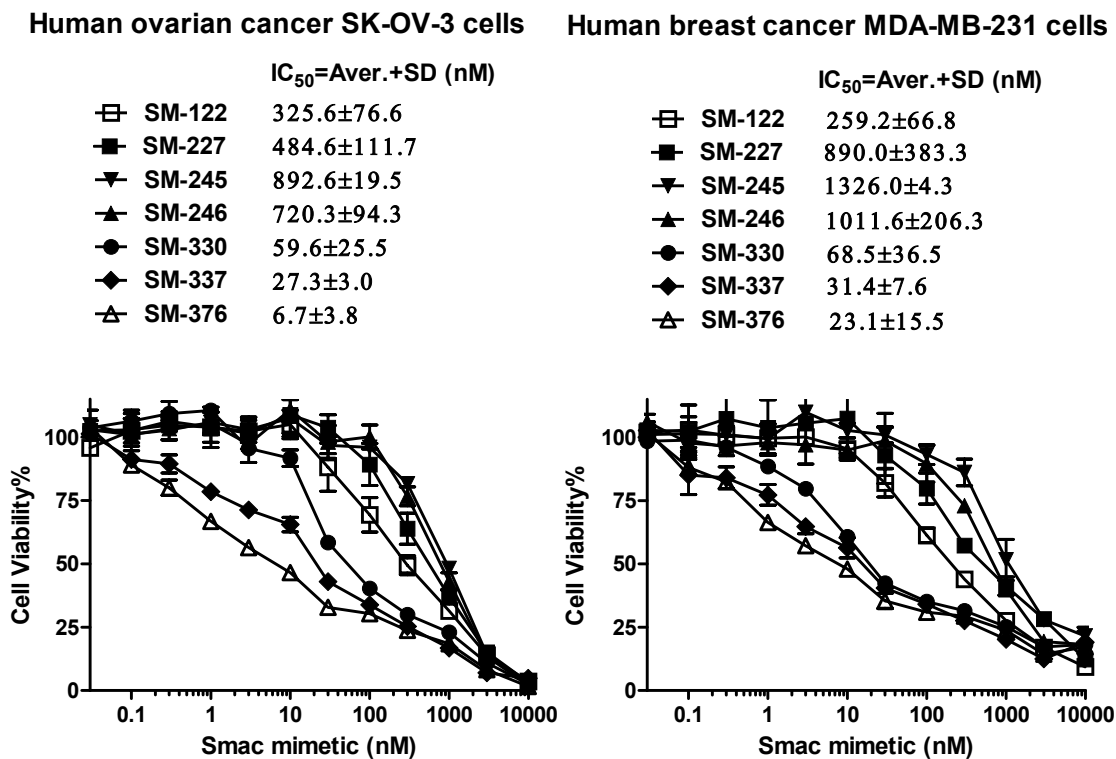
Figure 3.3 Inhibition of tumor cell growth by monovalent Smac mimetics in human breast cancer MDA-MB-231 cells and human ovarian cancer SK-OV-3 cells. Tumor cells were treated with Smac mimetics for 96 hours and cell growth was determined using a WST-based cell growth assay.

After human breast cancer MDA-MB-231 cells and human ovarian cancer SK-OV-3 cells were treated with Smac mimetics for 96 hours, tumor cell viabilities were analyzed by using WST-based cell growth assay. As shown in Figure 3.3, the potency of monovalent Smac mimetics in inhibiting tumor cell growth is consistent with the binding potency with XIAP, c-IAP1/2. In both tumor cell lines, Smac mimetics SM-227, SM-245, and SM-246 have less potency than the lead compound SM-122 in tumor cell growth inhibition. The Smac mimetics SM-330 and SM-337, with improved binding potency with XIAP, are 4 to 10 times more potent than SM-122 in both tumor cell lines. SM-376,

71

with an (*R*)-tetrahydronaphthyl group which serves to increase the hydrophobic interaction with the large hydrophobic pocket formed by lysine 297 and lysine 299 of the XIAP BIR3 domain, has the best potency in inhibition of cell growth in both tumor cell lines, consistent with its significant binding potency with the XIAP BIR 3 domain.

3.3 Tumor Cell Death Induction Activity of Monovalent Smac Mimetics
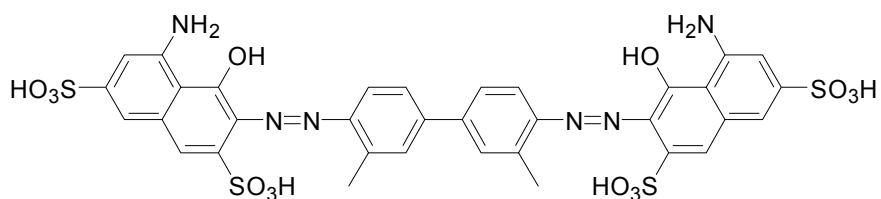
Figure 3.4 Chemical structure of Trypan blue.

Trypan blue cell death assays were performed to evaluate the activity of monovalent Smac mimetics in tumor cell death induction. Trypan blue (Figure 3.4) can pass through the cell membrane of dead cells to color the cells in dark blue, while live cells remain unaffected. Therefore, cell viabilities can be obtained after counting both live and non-live cells distinguished by Trypan blue.

After human breast cancer MDA-MB-231 cells and human ovarian cancer SK-OV-3 cells were treated with 0.1, 1, and 3 μM of the monovalent Smac mimetics SM-122, SM-245, SM-246, SM-337, SM-350, or SM-376 for 24 and 48 hours, tumor cell viabilities were analyzed by using Trypan-blue-based cell death assay. As shown in Figure 3.5, every tested monovalent Smac mimetic can dose- and time-dependently induce tumor cell death in both SK-OV-3 and MDA-MB-231 cells. Smac mimetics

SM-245 and SM-246 have same potency compared with lead compound SM-122 in both tumor cell lines, while SM-337 and SM-350 are more potent than SM-122, consistent with their better binding potency against XIAP BIR 3 domain. As expected, SM-376, with the best binding potency among all the monovalent Smac mimetics, shows the best potency in tumor cell death induction in both MDA-MB-231 and SK-OV-3 cells.
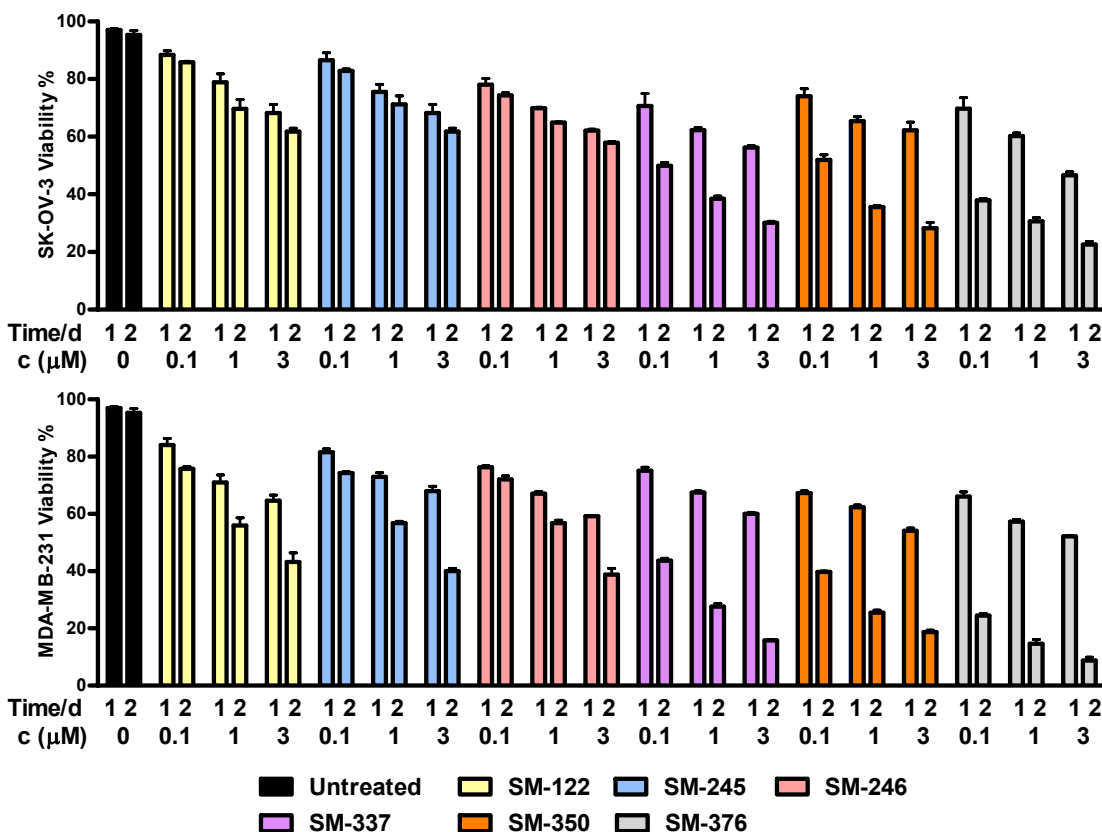
Figure 3.5 Cell viabilities of human ovarian cancer SK-OV-3 cells and human breast cancer MDA-MB-231 cells treated with different concentrations of monovalent Smac mimetics for 24 or 48 hours, as determined by Trypan blue cell death assays.

3.4 Apoptosis Induction Activity of Monovalent Smac Mimetics

Our hypothesis is that Smac mimetics induce tumor cell death and inhibit tumor cell growth by inhibiting IAPs and activating apoptosis in tumor cells. To further test this

hypothesis, the abilities of monovalent Smac mimetics in tumor apoptosis induction were analyzed by using Annexin V and Propidium Iodide (P.I.) double staining flow cytometry.
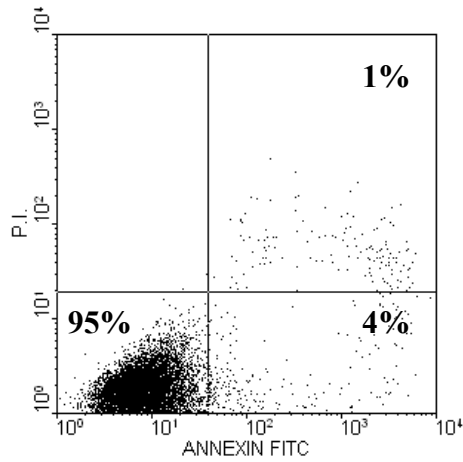
Figure 3.6 Annexin V and P.I. double staining flow cytometry of untreated MDA-MB-231 cells.

UT	SM245	SM337	SM376
	10 nM	10 nM	10 nM
	100 nM	100 nM	100 nM
	1 µM	1 µM	1 µM
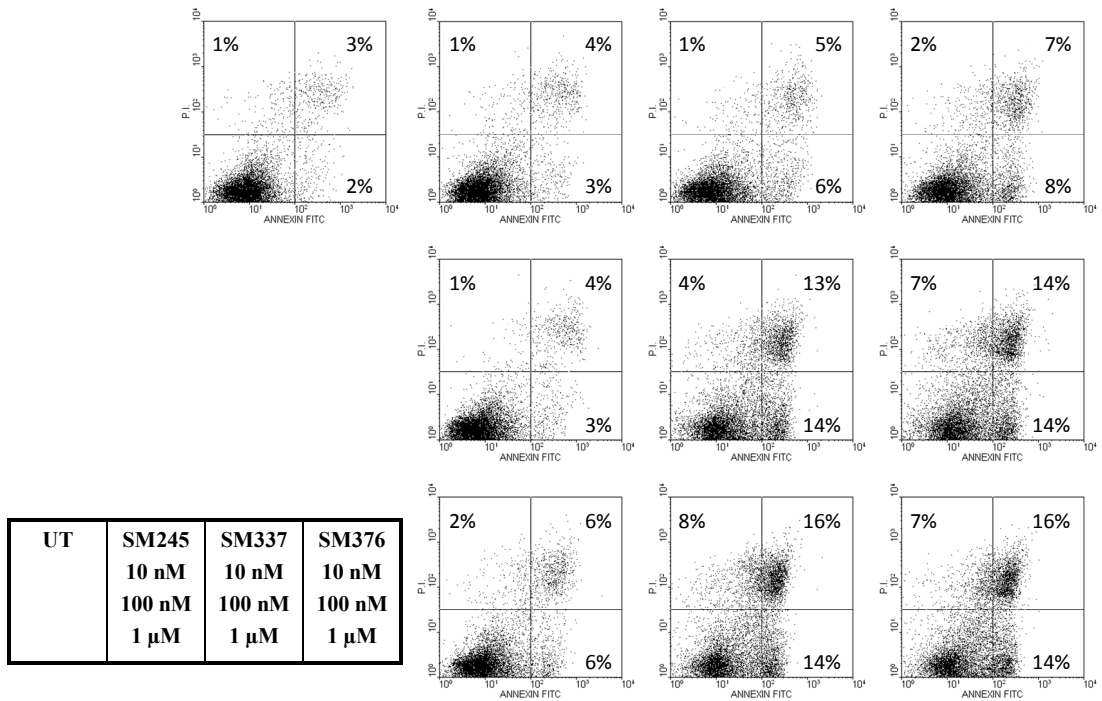
Figure 3.7 Annexin V and P.I. double staining flow cytometry of human breast cancer MDA-MB-231 cells treated with different concentrations of monovalent Smac mimetic SM-245, SM-337, or SM-376 for 24 hours.
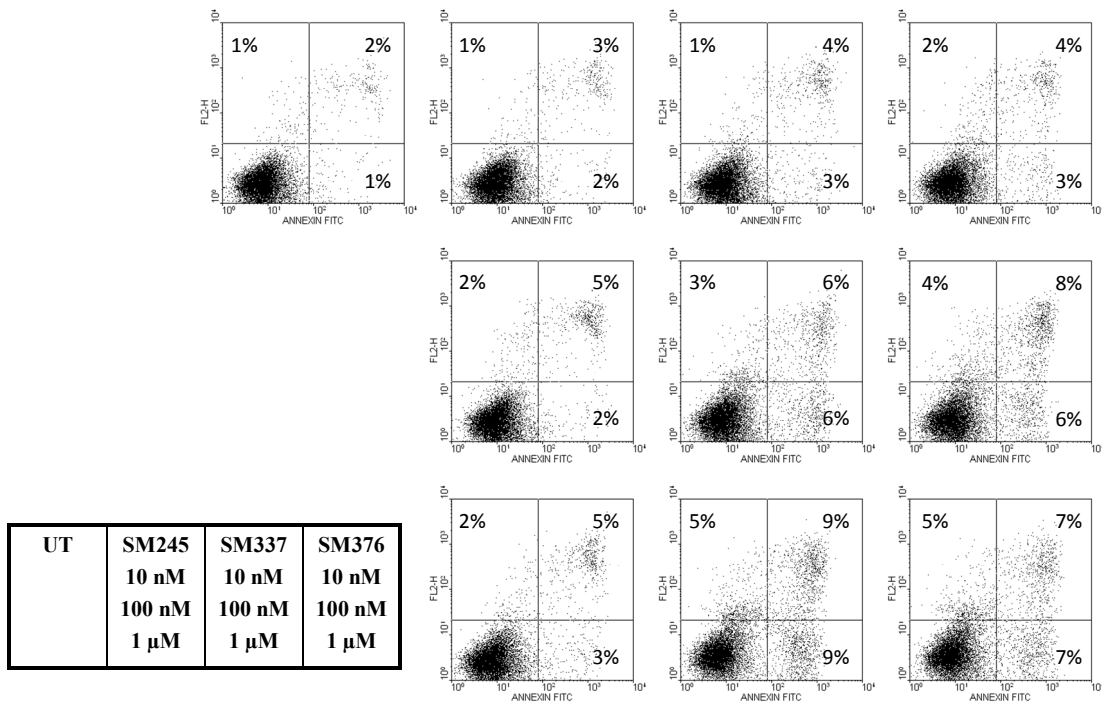
Figure 3.8 Annexin V and P.I. double staining flow cytometry of human ovarian cancer SK-OV-3 cells treated with different concentrations of monovalent Smac mimetic SM-245, SM-337, or SM-376 for 24 hours.

Figure 3.6 shows the results of Annexin V and P.I. double staining flow cytometry of untreated MDA-MB-231 cells. Annexin V competes for the binding site of phosphatidylserine, which is normally confined to the inner leaflet of the cell membrane and is externalized in the early stages of apoptosis, while P.I. can intercalate DNA which is released after damage of the cell nucleus in the late stage of apoptosis.[170-179] Hence, cells in the lower right quadrant are in the early phase of apoptosis, binding Annexin V but not taking up P.I. Cells in the upper right quadrant are in the late phase of apoptosis, both binding Annexin V and taking up P.I.. Cells in the lower left quadrant are live cells, neither binding Annexin V nor taking up P.I., while cells in the upper left quadrant are dead cells, only taking up P.I.. Therefore, flow cytometry with Annexin V and P.I. double

75

staining can be used to evaluate the ability of Smac mimetics in inducing apoptosis, since it can successfully distinguish the different apoptosis phases in which cells are present.[180-191]
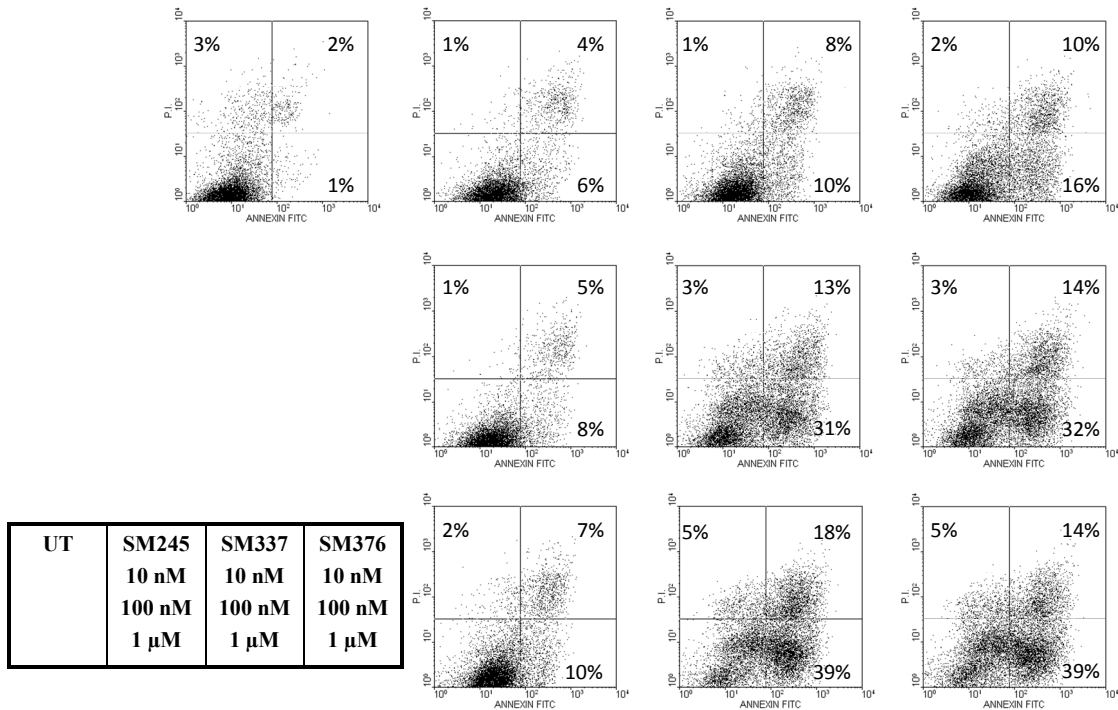
Figure 3.9 Annexin V and P.I. double staining flow cytometry of human breast cancer MDA-MB-231 cells treated with different concentrations of monovalent Smac mimetic SM-245, SM-337, or SM-376 for 48 hours.

After human breast cancer MDA-MB-231 cells and human ovarian cancer SK-OV-3 cells were treated with 10, 100, and 1000 nM of the Smac mimetic SM-245, SM-337, or SM-376 for 24 hours, apoptosis in tumor cells was analyzed using Annexin V and P.I. double staining flow cytometry. As shown in Figure 3.7 and 3.8, every Smac mimetic can induce apoptosis in both tumor cell lines in a dose-dependent manner. SM-337 and SM-376 show similar potency in inducing apoptosis in both MDA-MB-231

and SK-OV-3 cells, while both Smac mimetics are more potent than SM-245, consistent with their superior potency in binding against XIAP BIR 3 domain.

After human breast cancer MDA-MB-231 cells were treated with 10, 100, and 1000 nM of Smac mimetic SM-245, SM-337, or SM-376 for 48 hours, apoptosis in tumor cells was analyzed by Annexin V and P.I. double staining flow cytometry, as shown in Figure 3.9. As expected, each Smac mimetic can dose-dependently induce apoptosis in MDA-MB-231 cells. Meanwhile, each Smac mimetic time-dependently induces apoptosis in MDA-MB-231 cells, when compared with the results in Figure 3.7. Similarly, SM-337 and SM-376 have better potency than SM-245, which bears a relatively lower binding affinity against XIAP BIR 3 domain.

3.5 Caspase Activation of Monovalent Smac Mimetics

A cell-free functional assay was performed to test further whether Smac mimetics can function as antagonists of XIAP. While the XIAP protein effectively inhibits the activity of caspase-3/7, the Smac mimetics SM-122, SM-227, SM-330, and SM-337 can all dose-dependently antagonize XIAP and restore the activity of casapase-3/7. As shown in Figure 3.10, newly developed Smac mimetic SM-227, SM-330, and SM-337 all have better potency than original lead compound SM-122 in caspase activity recovery.
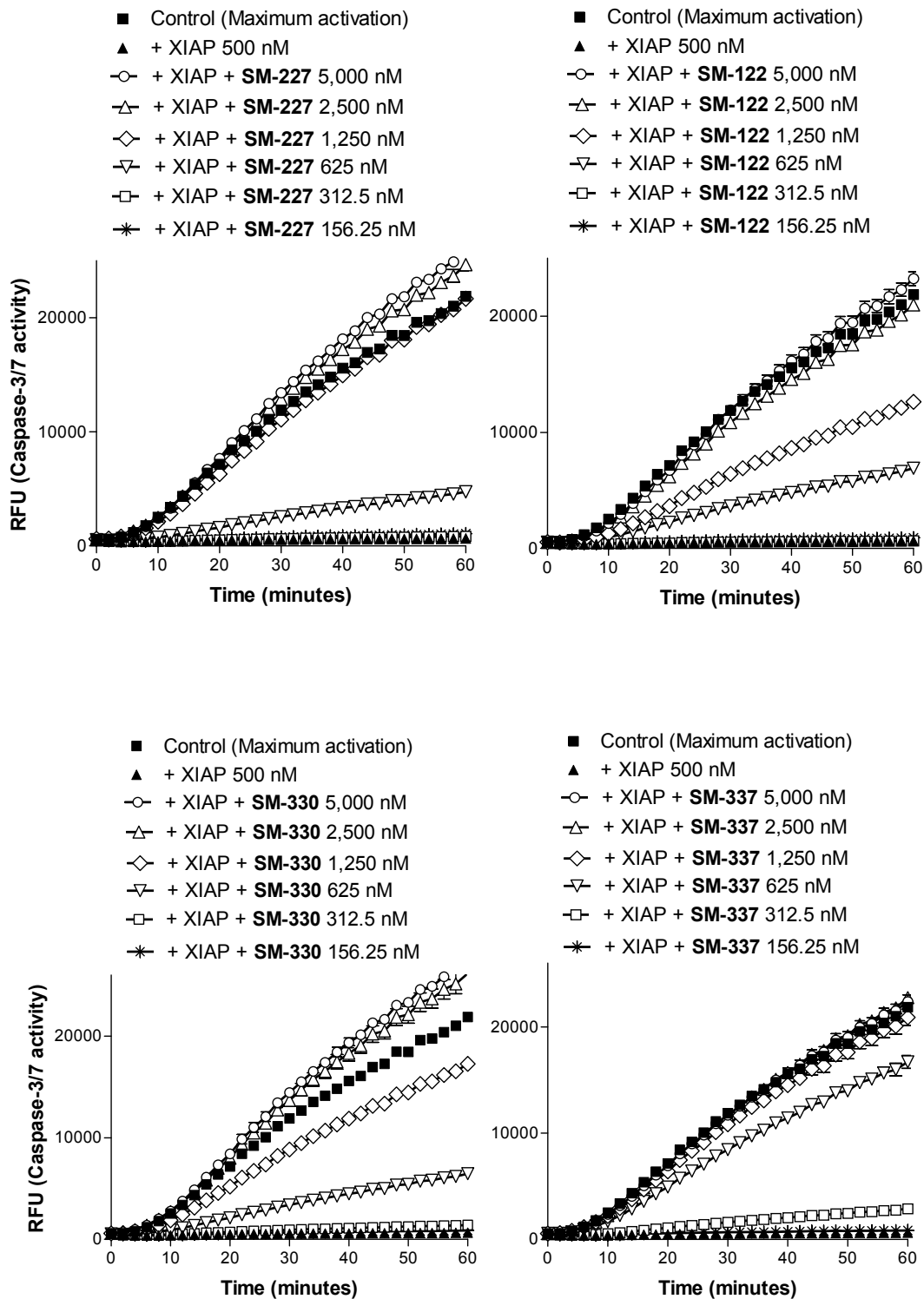
Figure 3.10 Inhibition of caspase-3/7 activity by XIAP and antagonism of Smac mimetics to XIAP to recover the activity of caspase-3/7 in a cell-free functional assay.
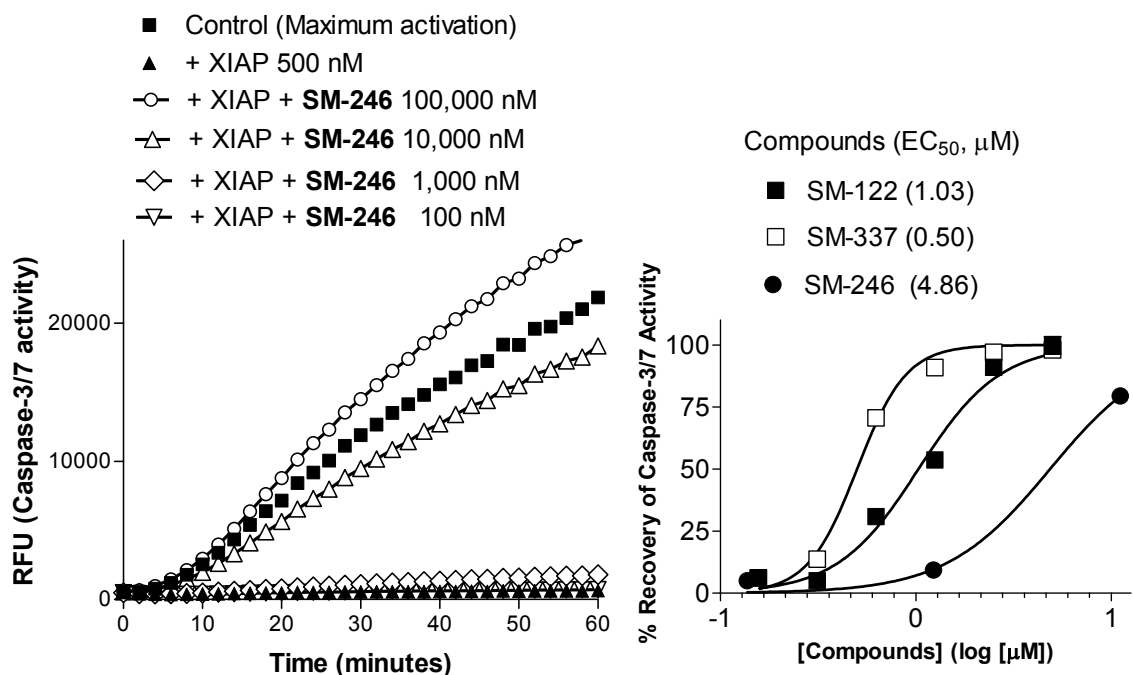
Figure 3.11 Left: Inhibition of caspase-3/7 activity by XIAP and antagonism of Smac mimetic SM-246 to XIAP to recover the activity of caspase-3/7 in a cell-free functional assay. Right: Dose-dependent recovery of caspase-3/7 activity by SM-122, SM-246, and SM-337 to the maximum activation. Caspase-3/7 activity at 30 minute point was used.

The ability of Smac mimetic SM-246 in caspase-3/7 activity recovery was also analyzed in a cell-free functional assay. The result shows that SM-246 can dose-dependently recover the activity of caspase-3/7 by antagonizing XIAP. However, as shown in Figure 3.11, SM-246 has less potency in caspase activity recovery than SM-122 and SM-330, consistent with its lower binding potency with the XIAP BIR 3 domain.

3.6 Drug Synergy Effect of Monovalent Smac Mimetics with TRAIL

TRAIL + SM-337 wst assay in MDA-MB-435 cells

TRAIL	(IC$_{50}$=280)
T + 0.1nM of SM-337	(IC$_{50}$=180)
T + 1nM of SM-337	(IC$_{50}$=80)
T + 10nM of SM-337	(IC$_{50}$=10)

TRAIL + SM-376 wst assay in MDA-MB-435 cells

TRAIL	(IC$_{50}$=220)
T + 0.1nM of SM-376	(IC$_{50}$=95)
T + 1nM of SM-376	(IC$_{50}$=12)
T + 10nM of SM-376	(IC$_{50}$=2.8)

TRAIL + SM-377 wst assay in MDA-MB-435 cells

TRAIL	(IC$_{50}$=210)
T + 0.1nM of SM-377	(IC$_{50}$=190)
T + 1nM of SM-377	(IC$_{50}$=18)
T + 10nM of SM-377	(IC$_{50}$=3)
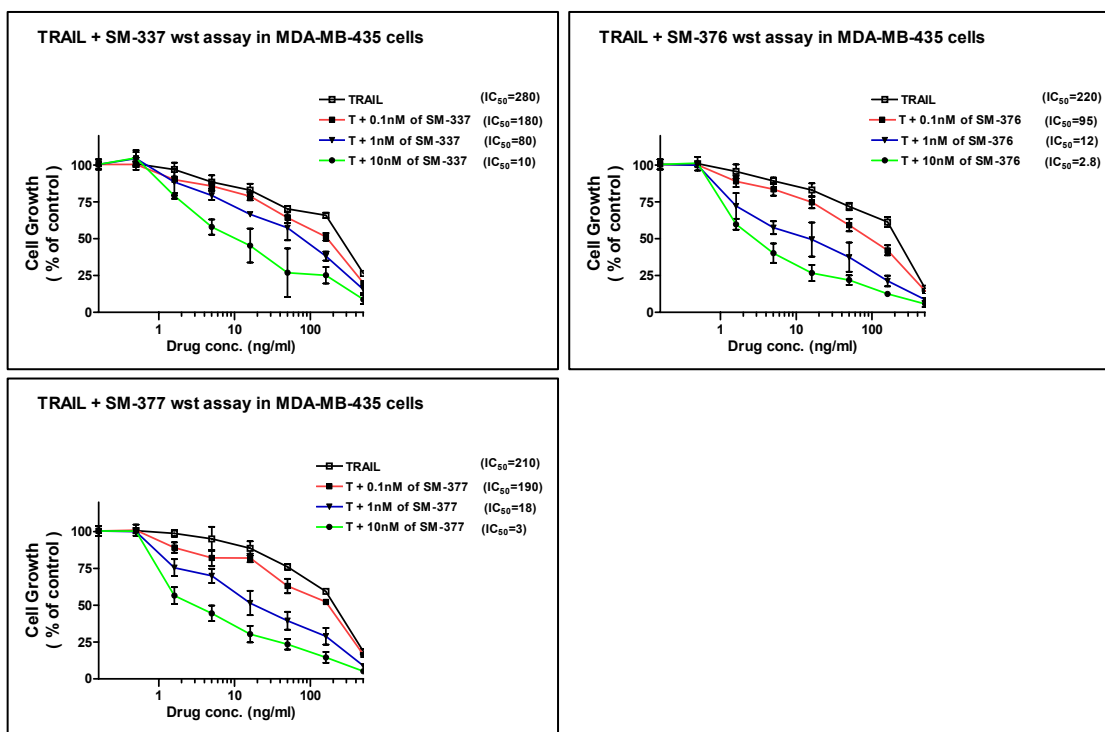
Figure 3.12 Inhibition of cell growth by Smac mimetics SM-337, SM-376, and SM-377 in combination with TRAIL in human breast cancer MDA-MB-231 cell lines. Cells were treated with TRAIL only or TRAIL in combination with Smac mimetics for 4 days and cell growth was analyzed by WST-based cell growth assay.

We hypothesize that our Smac mimetics can inhibit tumor cell growth by inhibiting XIAP thus promoting apoptosis in tumor cells. Hence, our Smac mimetics may synergize with Tumor necrosis factor-Related Apoptosis Inducing Ligand (TRAIL) which can induce the extrinsic apoptotic pathway. To verify this, WST-based cell growth assays of human breast cancer MDA-MB-435 cells treated with TRAIL alone or in combination with different concentrations of Smac mimetic SM-337, SM-376, or SM-377, were performed. As shown in Figure 3.12, each monovalent Smac mimetic is dose-dependently synergistic with TRAIL in inhibiting MDA-MB-435 cell growth. SM-376 and SM-377 have similar potency in tumor cell growth inhibition, while both are more potent than SM-337, consistent with their better binding potency to XIAP protein.
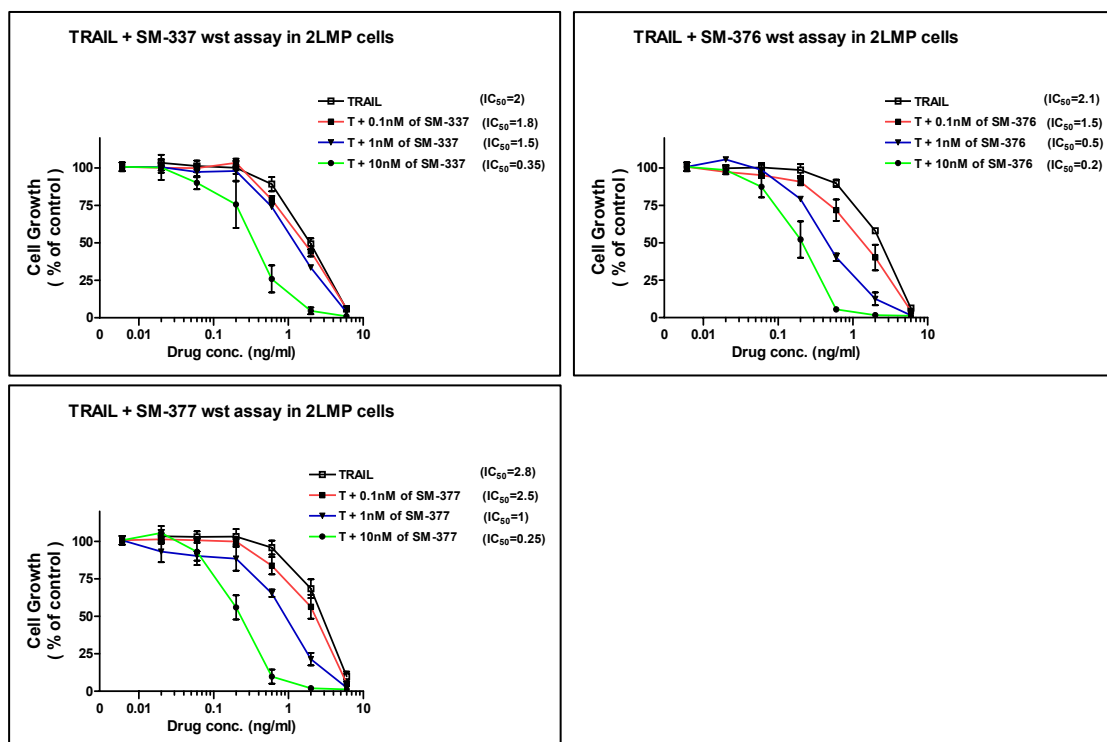
Figure 3.13 Inhibition of cell growth by Smac mimetics SM-337, SM-376, and SM-377 in combination with TRAIL in human breast cancer 2LMP cell lines. Cells were treated with TRAIL only or TRAIL in combination with Smac mimetics for 4 days and cell growth was analyzed by WST-based cell growth assay.

The synergistic effect of Smac mimetics with TRAIL in human breast cancer 2LMP cells was also analyzed by using WST-based cell growth assay. As shown in Figure 3.13, SM-337, SM-376, and SM-377 can all dose-dependently synergize with TRAIL in inhibiting 2LMP cell growth. Similarly, in MDA-MB-435 cells, SM-376 and SM-377 are slightly more potent than SM-337 in inhibiting 2LMP cell growth, consistent with their better binding potency to XIAP protein.

3. 7 Cellular Molecular Effects of Monovalent Smac Mimetics
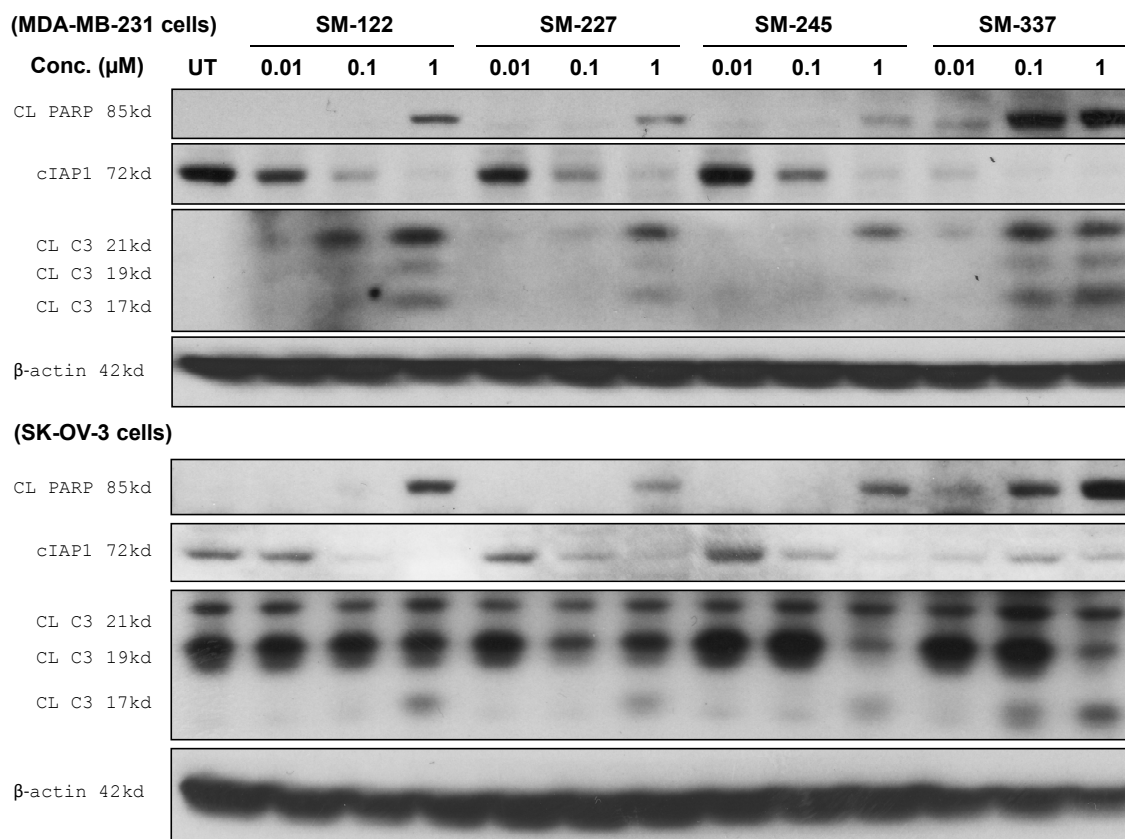
Figure 3.14 Western blot assays of human breast cancer MDA-MB-231 cells and human ovarian cancer SK-OV-3 cells treated with different concentrations of Smac mimetic SM-122, SM-227, SM-245, or SM-337 for 24 hours.

To further explore the cellular molecular effects induced by our monovalent Smac mimetics, human breast cancer MDA-MB-231 cells and human ovarian cancer SK-OV-3 cells were treated with 10, 100, and 1000 nM of Smac mimetic SM-122, SM-227, SM-245, or SM-337 for 24 hours, and then Poly ADP Ribose Polymerase (PARP) cleavage. Degradation of c-IAP1, and caspase activation were analyzed with Western blotting assays. As shown in Figure 3.14, each Smac mimetic can dose-dependently induce the cleavage of PARP, a substrate of active caspase-3, and also a marker of cells undergoing apoptosis in both tumor cell lines. Our designed Smac mimetics bind to cIAP-1 with very high affinities (Table 3.1) and recent studies have shown that Smac

mimetics induce cIAP-1 degradation in cancer cells, mediating apoptosis induction.[192-195] Hence, the ability of Smac mimetic in inducing cIAP-1 degradation was also analyzed. As expected, each Smac mimetic can effectively induce c-IAP1 degradations in both tumor cell lines. Consistent with the ability of Smac mimetics in inducing PARP cleavage, each Smac mimetic dose-dependently induces the activation of caspase-3 in both tumor cell lines.

3.8 Conclusion

A series of potent non-peptidic small molecular Smac mimetics has been successfully developed. SM-330, SM-337, SM-376, and SM-377 with improved binding potency with XIAP and c-IAP1/2, compared with our original lead compound SM-122, are cell-permeable and have excellent activity in inhibiting tumor cell growth, inducing tumor cell death, and inducing apoptosis in tumor cells, as tested in both human breast cancer MDA-MB-231 cells and human ovarian cancer SK-OV-3 cells. As expected, our Smac mimetics can synergize with TRAIL in inhibiting tumor cell growth, as tested in both human breast cancer MDA-MB-435 cells and 2LMP cells. Cell-free functional assays verify that our Smac mimetics can recover the activity of caspase-3,7 previously inhibited by XIAP protein. The cellular molecular events induced by our Smac mimetics were also analyzed with Western blotting assays, which show that each Smac mimetic can dose-dependently induce PARP cleavage, c-IAP1 degradation and caspase activation in tumor cells. Overall, these potent Smac mimetics with excellent cellular activity are

currently being used as our new lead template to develop future drug candidates with

excellent PK (pharmacokinetic) properties.

CHAPTER 4

BIOLOGICAL EVALUATION OF BIVALENT SMAC MIMETICS

4.1 Binding Potency of Bivalent Smac Mimetics

To further explore the optimal length of the linker for the bivalent Smac mimetics, bivalent Smac mimetics SM-1252 and SM-1253 were recently developed. A series of bivalent Smac mimetics with linkers of different lengths were tested for their binding potency against both XIAP BIR3 protein and XIAP linker-BIR2-BIR3 protein, using our fluorescence-polarization based assays. As shown in Table 4.1, as the length of the bivalent linker increases, the binding potency against XIAP BIR3 domain decreases. However, all the five bivalent Smac mimetics show similar excellent potency in binding against XIAP linker-BIR2-BIR3 domains. All the bivalent Smac mimetics show excellent binding potency in binding with linker-BIR2-BIR3 protein compared with BIR3 protein only. Their cellular activities were explored in detail in the subsequent parts of this chapter.

Comp. (linker)	Structure	BIR3 $K_i \pm$ SD (nM)	L-BIR2-BIR3 $K_i \pm$ SD (nM)
SM-1252 (2C)		9.7 ± 3.8	1.0 ± 0.7
SM-1253 (4C)		7.6 ± 2.3	0.3 ± 0.2
SM-385 (6C)		12.7 ± 3.9	1.0 ± 0.5
SM-381 (8C)		27.5 ± 6.2	1.8 ± 0.6
SM-383 (10C)		43.1 ± 3.6	1.8 ± 0.5

Table 4.1 Binding affinities of bivalent Smac mimetics against XIAP BIR3 and XIAP linker-BIR2-BIR3 domains, as measured by fluorescence-polarization based assays

4.2 Tumor Cell Growth Inhibition Activity of Bivalent Smac Mimetics

SM-1252, SM-1253, SM-385, SM-381, and SM-383 have 2, 4, 6, 8, and 10 methylene groups respectively in the bivalent linker. To explore the ability of these

bivalent Smac mimetics in inhibition of tumor cell growth, WST-based cell growth assays were performed. Human breast cancer MDA-MB-231 cells and human ovarian cancer SK-OV-3 cells were treated with bivalent Smac mimetics for 96 hours, and then cell viabilities were analyzed by using WST-based cell growth assay.
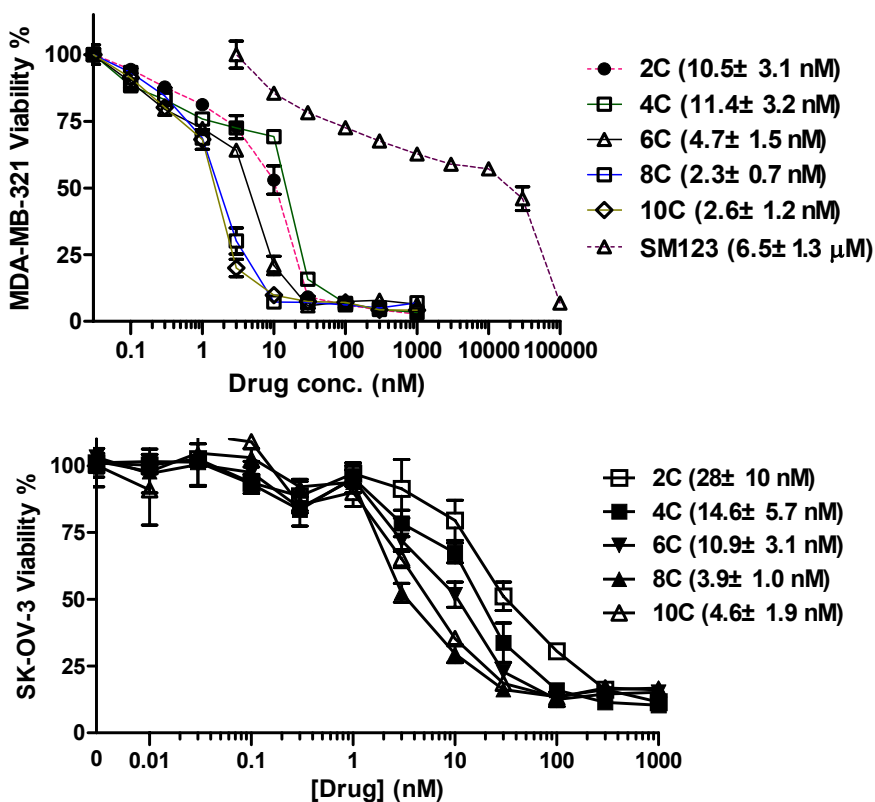
Figure 4.1 WST cell growth assays of human breast cancer MDA-MB-231 cells and human ovarian cancer SK-OV-3 cells treated with bivalent Smac mimetics for 96 hours. Experiments were performed three times. Data are reported in the form of $IC_{50} \pm SD$. 2C (SM-1252), 4C (SM-1253), 6C (SM-385), 8C (SM-381), 10C (SM-383).

As shown in Figure 4.1, all the bivalent Smac mimetics show excellent potency in tumor cell growth induction with IC_{50} values (the concentration in which Smac mimetic inhibits 50% tumor cell growth compared with untreated group) in the neighborhood of 30 nM in both MDA-MB-231 and SK-OV-3 cells. In comparison, the inactive control SM-123 is over 600 times less potent than the weakest bivalent Smac mimetic SM-1252. In both tumor models, SM-1252, with the shortest linker, has the weakest potency among

all the bivalent Smac mimetics. As the linker increases in length, the cellular potency increases. However, SM-381 and SM-383, with 8 and 10 methylenes in the bivalent linker respectively, have equivalent cellular potency in tumor cell growth inhibition.
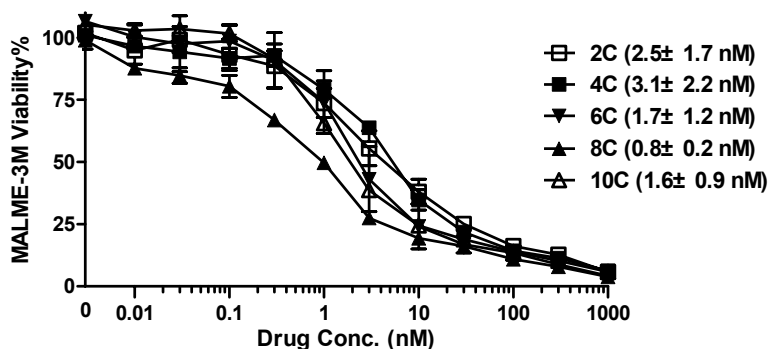
Figure 4.2 WST cell growth assay of human melanoma MALME-3M cells treated with bivalent Smac mimetics for 96 hours. Experiments were performed three times. Data are reported in the form of IC_{50} ± SD. 2C (SM-1252), 4C (SM-1253), 6C (SM-385), 8C (SM-381), 10C (SM-383).

Human melanoma MALME-3M cells were also treated with bivalent Smac mimetics for 96 hours, and then cell viabilities were analyzed using WST cell growth assays. As shown in Figure 4.2, all the bivalent Smac mimetics show excellent cellular potency in tumor cell growth inhibition, with an IC_{50} of approximately 5 nM. As expected, the cellular potency of bivalent Smac mimetics increases as the linker increases in its length. Just as in MDA-MB-231 and SK-OV-3 cells, SM-381 and SM-383, with the longest linkers, have the best cellular potency in MALME-3M cells.

4.3 Tumor Cell Death Induction Activity of Bivalent Smac Mimetics

To further explore the ability of bivalent Smac mimetics in inducing tumor cell death, Trypan blue cell death assays were performed. Human breast cancer

MDA-MB-231 cells and human ovarian cancer SK-OV-3 cells were treated with 0.1, 1, 10, and 100 nM of bivalent Smac mimetic SM-1252 (2C), SM-381 (8C), and SM-383 (10C) for 2, 6, 12, and 24 hours respectively, and cell viabilities were analyzed by using Trypan blue assays.
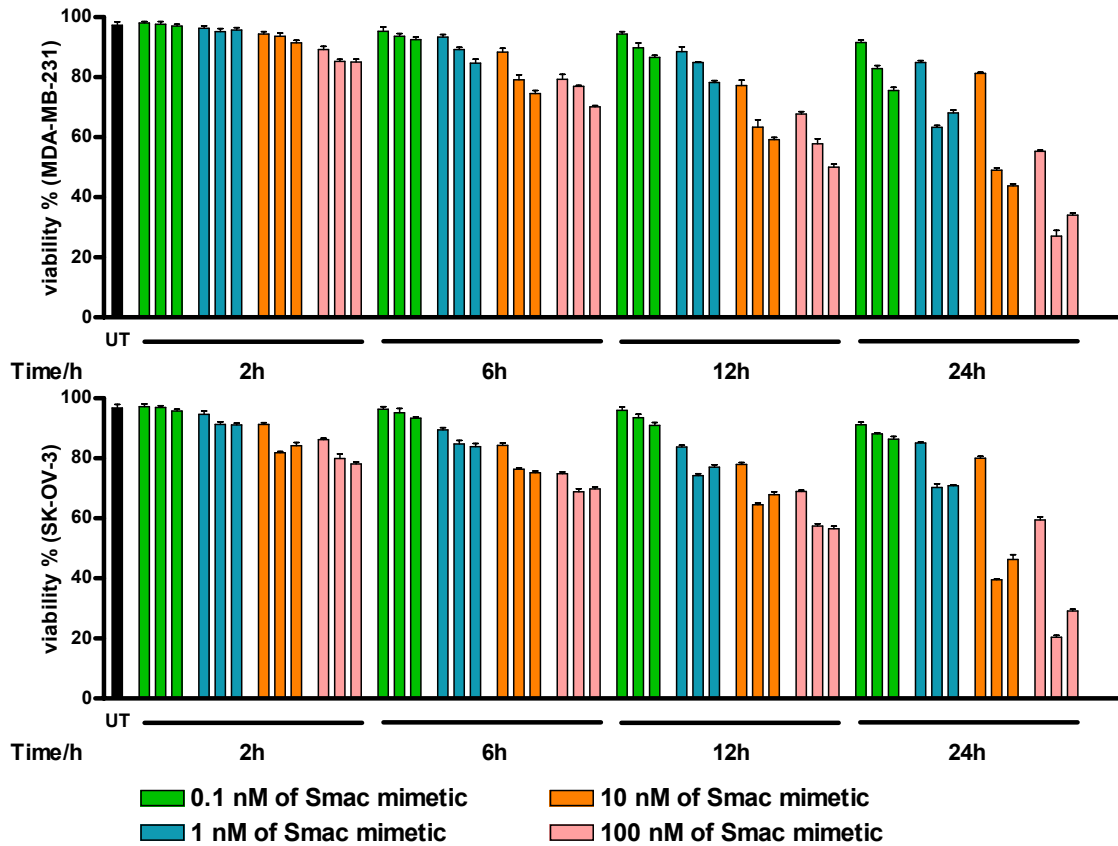
Figure 4.3 Trypan blue assays of human breast cancer MDA-MB-231 cells and human ovarian cancer SK-OV-3 cells treated with different concentrations of bivalent Smac mimetics for designated lengths of time. In each group of three, left is SM-1252 (2C), middle is SM-381 (8C), and right is SM-383 (10C).

As shown in Figure 4.3, each bivalent Smac mimetic can dose- and time-dependently induce tumor cell death in both MDA-MB-231 and SK-OV-3 cells. All the three bivalent Smac mimetics show similar potency within 12 hours of treatment in both tumor cell lines. However, at higher concentrations (10 nM and 100 nM) of bivalent Smac mimetics for 24 hours, SM-381 and SM-383 are dramatically more potent than

SM-1252 in inducing tumor cell death in both tumor cell lines, consistent with the potency trend shown in the results in WST-based cell growth assays.

4.4 Tumor Apoptosis Induction Activity of Bivalent Smac Mimetics
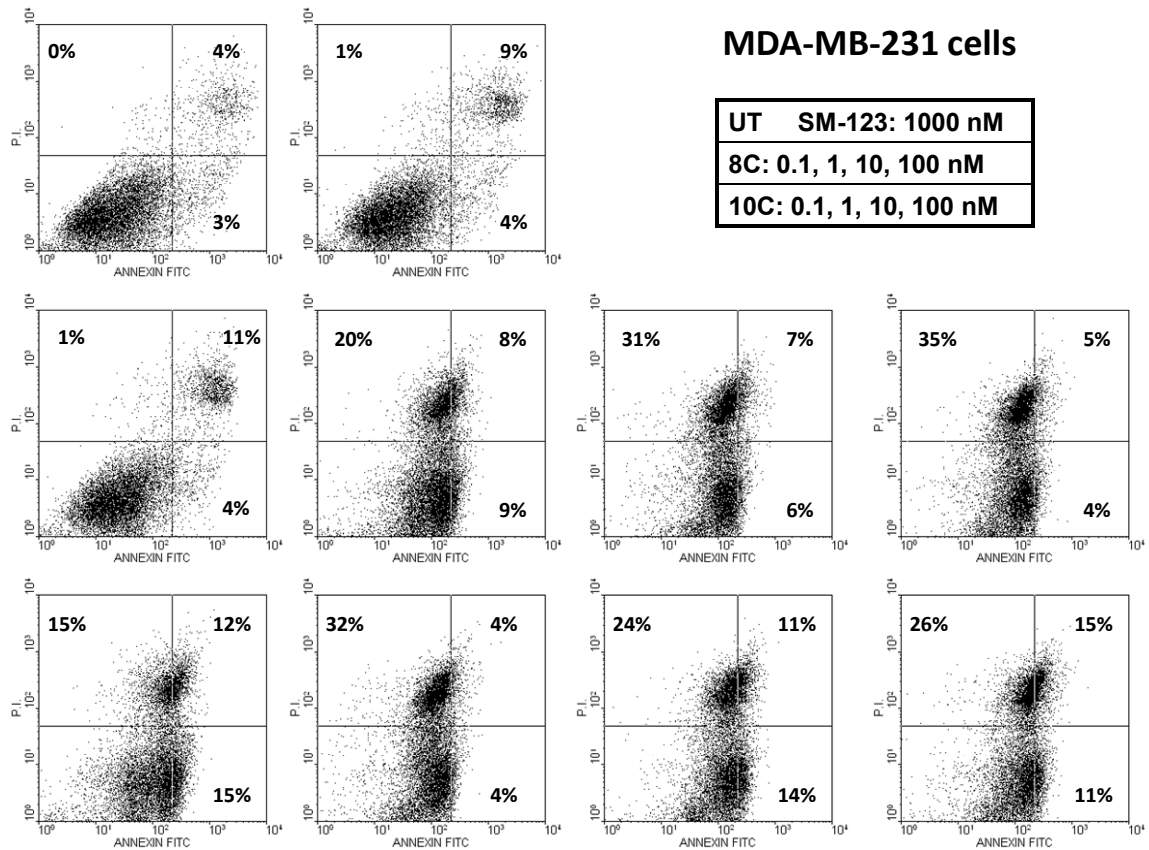
Figure 4.4 Human breast cancer MDA-MB-231cells were treated with different concentrations of bivalent Smac mimetic SM-381 (8C) and SM-383 (10C) or 1 μM of inactive control SM-122 for 24 hours. Apoptosis in tumor cells was analyzed by Annexin V and P.I. double staining flow cytometry.

To further explore the ability of bivalent Smac mimetics in inducing apoptosis in tumor cells, Annexin V and P.I. double staining flow cytometry was performed. Human breast cancer MDA-MB-231 cells were treated with 0.1, 1, 10, and 100 nM of the bivalent Smac mimetics SM-381 (8C) and SM-383 (10C) or 1000 nM of inactive control

SM-123 for 24 hours, and apoptosis was analyzed by flow cytometry. As shown in Figure 4.4, both bivalent these Smac mimetics can dose-dependently induce apoptosis in MDA-MB-231 cells. In contrast, the inactive control SM-123 can only induce a small percentage of apoptosis compared with the untreated group, although a high concentration of 1 μM was used.
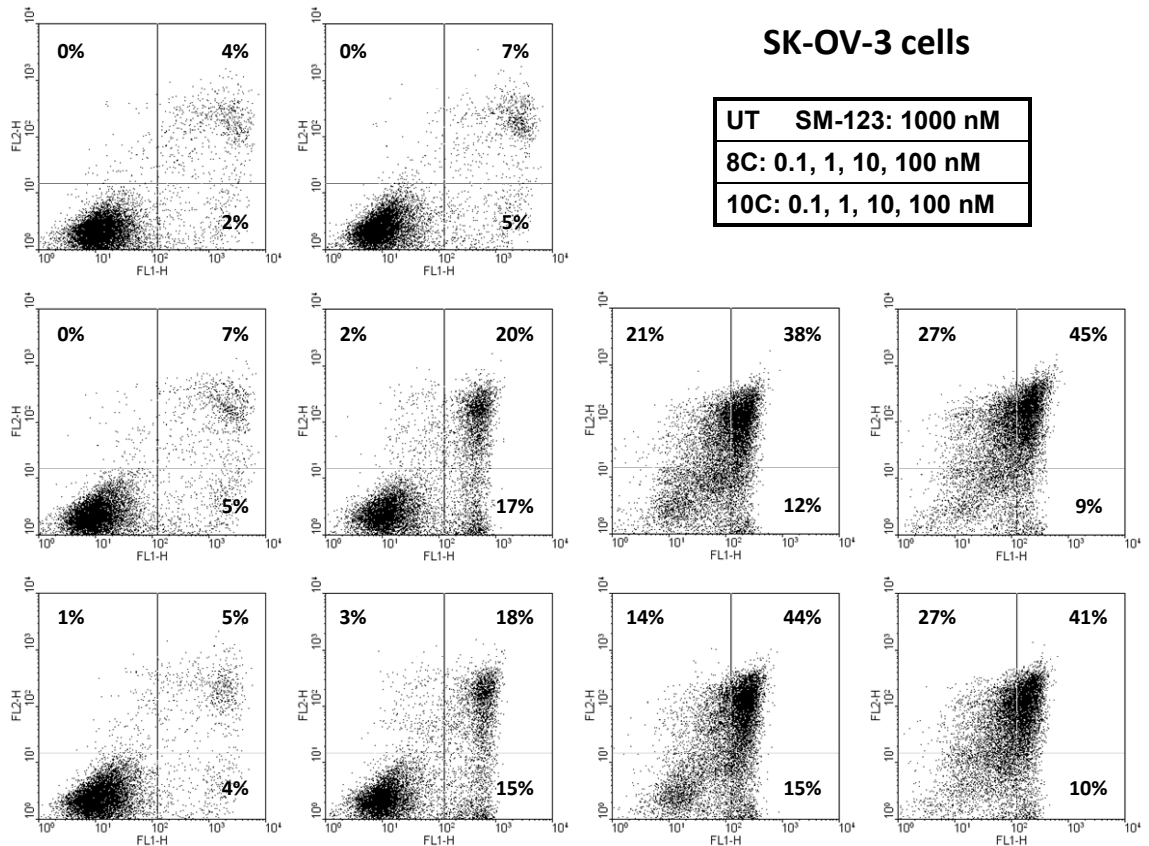
Figure 4.5 Human ovarian cancer SK-OV-3 cells were treated with different concentrations of bivalent Smac mimetic SM-381 (8C) and SM-383 (10C) or 1 μM of inactive control SM-122 for 24 hours. Apoptosis in tumor cells was analyzed by Annexin V and P.I. double staining flow cytometry.

The ability of bivalent Smac mimetics to induce apoptosis in human ovarian cancer SK-OV-3 cells was also analyzed. SK-OV-3 cells were treated with 0.1, 1, 10, and 100 nM of bivalent Smac mimetics SM-381 (8C) and SM-383 (10C) or 1000 nM of inactive control SM-123 for 24 hours, and apoptosis was analyzed by flow cytometry. As in

MDA-MB-231 cells, both bivalent Smac mimetics were found to dose-dependently induce apoptosis in SK-OV-3 cells, while the inactive control SM-123 fails to induce more apoptosis than the untreated group, as shown in Figure 4.5.

4.5 Cellular Molecular Effects of Bivalent Smac Mimetics
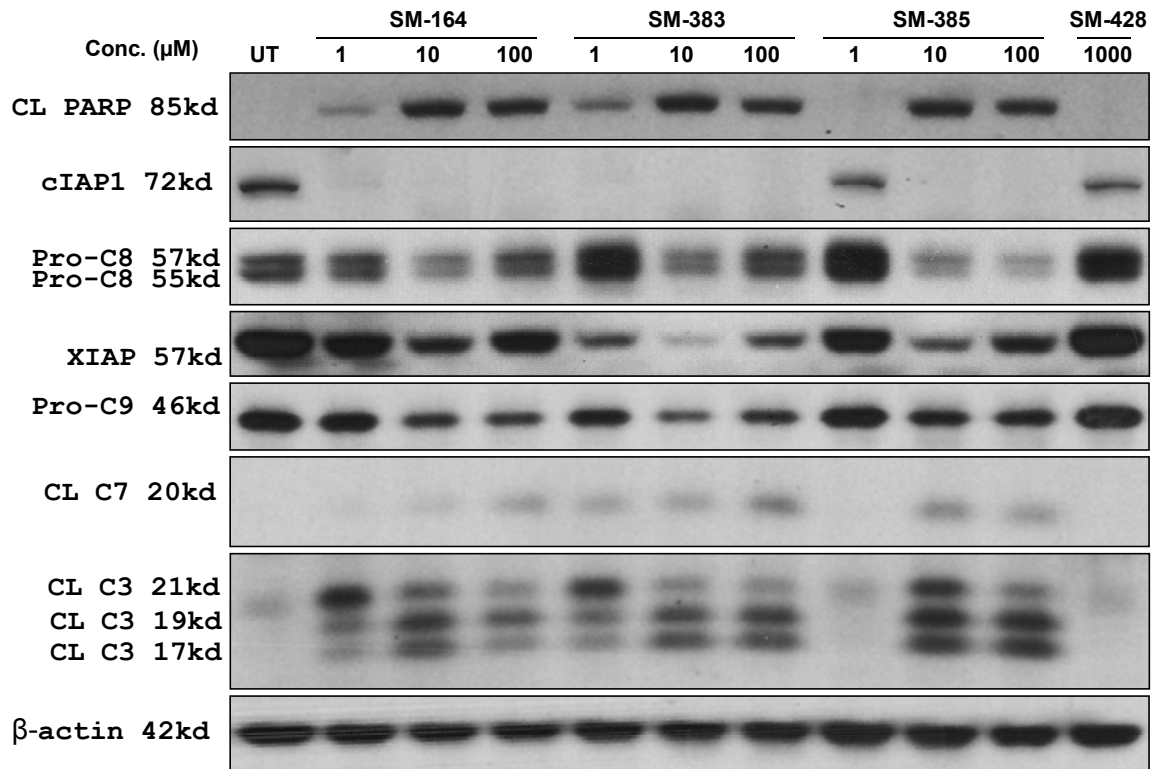
Figure 4.6 Western blotting assays of human breast cancer MDA-MB-231 cells treated with different concentrations of bivalent Smac mimetic SM-164, SM-381 and SM-383 for 24 hours.

To further probe the cellular molecular events induced by bivalent Smac mimetics, Western blotting assays were performed. Human breast cancer MDA-MB-231 cells were treated with 1, 10, and 100 nM of bivalent Smac mimetic SM-164, SM-381, and SM-383 for 24 hours, and then PARP cleavage, IAP degradations, and caspase activations were

analyzed using Western blotting assays. As shown in Figure 4.6, each bivalent Smac mimetic can dose-dependently induce PARP cleavage, c-IAP1 degradation and caspase-3/7 activations. SM-381 is as potent as the previously developed bivalent Smac mimetic SM-164,[135] while SM-383 is slightly less potent than SM-164. However, both SM-381 and SM-383 are dramatically more potent than the related monovalent Smac mimetics SM-330 and SM-337.
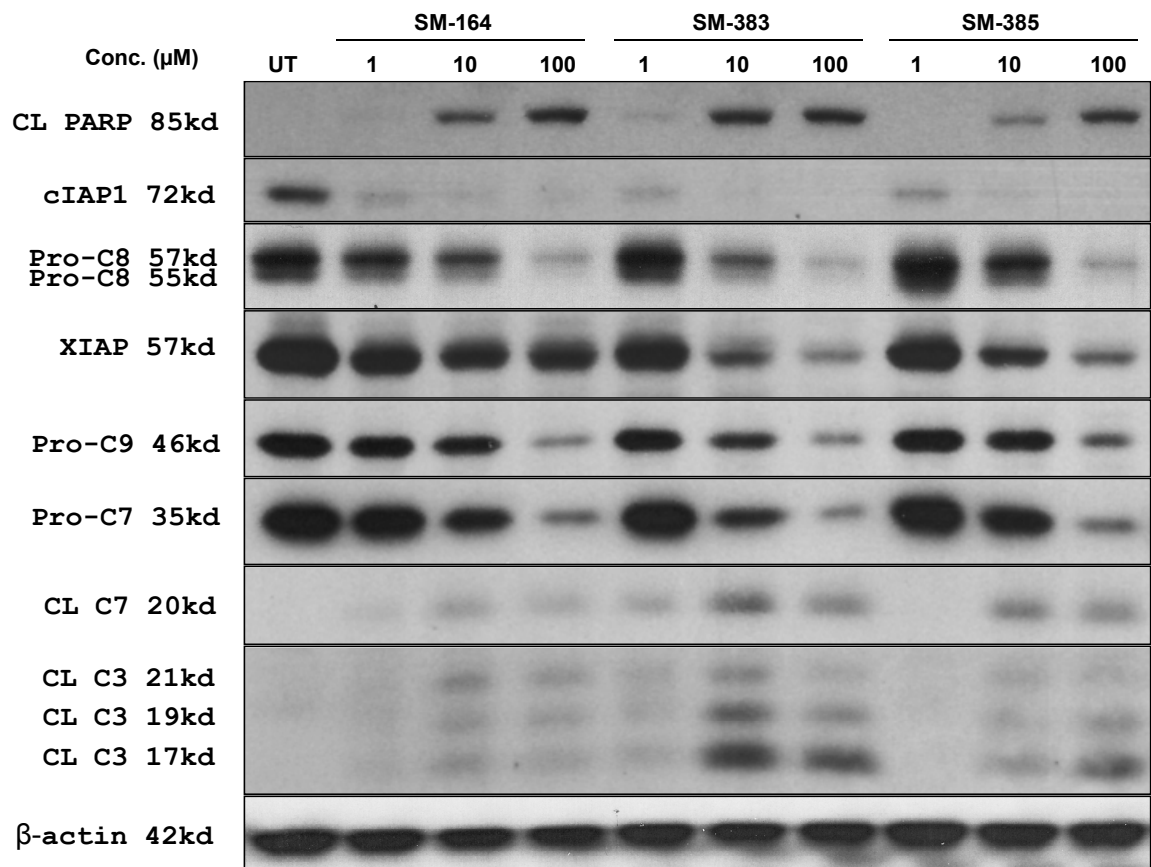
Figure 4.7 Western blotting assays of human ovarian cancer SK-OV-3 cells were treated with different concentrations of bivalent Smac mimetic SM-164, SM-381 and SM-383 for 24 hours.

The cellular activity of bivalent Smac mimetics in human ovarian cancer SK-OV-3 cells was also analyzed. SK-OV-3 cells were treated with 1, 10, and 100 nM of the bivalent Smac mimetics SM-164, SM-381, and SM-383 for 24 hours, and then PARP

cleavage, IAP degradations, and caspase activations were analyzed using Western blotting assays. Consistent with the results in MDA-MB-231 cells, SM-383 is as potent as SM-164 in PARP cleavage induction, c-IAP1 degradation, and caspase-3/7 activations, while SM-383 is slightly less potent than SM-164. However, both bivalent Smac mimetics SM-381 and SM-383 are 10 to 100 times more potent than monovalent Smac mimetics SM-227 and SM-337, whose performance is presented in a previous chapter.

4.6 Conclusion

Compared with monovalent Smac mimetics, all the bivalent Smac mimetics show excellent cellular activity as inhibitors of tumor cell growth of human breast cancer MDA-MB-231 cells, human ovarian cancer SK-OV-3 cells and human melanoma MALME-3M. As the length of bivalent linker increases, the cellular activity potency of bivalent Smac mimetics decreases. However, SM-381 and SM-383, with 8 and 10 methylene groups in the bivalent linker, have similar potency in all the tested tumor cell lines.

Bivalent Smac mimetics can dose- and time- dependently induce tumor cell death in both MDA-MB-231 and SK-OV-3 cells. In treatment of 12 hours, SM-1252, SM-381, and SM-383 show similar potency in tumor cell death induction. However, SM-381 and SM-383 are dramatically more potent than SM-1252 after 24 hours' treatment at higher concentrations, consistent with the potency trend shown in the WST-based cell growth assays.

The capability of bivalent Smac mimetic SM-381 and SM-383 in induction of apoptosis in MDA-MB-231 cells and SK-OV-3 cells was further analyzed. As expected, SM-381 and SM-383 were found to dose-dependently induce apoptosis in both tumor cell lines.

The cellular molecular effects of bivalent Smac mimetics were analyzed in MDA-MB-231 and SK-OV-3 cells. SM-381 shows excellent activity in PARP cleavage induction, c-IAP1 degradation induction, and caspase activations, and is as potent as our previously developed bivalent Smac mimetic SM-164.[135] Although SM-383 is slightly less potent than SM-381, both SM-381 and SM-383 are 10 to 100 times more potent than monomeric Smac mimetics SM-227 and SM-337 in cellular activities in tumor cells. Further modification of these bivalent Smac mimetics is in process, and we hope that our potent bivalent Smac mimetics can lead to excellent drug candidates in the future.

CHAPTER 5

CELLULAR MECHANISM STUDIES BASED ON SM-406

5.1 SM-406

The Smac mimetics SM-337, SM-350, SM-376 and SM-377 can potently inhibit tumor cell growth of human breast cancer MDA-MB-231 cells, MDA-MB-453 cells, 2LMP cells and human ovarian cancer SK-OV-3 cells, both alone and in combination with TRAIL, as shown in the results of our WST-based cell growth assays in Chapter 3. Pharmacokinetic studies, completed by Medicilon Company (Shanghai), showed that all of these potent Smac mimetics, in rats, have relatively low oral bioavailability (F%). With the lead compound SM-337 as template, a series of derived Smac mimetics were further designed and synthesized, with the aim of developing novel Smac mimetics with improved PK properties. The only difference between the newly developed Smac mimetics and SM-337 is the carboxylic acid tethering the cyclic amine of the 8-membered fused ring in the bicyclic structure. This modification has no detrimental effect on the potency of Smac mimetics, because the side chain tethered to the nitrogen atom in the bicyclic system is directed towards the solvent, and as predicted by our modeling studies (Figure 2.2), has no specific interaction with the XIAP protein.
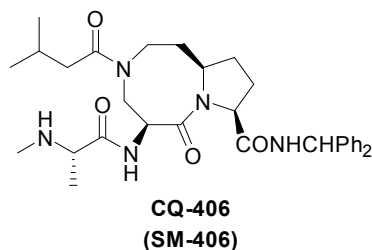
CQ-406
(SM-406)

Figure 5.1 Chemical structure of SM-406.

Among these newly developed Smac mimetics, compound CQ-406 (or SM-406),

in which a 3-methylbutanoic acid is attached to the cyclic amine in the left fused ring,

made by Dr. Cai Qian in our lab, has an excellent oral bioavailability (45%) in rats

compared with the previously synthesized Smac mimetics SM-337 (24%), SM-350

(22%), SM-376 (26%), and SM-377 (23%), although it has a slightly weaker potency in

binding with the XIAP BIR3 domain ($K_i = 13.80 \pm 2.93$ nM). Further pharmacokinetic

studies of the Smac mimetic SM-406 in dogs and monkeys are under investigation, and

the molecular cellular mechanism studies of our Smac mimetics detailed here are based

on this promising drug candidate SM-406.

5.2 Further Biological Studies Based on SM-406

5.2.1 Apoptosis induction activity of SM-406

To test the ability of SM-406 in inducing apoptosis in tumor cells, Annexin V and

P.I. (Propidium Iodide) double staining flow cytometry was performed to monitor the

apoptosis process in tumor cells treated with SM-406.
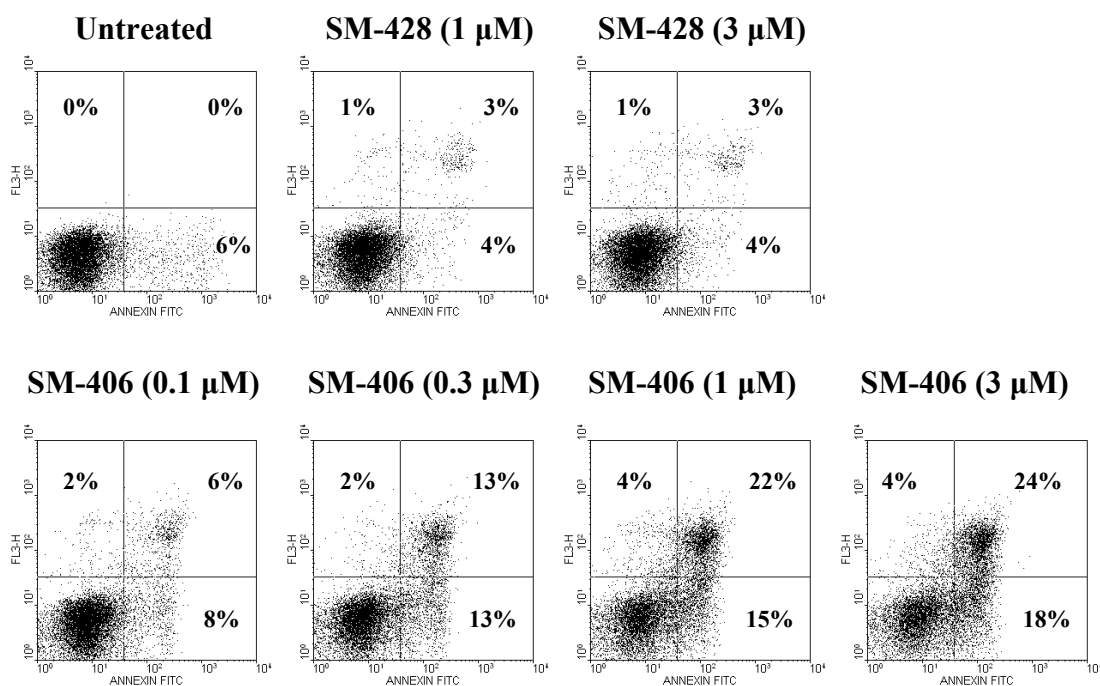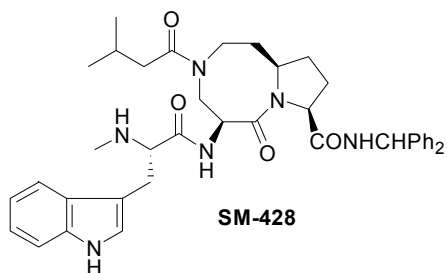
SM-428

Figure 5.2 Top: Chemical structure of SM-428, inactive control of Smac mimetics. Bottom: Annexin V and P.I. double staining flow cytometry of human ovarian cancer SK-OV-3 cells treated Smac mimetic SM-406 and inactive control SM-428 for 24 hours.

SM-428, used as an inactive control of Smac mimetics, is a derivative of the Smac mimetic SM-406, in which the methyl side chain of the amino terminal alanine moiety is substituted with an indole ring, yielding compound SM-428. The methyl side chain in the amino terminal alanine residue of mature Smac protein penetrates the small hydrophobic pocket formed by the side chains of leucine 307, tryptophan 310, and glutamine 319 in XIAP.[122] Further study showed that this small hydrophobic pocket can also accommodate an ethyl group, however, larger hydrophobic groups can eliminate this hydrophobic interaction.[127] Predictably, the newly introduced large indole ring completely abolishes

98

this interaction and dramatically reduces the binding affinity of SM-428 with the XIAP BIR3 domain, as verified by our fluorescence-polarization-based binding assay ($K_i = 45.0 \pm 8.7$ μM). Consequently, compound SM-428 was used as an inactive control in our molecular biological studies of Smac mimetics.

Untreated

Human ovarian cancer SK-OV-3 cells were treated with SM-406 (3 μM) for designated lengths of time.

SM-406 (3 hours)   SM-406 (6 hours)   SM-406 (12 hours)   SM-406(24 hours)
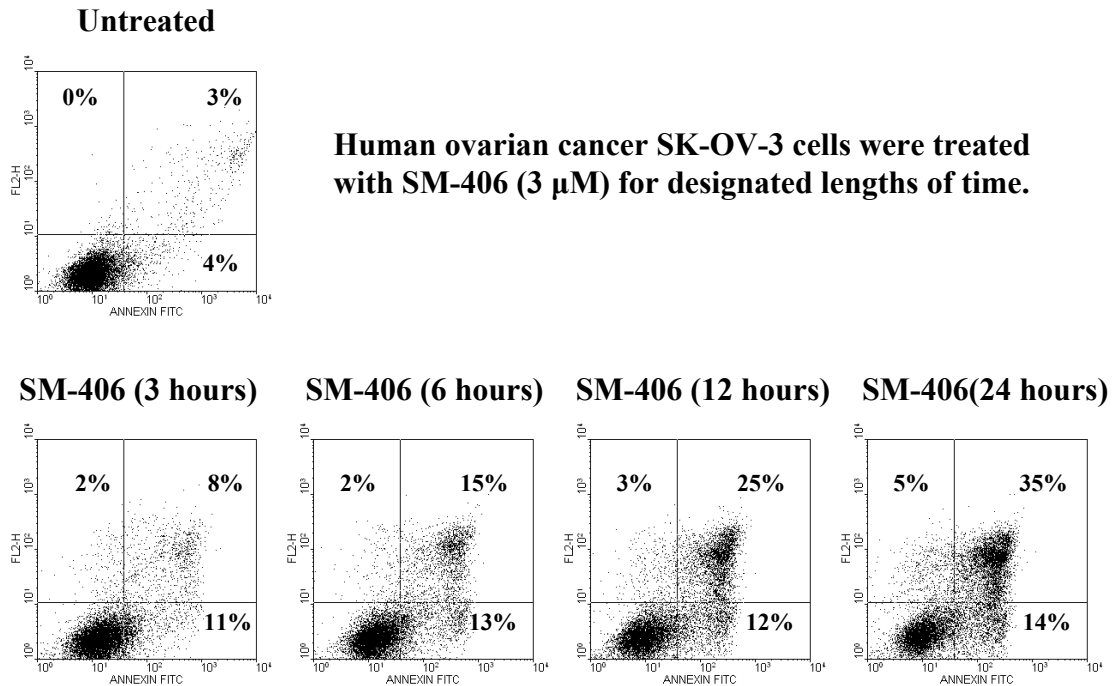
Figure 5.3 Annexin V and P.I. double staining flow cytometry of human ovarian cancer SK-OV-3 cells treated with 3 μM of Smac mimetic SM-406 for designated lengths of time.

Human ovarian cancer SK-OV-3 cells were first treated with different doses of Smac mimetic SM-406 and 3 μM of inactive control SM-428 for 24 hours, and then the apoptosis of SK-OV-3 cells was analyzed by Annexin V and P.I. double staining flow cytometry, as shown in Figure 5.2. As expected, SM-406 can induce apoptosis of SK-OV-3 cells in a dose-dependent manner.

The apoptosis induction behavior of SM-406 in SK-OV-3 cells was also studied in a time course. SK-OV-3 cells were treated with 3 μM of Smac mimetic SM-406 for

different lengths of time, and the apoptosis of SK-OV-3 cells was analyzed by using flow cytometry, as shown in Figure 5.3. The Smac mimetic SM-406 was shown to induce apoptosis of human ovarian cancer SK-OV-3 cells in a time-dependent manner.
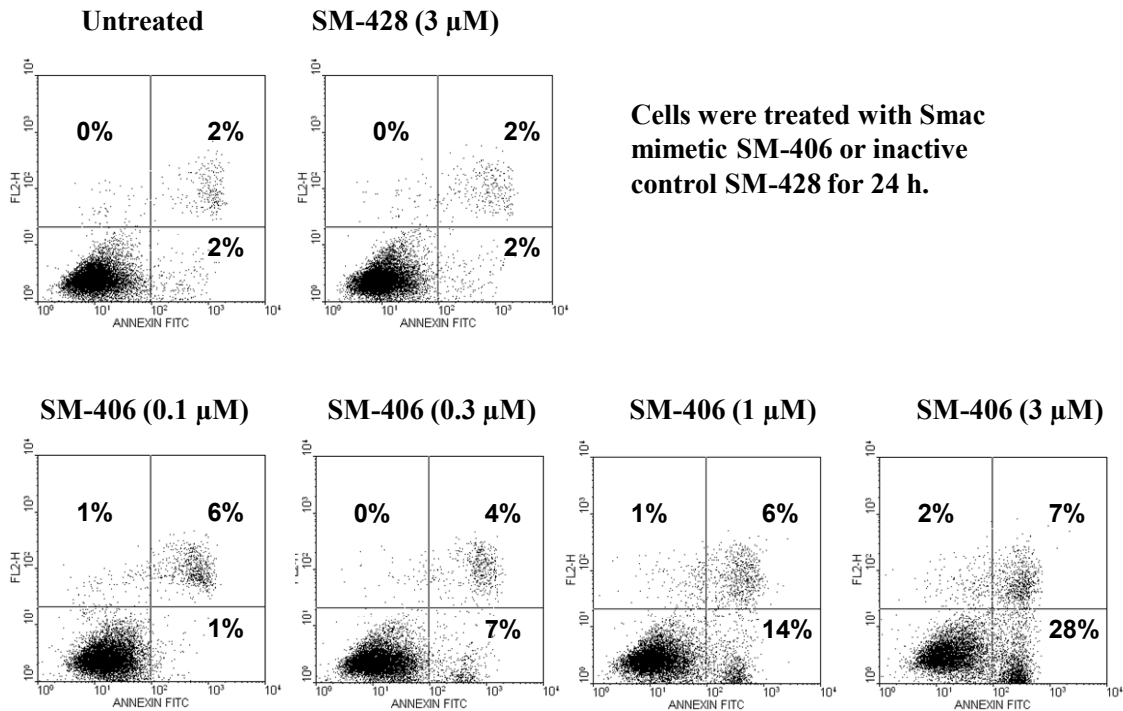
Figure 5.4 Annexin V and P.I. double staining flow cytometry of human breast cancer MDA-MB-231 cells treated with different doses of Smac mimetic SM-406 or inactive control SM-428 for 24 hours.

Human breast cancer MDA-MB-231 cells were also treated with different doses of Smac mimetic SM-406 or 3 μM of inactive control SM-428 for 24 hours. Apoptosis was analyzed by using flow cytometry as shown in Figure 5.4. The result shows that SM-406 can also induce apoptosis of MDA-MB-231 cells in a dose-dependent manner, while the inactive control SM-428 fails to induce apoptosis of tumor cells, compared with an untreated group. The time dependency of apoptosis induction of SM-406 in MDA-MB-231 cells was also studied. After MDA-MB-231 cells were treated with 3 μM

of Smac mimetic SM-406 or 3 μM of inactive control SM-428 for different lengths of time, the apoptosis of MDA-MB-231 cells was analyzed by Annexin V and P.I. double staining flow cytometry, as shown in Figure 5.5. Consistent with the results in human ovarian cancer SK-OV-3 cells, our Smac mimetic SM-406 was found to induce apoptosis in human breast cancer MDA-MB-231 cells in a time-dependent manner.

Untreated (24 hours)   **SM-428 (24 hours)**

Cells were treated with Smac mimetic SM-406 (3 μM) or inactive control SM-428 (3 μM) for designated time.

SM-406 (3 hours)   **SM-406 (6 hours)**   **SM-406 (12 hours)**   **SM-406 (24 hours)**
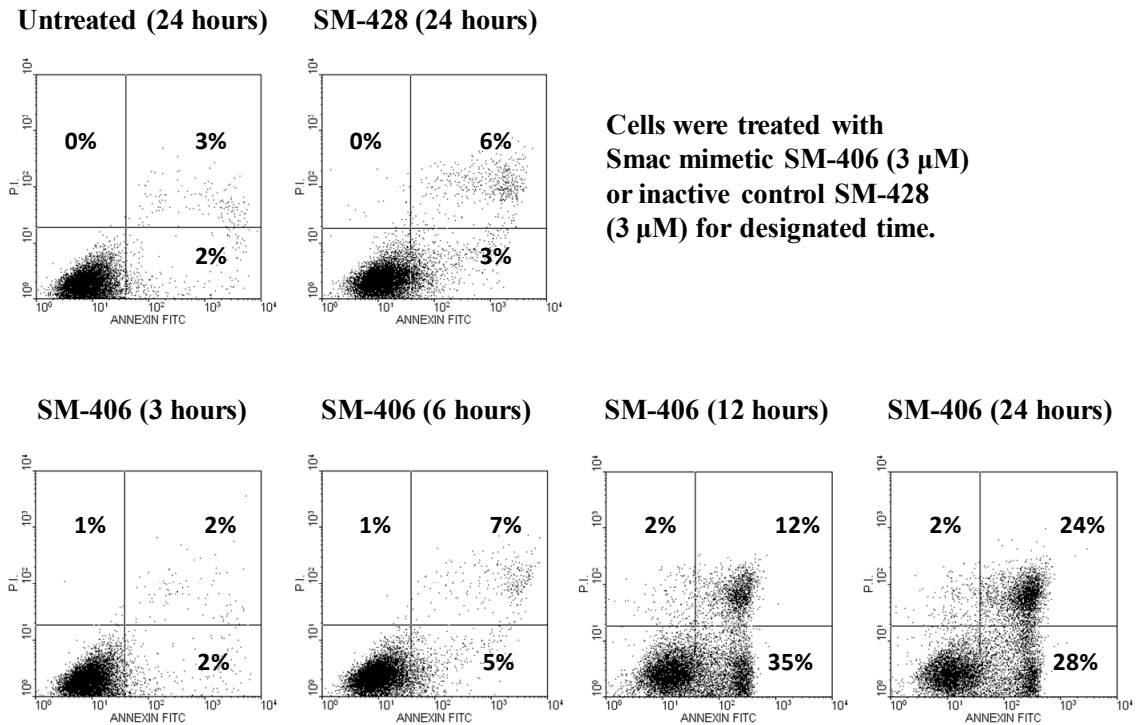
Figure 5.5 Annexin V and P.I. double staining flow cytometry of human breast cancer MDA-MB-231 cells treated with 3 μM of Smac mimetic SM-406 or 3 μM of inactive control SM-428 for designated lengths of time.

The apoptosis induction behavior of the Smac mimetic SM-406 in human melanoma MALME-3M cells were also analyzed by using Annexin V and P.I. double staining flow cytometry. As shown in Figure 5.6, the Smac mimetic SM-406 can dose-dependently induce apoptosis in MALME-3M cells, while the inactive control SM-428 cannot induce apoptosis of tumor cells compared with the untreated group.

101

Similarly, Smac mimetic SM-406 can also time-dependently induce apoptosis in MALME-3M cells, while the group treated with the same concentration of the inactive control SM-428 has almost no further induced apoptosis compared with the untreated group of MALME-3M cells, as shown in Figure 5.7.
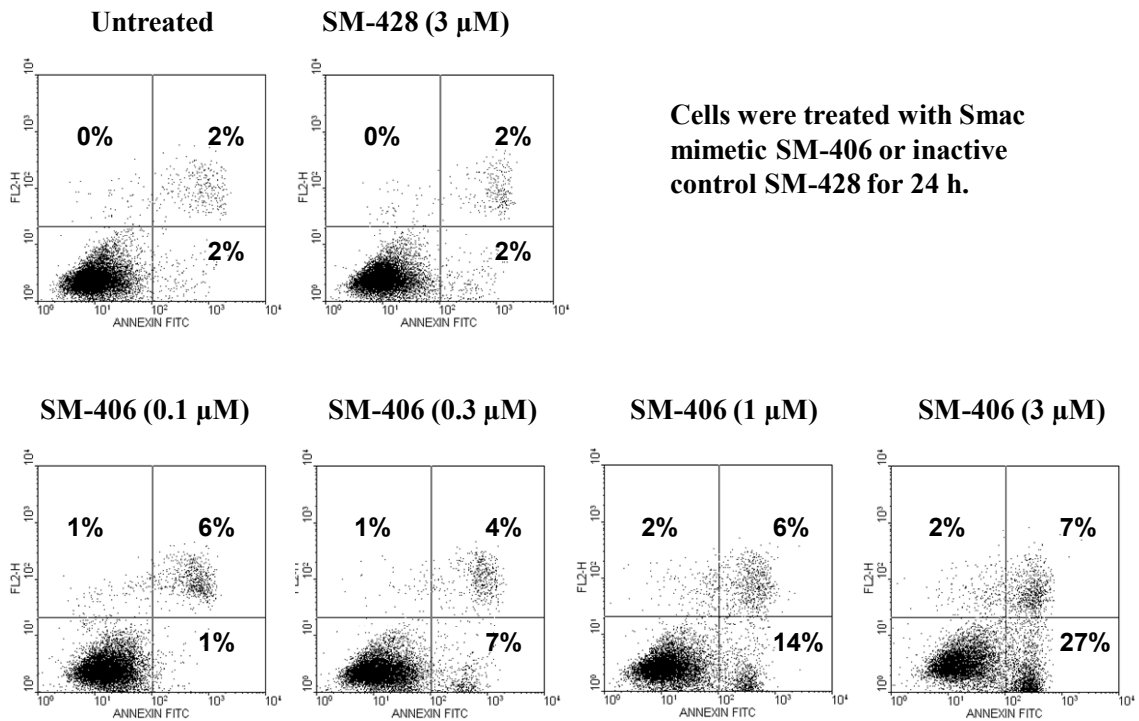
Figure 5.6 Annexin V and P.I. double staining flow cytometry of human melanoma MALME-3M cells treated with different doses of Smac mimetic SM-406 or inactive control SM-428 for 24 hours.

Untreated   SM-428 (3 µM) (24h)

Cells were treated with 3 µM of Smac mimetic SM-406 or inactive control SM-428 for designated lengths of time.

SM-406 (3 µM) 1h   3h   12h   24h
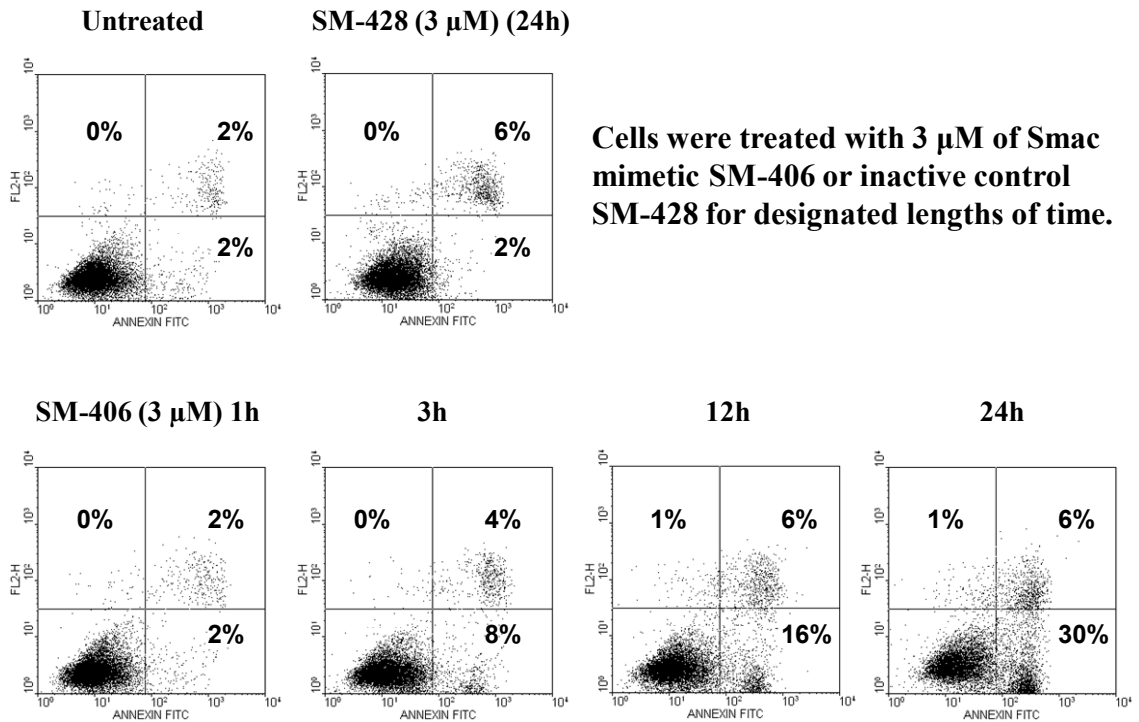
Figure 5.7 Annexin V and P.I. double staining flow cytometry of human melanoma MALME-3M cells treated with 3 µM of Smac mimetic SM-406 or 3 µM of inactive control SM-428 for designated lengths of time.

5.2.2 Tumor cell death induction activity of SM-406.

MDA-MB-231 cells treated with Smac mimetic SM-406 and inactive control SM-428 for 24 hours.   **SK-OV-3 cells treated with Smac mimetic SM-406 and inactive control SM-428 for 24 hours.**
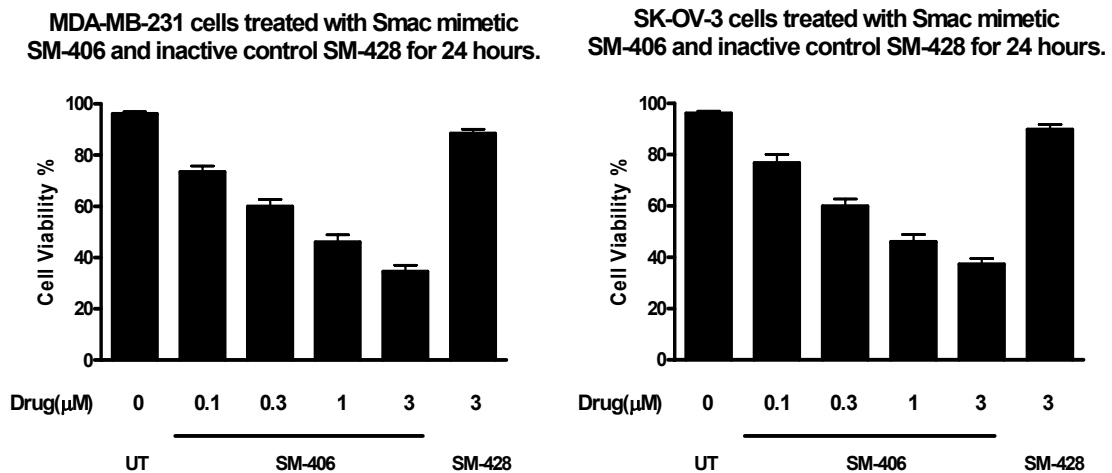
Figure 5.8 Cell viabilities of human breast cancer MDA-MB-231 cells and human ovarian cancer SK-OV-3 cells treated with different concentrations of Smac mimetic SM-406 or inactive control SM-428 for 24 hours, as analyzed by Trypan-blue-based cell death assay.

103

MDA-MB-231 cells treated by Smac mimetic SM-406 or inactive control SM-428 for designated lengths of time.
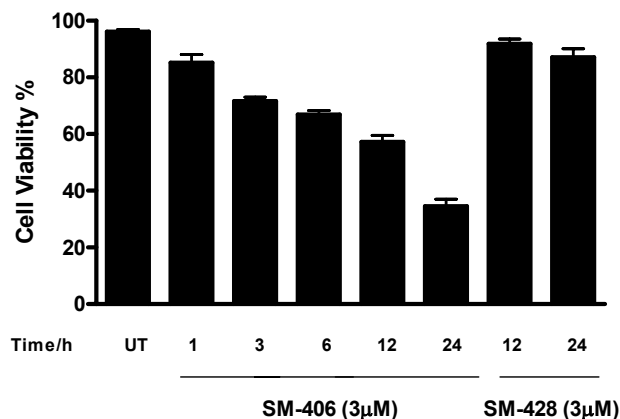
SK-OV-3 cells treated by Smac mimetic SM-406 or inactive control SM-428
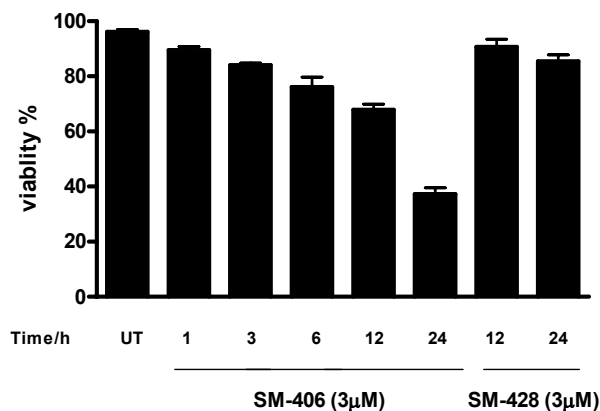
Figure 5.9 Cell viabilities of human breast cancer MDA-MB-231 cells and human ovarian cancer SK-OV-3 cells treated with 3 μM of Smac mimetic SM-406 or 3 μM of inactive control SM-428 for designated lengths of time, as analyzed by Trypan-blue-based cell death assay.

The cell death induction activity of Smac mimetic SM-406 in human breast cancer MDA-MB-231 cells and human ovarian cancer SK-OV-3 cells was investigated. Tumor cell lines were treated with different doses of Smac mimetic SM-406 or 3 μM of inactive control SM-428 for 24 hours. Then cell viabilities in these tumor cell lines were analyzed by using Trypan-blue based assay, in which Trypan blue can color dead cells blue but fails to color live cells with intact cell membranes. As shown in Figure 5.8, SM-406 can induce cell death in both human breast cancer MDA-MB-231 cells and

human ovarian cancer SK-OV-3 cells in a dose-dependent manner, while the inactive control SM-428 exhibits no tumor cell death induction activity.

The tumor cell death induction activity of SM-406 was also studied in a time course. MDA-MB-231 cells and SK-OV-3 cells were treated with 3 μM of Smac mimetic SM-406 or 3 μM of inactive control SM-428 for different lengths of time as shown in Figure 5.9, and tumor cell viabilities were analyzed by using Trypan-blue-based cell death assay. As expected, it was found that the Smac mimetic SM-406 can induce tumor cell death in these two different types of tumor cell lines in a time-dependent manner.

5.2.3 Cellular molecular effects of SM-406.

Figure 5.10 Western blotting assays of human breast cancer MDA-MB-231 cells and human ovarian cancer SK-OV-3 cells treated with different concentrations of Smac mimetic SM-406 or 3 μM of inactive control SM-428 for 24 hours.

To further explore the cellular activity of Smac mimetic SM-406 in tumor cells, PARP cleavage, IAP degradations, and caspase activations were monitored with Western blotting assays. Human breast cancer MDA-MB-231 cells and human ovarian cancer SK-OV-3 cells were treated with different doses of Smac mimetic SM-406 or 3 μM of inactive control SM-428. Then the cells were harvested, lysed and analyzed by Western blotting assays. As shown in Figure 5.10, Smac mimetic SM-406 can induce c-IAP1 and XIAP degradation, caspase-8, -3 and -7 activations in a dose-dependent manner in both MDA-MB-231 cells and SK-OV-3 cells. As expected, SM-406 can dose-dependently induce the cleavage of PARP (Poly ADP Ribose Polymerase), a substrate of active caspase-3 and also a marker of cells undergoing apoptosis in both tumor cell lines, consistent with the results of apoptosis analysis by using Annexin V and P.I. double staining flow cytometry. In contrast, inactive control SM-428 fails to induce PARP cleavage, IAP degradation, or caspase activation in either MDA-MB-231 cells or SK-OV-3 cells.

Smac mimetic SM-406 can induce PARP cleavage, cIAP-1 and XIAP degradation, caspase-8,9,3 and 7 activation and Smac release in both MDA-MB-231 and SK-OV-3 cells in a time-dependent manner.

Figure 5.11 Western blotting assays of human breast cancer MDA-MB-231 cells and human ovarian cancer SK-OV-3 cells treated with 3 μM of Smac mimetic SM-406 or 3 μM of inactive control SM-428 for designated lengths of time.

To explore the cellular molecular events induced by the Smac mimetic SM-406, MDA-MB-231 cells and SK-OV-3 cells treated with 3 μM of Smac mimetic SM-406 or 3 μM of the inactive control SM-428 for different lengths of time, and then PARP cleavage, IAP degradation and caspase activation were analyzed using Western blotting assays. As shown in Figure 5.11, SM-406 can induce PARP cleavage, c-IAP1 and XIAP degradation, and caspase-8, -9, -3 and -7 activations in a time-dependent manner in both MDA-MB-231 cells and SK-OV-3 cells. Smac proteins in cell cytosol were also probed, and the results show that SM-406 can also induce the release of Smac proteins in a time-dependent manner in both MDA-MB-231 cells and SK-OV-3 cells. In contrast, the

inactive control SM-428 cannot induce PARP cleavage, IAP degradation, caspase activation, or Smac release in either MDA-MB-231 cells or SK-OV-3 cells.

5.2.4 Co-immunoprecipitation assays confirm c-IAP1 and XIAP as the cellular targets of SM-406.
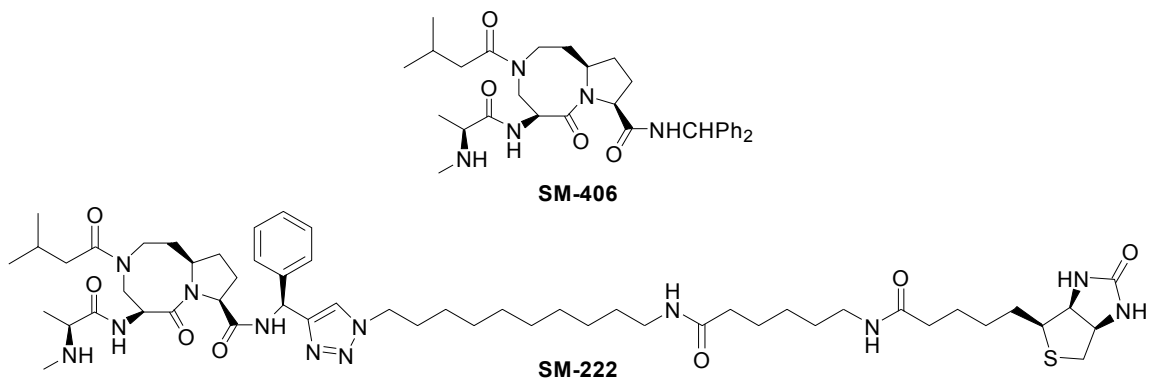
Figure 5.12 Chemical structures of Smac mimetic SM-406 and biotinylated Smac mimetic SM-222.

To provide direct evidence that SM-406 targets XIAP and c-IAP1 in cells, a biotinylated Smac mimetic SM-222 (Figure 5.12) was developed in our lab, and co-immunoprecipitation (co-IP) pull-down assays were performed using this biotinylated Smac mimetic SM-222 in both human breast cancer MDA-MB-231 cell lysates and human ovarian cancer SK-OV-3 cell lysates.

Our computational modeling studies show that the pro-(S) phenyl group in the tail region of SM-406 is oriented toward the solvent and has no specific interaction with the XIAP BIR3 domain. Hence, a linker tethering a biotin moiety can be linked to this pro-(S) phenyl ring to yield the biotinylated Smac mimetic SM-222. For ease of synthesis, this phenyl ring was replaced with a triazole ring, which can be easily linked by "click chemistry".[136-142] As shown in Figure 5.12, biotinylated Smac mimetic SM-222 shares the

same core structure with Smac mimetic SM-406. Our Fluorescence Polarization-based

assay showed that biotinylated Smac mimetic SM-222 ($K_i = 6.19 \pm 3.0$ nM) can bind with

the XIAP BIR 3 domain as effectively as SM-406.

SM-222 (uM)	-	0.3	1	3	3	3	3	3	3
SM-406 (uM)	-	-	-	-	0.3	1	3	-	-
SM-428 (uM)	-	-	-	-	-	-	-	3	10

cIAP1 72kd
XIAP 57kd
MDA-MB-231 cells

cIAP1 72kd
XIAP 57kd
SK-OV-3 cells
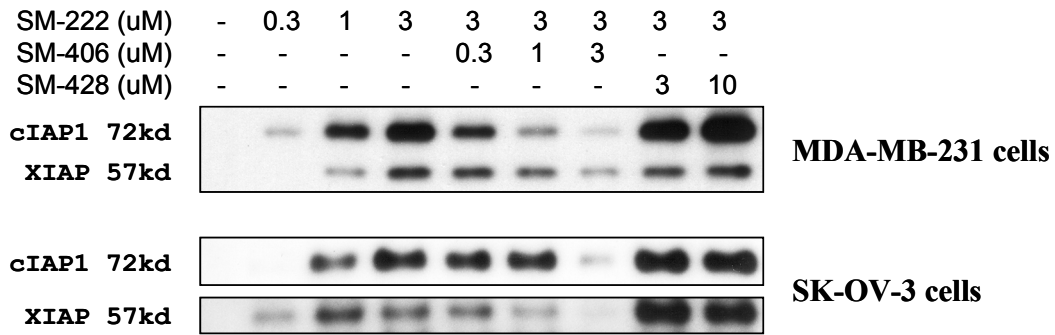
Figure 5.13 Probing the interaction of Smac mimetics to cellular XIAP and c-IAP1 in human breast cancer MDA-MB-231 cells and human ovarian cancer SK-OV-3 cells by competitive, co-immunoprecipitation pull-down assays using biotinylated Smac mimetic SM-222. MDA-MB-231 and SK-OV-3 cell lysates were incubated with SM-222 alone, or followed by co- incubation with Smac mimetic SM-406. Complexes formed between SM-222 and its targeted proteins were recovered by incubation with Streptavidin-argarose beads. XIAP and c-IAP1 proteins associated with beads were eluted by heating and detected by western blotting using monoclonal XIAP and c-IAP1 antibodies.

In Figure 5.13, the results of co-immunoprecipitation pull-down assays showed

that biotinylated Smac mimetic SM-222 can dose-dependently pull down XIAP and

c-IAP1 proteins in both human breast cancer MDA-MB-231 cell lysates and human

ovarian cancer SK-OV-3 cell lysates. Meanwhile, Smac mimetic SM-406 can effectively

compete off the binding between the biotinylated Smac mimetic SM-222 and c-IAP1 or

XIAP in a dose-dependent manner in lysates of both MDA-MB-231 cells and SK-OV-3

cells. In contrast, the inactive control SM-428 cannot compete off the binding between

SM-222 and c-IAP1 or XIAP in either MDA-MB-231 cell lysates or SK-OV-3 cell

lysates. Thus, the results of co-immunoprecipitation assays verify XIAP and c-IAP1 as

the intracellular targets of our Smac mimetics.

5.2.5 SM-406 can compensate for Smac knockdown in tumor cells.
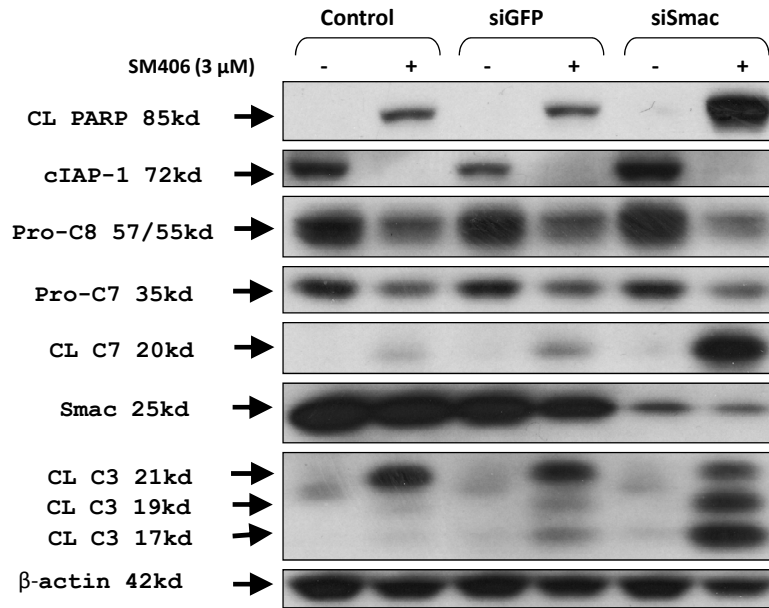
Figure 5.14 Western blotting assay of human ovarian cancer SK-OV-3 cells transfected with control siRNA oligonucleotides targeting GFP, or siRNA oligonucleotides targeting Smac for 48 hours, then treated with 3 μM of Smac mimetic SM-406 for 24 hours.

Cellular activities of SM-406 in Smac knockdown cells were tested to further verify the hypothesis that our small molecular Smac mimetics acquire cellular activity in tumor cells by mimicking Smac proteins,. Human ovarian cancer SK-OV-3 cells were first transfected with control Small Interfering RNA or Silencing RNA (siRNA) oligonucleotides targeting Green Fluorescent Protein (GFP) or Smac proteins for 48 hours, then treated with 3 μM of the Smac mimetic SM-406 for 24 hours. PARP cleavage, c-IAP1 and XIAP degradations, and caspase activations were analyzed by a Western blotting assay. As shown in Figure 5.14, SM-406 shows the same cellular activities in inducing PARP cleavage, IAP degradation and caspase activation in Smac protein knockdown SK-OV-3 cells, compared with untreated group and GFP knockdown group, verifying that Smac mimetic SM-406 can fully compensate for the reduction of Smac

proteins in SK-OV-3 cells.

   Similarly, human breast cancer MDA-MB-231 cells were also transfected with siRNA oligonucleotides targeting GFP or Smac proteins for 48 hours, and then treated with 3 μM of Smac mimetic SM-406 for 24 hours. As shown in Figure 5.15, Smac mimetic SM-406 can fully compensate the reduction of Smac proteins in MDA-MB-231 cells in the activity of inducing PARP cleavage, IAP degradation and caspase activation in tumor cells.
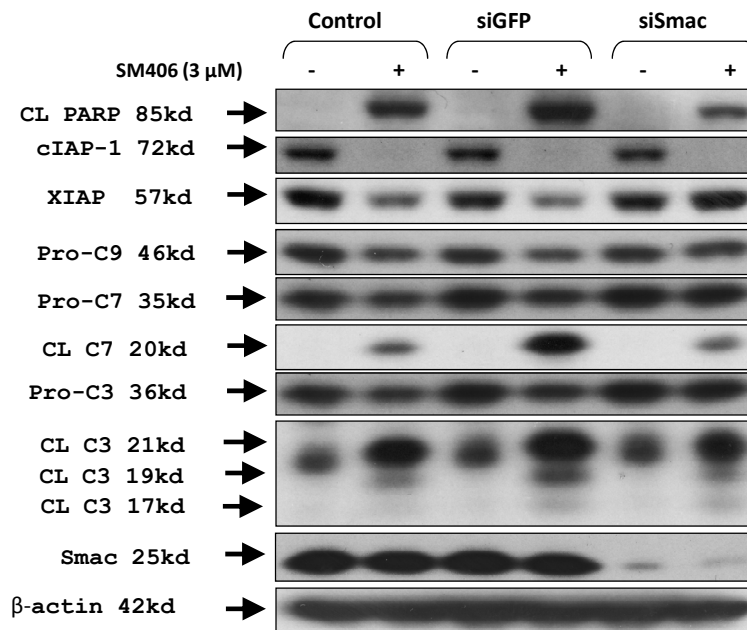
Figure 5.15 Western blotting assay of human breast cancer MDA-MB-231 cells transfected with control siRNA oligonucleotides targeting GFP, or siRNA oligonucleotides targeting Smac for 48 hours, then treated with 3 μM of Smac mimetic SM-406 for 24 hours.

   The ability of Smac mimetic SM-406 to induce tumor cell death in MDA-MB-231 cells and SK-OV-3 cells which were transfected with siRNA against Smac protein, was analyzed by using Trypan blue cell death assay. As shown in Figure 5.16, Smac knockdown has no influence on the ability of the Smac mimetic SM-406 in inducing

tumor cell death in both MDA-MB-231 and SK-OV-3 cells, further verifying that Smac mimetic SM-406 can fully compensate the reduction of Smac proteins in tumor cells, consistent with the results of Western blotting assays.
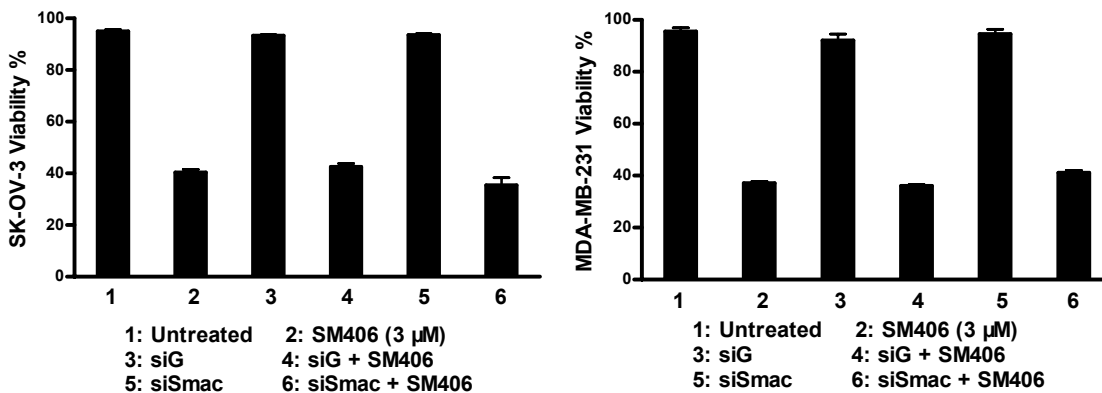
Figure 5.16 Human ovarian cancer SK-OV-3 cells and human breast cancer MDA-MB-231 cells were first transfected with control siRNA oligonucleotides targeting GFP, or siRNA oligonucleotides targeting Smac for 48 hours, then treated with 3 μM of Smac mimetic SM-406 for 24 hours. Cell viabilities were analyzed by using Trypan-blue-based cell death assay.

5.2.6 Study of caspase dependence in the cellular activity of SM-406 in tumor cells

To further investigate caspase dependence in the cellular activity of the Smac mimetic SM-406, caspase inhibitors were used to inhibit caspase activity in tumor cells. After human breast cancer MDA-MB-231 cells and human ovarian cancer SK-OV-3 cells were treated with Smac mimetic SM-406 alone or in combination of 25 μM of caspase-9, -8, -3 inhibitors respectively, cell viabilities were analyzed by using Trypan blue cell death assays. As shown in Figure 5.17, the Smac mimetic SM-406 can induce cell death in both tumor cell lines in a dose-dependent manner, consistent with the previous study. Inhibition of active caspase-3 can rescue cells from death in both tumor cell lines, suggesting that the ability of SM-406 in dose-dependently inducing cell death in these two tumor cell lines is dependent on the activation of caspase-3. However, inhibition of

active caspase-9 cannot rescue tumor cells from death in either MDA-MB-231 cells or SK-OV-3 cells; in contrast, inhibition of active caspase-8 can rescue cells from death in both tumor cell lines.
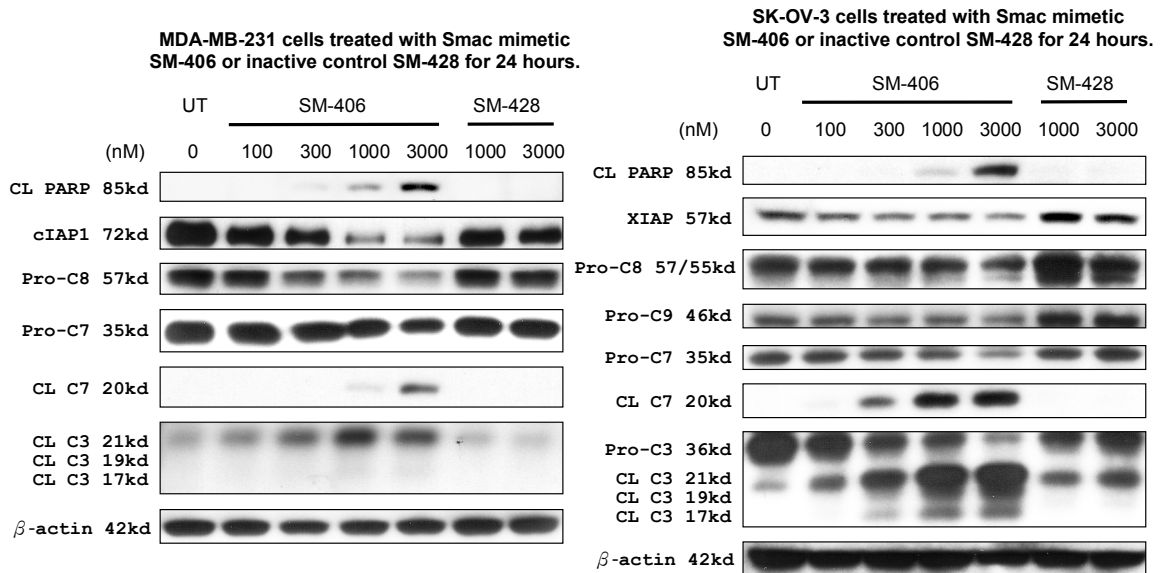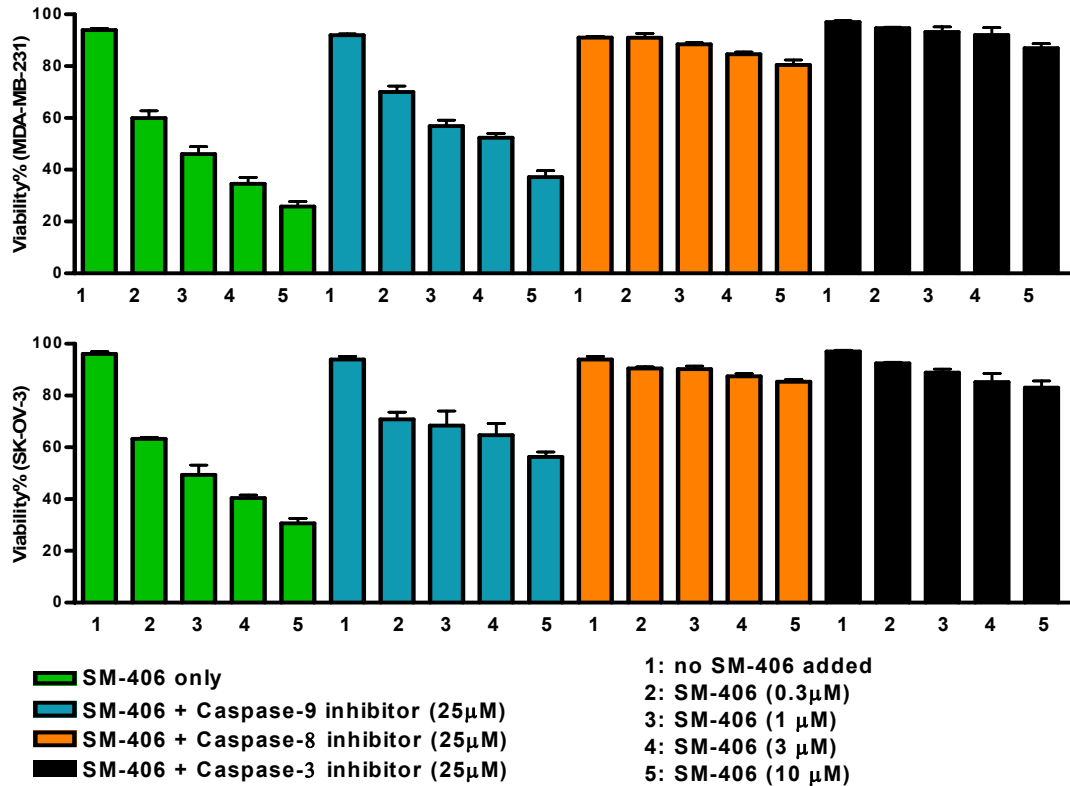

Figure 5.17 Cell viabilities of human breast cancer MDA-MB-231 cells and human ovarian cancer SK-OV-3 cells treated with designated concentrations of Smac mimetic SM-406 alone or in combination with 25 μM of caspase-9, -8, and -3 inhibitors for 24 hours, as analyzed by Trypan-blue-based cell death assay.

Therefore, Trypan-blue assay results show that the ability of Smac mimetic SM-406 in dose-dependently inducing cell death in MDA-MB-231 cells and SK-OV-3 cells is dependent on the activities of caspase-8 and caspase-3, but only partially on the activity of caspase-9. This interesting result contradicts our hypothesis that the Smac mimetic SM-406 induces tumor cell death by binding with XIAP and antagonizing its inhibition of caspase-9 to promote apoptosis in tumor cells. In order to further investigate the importance of caspase-9, -8 and -3, Western blotting assays were performed to

monitor caspase activation and cleavage of PARP by using caspase inhibitors and

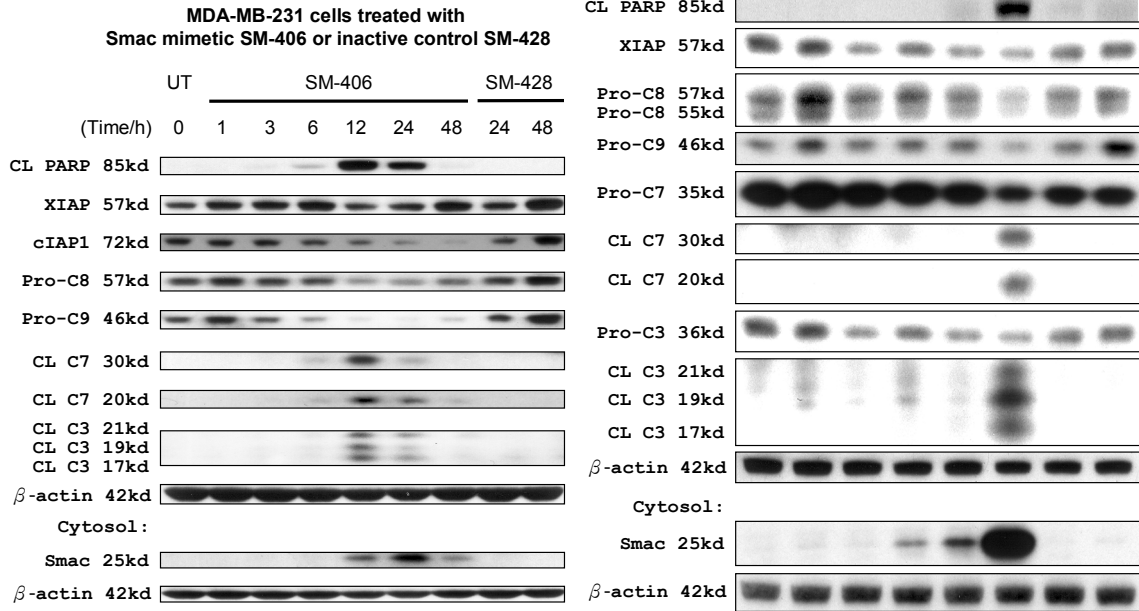siRNAs against caspase-9, -8, and -3 (Figure 5.18 and 5.19).
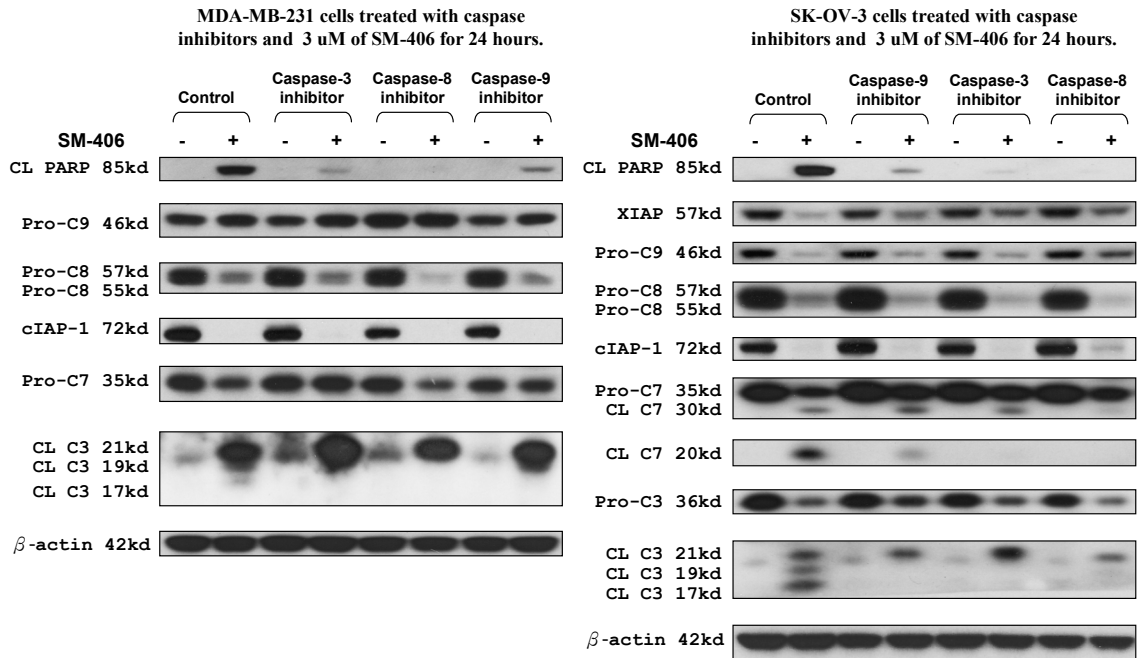
Figure 5.18 Western blotting assays of human breast cancer MDA-MB-231 cells and human ovarian cancer SK-OV-3 cells treated with 3 μM of Smac mimetic SM-406 alone or in combination with 25 μM of caspase-9, -8, and -3 inhibitors for 24 hours.

Consistent with the results of Trypan-blue-based cell death assays, Western

blotting assays of MDA-MB-231 cells and SK-OV-3 cells treated with 3 μM of Smac

mimetic SM-406 alone or in combination with 25 μM of caspase-9, -8, and -3 inhibitors

respectively, show that SM-406 with the caspase-9 activity blocked can still induce

PARP cleavage and caspase-3 and -7 activations, but has less potency compared with the

treatment of SM-406 alone in both tumor cell lines. In contrast, SM-406 loses its ability

in inducing PARP cleavage and caspase-3 and -7 activations, when the activity of

caspase-8 is blocked by caspase-8 inhibitor. Interestingly, our Smac mimetic SM-406 can

114

induce the degradation of c-IAP1 in both tumor cell lines, whether caspase-9, -8, or -3 is

blocked or not. However, there was no dramatic degradation of XIAP compared with

c-IAP1, when cells were with SM-406.
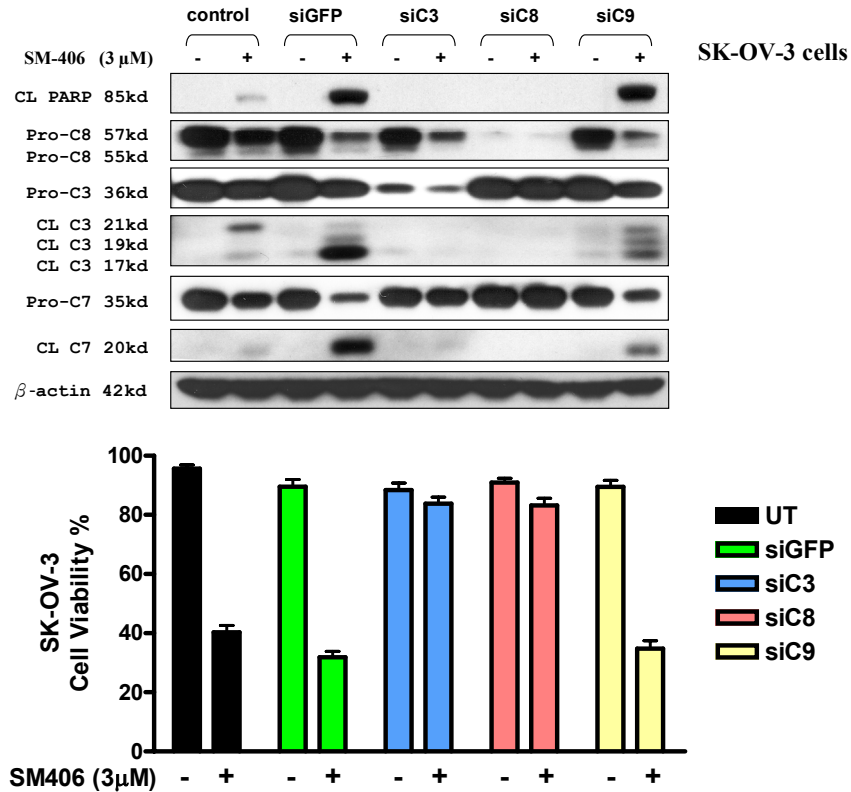
Figure 5.19 Top: Western blotting assay of human ovarian cancer SK-OV-3 cells transfected with control siRNA oligonucleotides targeting GFP, or siRNA oligonucleotides targeting caspase-9, -8 and -3 for 48 hours, then treated with 3 μM of Smac mimetic SM-406 for 24 hours. Bottom: Cell viability of SK-OV-3 cells, as analyzed by Trypan-blue based cell death assay.

SiRNAs against caspase-9, -8, and -3 were used to further investigate caspase

dependence in the activity of SM-406 in tumor cells,. Human ovarian cancer SK-OV-3

cells were first transfected for 48 hours with control siRNA oligonucleotides targeting

either GFP or caspase-9, -8, and -3, then treated with 3 μM of the Smac mimetic SM-406

for 24 hours. SK-OV-3 cell viability was analyzed by Trypan-blue based cell death assay,

giving results consistent with the previous studies. SM-406 induced tumor cell death even

though caspase-9 was reduced; however, tumor cells were almost completely rescued from the treatment with SM-406 when caspase-8 or caspase-3 was reduced. Western blotting assays show the same result: SM-406 still induces PARP cleavage and caspase-3 and -7 activations when caspase-9 is reduced; however, SM-406 loses its activity when either caspase-8 or caspase-3 was reduced by siRNAs.

Hence, from the above investigations by using both caspase inhibitors and siRNAs, it appears that the activity of SM-406 in inducing cell death, PARP cleavage, and caspase-3 and -7 activations in MDA-MB-231 cells and SK-OV-3 cells is mainly dependent on caspase-8 and caspase-3 rather than caspase-9.

5.2.7 SM-406 can induce fast degradation of c-IAP1 but not XIAP.

Recently, it was found that Smac mimetics can induce fast degradation of c-IAP1 but not XIAP,[192-194] and this may assist in elucidation of the molecular mechanism of Smac mimetics in inducing tumor cell apoptosis.[195] The ability of our Smac mimetic SM-406 in inducing c-IAP1 and XIAP degradations was further probed. As shown in Figure 5.20, SM-406 can induce fast degradation of c-IAP1 but not XIAP in both human breast cancer MDA-MB-231 cells and human ovarian cancer SK-OV-3 cells. Complete degradation of c-IAP1 was complete within five minutes of treatment; however, the degradation of XIAP was not observed until 12 hours of treatment in SK-OV-3 cells or 6 hours in MDA-MB-231 cells, when tumor cells were treated with 3 μM of SM-406.

**Human ovarian cancer SK-OV-3 cells treated with
3 μM of Smac mimetic SM 406 for designated lengths of time.**

	UT	5min	15min	30min	1h	3h	6h	12h	24h
c-IAP1 72kd ➡									
XIAP 57kd ➡									
β-actin 42kd ➡									

**Human breast cancer MDA-MB-231 cells treated with
3 μM of Smac mimetic SM 406 for designated lengths of time.**

	UT	5min	15min	30min	1h	3h	6h	12h	24h
c-IAP1 72kd ➡									
XIAP 57kd ➡									
β-actin 42kd ➡									
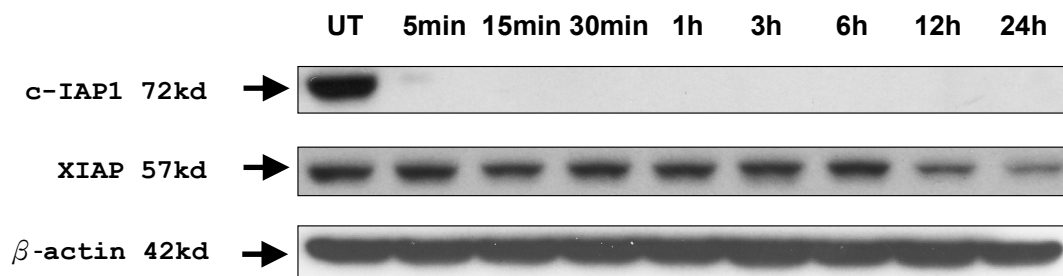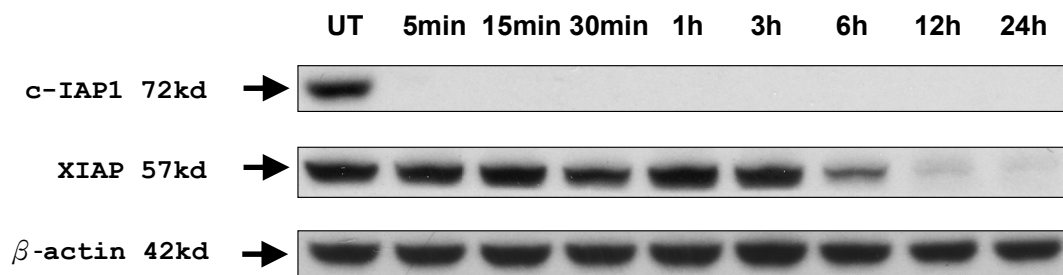
Figure 5.20 Western blotting assays of human ovarian cancer SK-OV-3 cells and human breast cancer MDA-MB-231 cells treated with 3 μM of Smac mimetic SM-406 for designated lengths of time.

The results that Smac mimetic SM-406 can induce fast c-IAP1 degradation but not XIAP are consistent with the recently published work,[192-195] in which a plausible cellular mechanism of IAC (IAPs Antagonist Compound)-induced tumor cell death in IAC sensitive cells was advanced. Fast degradation of c-IAP1 caused by the Smac mimetic SM-406 recruits Receptor-Interacting Protein (RIP) and activates canonical NF-κB (Nuclear Factor-κB) pathway. The non-canonical pathway is also activated by the inhibition of c-AIP1 with an increase in levels of Nim1-like Protein Kinase (NIK1) and processing of p100. In IAC-sensitive cells such as MDA-MB-231 and SK-OV-3 cells, the activation of NF-κB causes an increase in levels of TNFα, killing these tumor cells through enhanced apoptotic TNF-R1 signaling.[192-194] A recent study also shows that the

degradation of c-IAP1/2 caused by Smac mimetics leads to the release of receptor interacting protein kinase (RIPK1) from the activated TNF receptor complex to form a caspase-8-activating complex consisting of RIPK1, FADD, and caspase-8. The activated initiator caspase-8 then activates effector caspases to promote apoptosis in tumor cells.[195]

5.3 Conclusion

The investigations of cellular molecular activity based on the potent Smac mimetic SM-406 show that SM-406 can induce apoptosis and cell death in MDA-MB-231 cells and SK-OV-3 cells in a dose- and time-dependent manner, as analyzed by Annexin V, P.I. double staining flow cytometry and Trypan-blue based cell death assays respectively. SM-406 can also dose- and time-dependently induce PARP cleavage, c-IAP1 and XIAP degradation, and caspase activation in MDA-MB-231 cells and SK-OV-3 cells, as tested by Western blotting assays. Co-immunoprecipitation assays using both the biotinylated Smac mimetic SM-222 and potent Smac mimetic SM-406 verify c-IAP1 and XIAP as the cellular targets of our Smac mimetics.

Caspase dependence in the cellular activity of SM-406 was studied by blocking caspase-9, -8, and -3 activities with either caspase inhibitors or siRNAs against each caspase. Both Trypan-blue based cell death assays and Western blotting assays show that the ability of SM-406 in inducing tumor cell death, PARP cleavage, and caspase activations is mainly dependent on caspase-8 and caspase-3, but only partially dependent on caspase-9.

The Smac mimetic SM-406 can induce a complete and fast degradation of c-IAP1 but not XIAP. The complete degradation of c-IAP1 was finished within 5 minutes, while the degradation of XIAP did not show up until 6 hours of treatment in either MDA-MB-231 or SK-OV-3 cells. As the half life of SM-406 determined bypharmacokinetic studies (Table 5.1) is 1.78 hours, the main cellular target of SM-406 can be c-IAP1 instead of XIAP. Recently, a possible cellular mechanism of SM-406 in inducing tumor cell apoptosis was proposed: fast degradation of c-IAP1 caused by the Smac mimetic SM-406 recruits RIP (Receptor-Interacting Protein) and activates the canonical NF-κB pathway. The non-canonical pathway is also activated by the inhibition of c-IAP1 with an increase in levels of NIK1 and processing of p100. In IAC-sensitive cells such as MDA-MB-231 and SK-OV-3 cells, the activation of NF-κB causes an increase in levels of TNFα, killing these tumor cells through enhanced apoptotic TNF-R1 signaling.[192-194] Recent study also showed that the degradations of c-IAP1/2 caused by Smac mimetics lead to the release of RIPK1 from the activated TNF receptor complex to form a caspase-8-activating complex consisting of RIPK1, FADD, and caspase-8. The activated initiator caspase-8 then activates effector caspases to promote apoptosis in tumor cells.[195] Further studies aimed at elucidating the cellular mechanism of Smac mimetics are continuing.[196]

5.4 Methods and Materials

Cell Culture: Human breast cancer cells (ATCC$^®$) were maintained at 37ºC, 95% air, 5% carbon dioxide in modified IMEM (with L-glutamine, without gentamicin sulfate, GIBCO™, Invitrogen Corp.) supplemented with 10% Fetal Bovine Serum (FBS, Hyclone$^®$, QB Perbio) and passaged twice weekly. Human ovarian cancer cells (ATCC$^®$) were maintained at 37ºC, 95% air, 5% carbon dioxide in HyQ$^®$ RPMI-1640 medium (with 2.05 mM L-glutamine, 0.1 μM sterile filtered, Hyclone$^®$, QB Perbio) supplemented with 10% FBS and passaged twice weekly. Human melanoma MALME-3M cells were maintained at 37ºC, 95% air, 7% carbon dioxide in HyQ$^®$ RPMI-1640 medium supplemented with 15% FBS and passaged twice weekly.

Cell Transient Transfection by siRNA: To 1 mL of reduced serum medium (Opti-MEM$^®$, GIBCO$^®$, Invitrogen™ Inc.) in a 50 mm Petri Dish were added 100 pmol of siRNA and 10 μL of Lipofectamine RNAiMAX reagent (Lipofectamine™, Invitrogen™ Inc.) The mixture was incubated at room temperature for 15 minutes, followed by adding 5 mL of diluted cells in medium without antibiotics, and mixed gently and were allowed to grow for 48 hours in the incubator. Western Blotting assay was performed to determine the efficiency when downregulation of targeting genes and transfected cells were subjected to further experiments. For studying the effect of siRNA knockdown on cell growth inhibition, after mixing with reduced serum medium containing siRNA and Lipofectamine RNAiMAX, cells were transferred into 96-well plates, and subjected to WST-based cell growth assay. Small interfering RNA oligonucleotides (siRNAs): against Smac (targets 156-176 aaccctgtgtgcggttcctat, QIAGEN Inc.); against caspase-3 (Singal Silence™ pool caspase-3 siRNA, Cell Signaling Technology$^®$); against caspase-8

(caspase-8 siRNA pool, Eurogentec Corp.); against caspase-9 (Smart Pool™ caspase-9 siRNA, Dharmacon Inc.); against negative control nonsilencing GFP (Green Fluorescence Protein) (targets 322-342 aagacccgcgccgaggtgaag, QIAGEN Inc.).

Antibodies and Caspase Inhibitors: Primary antibodies against cleaved PARP (85 kDa, source: rabbit, Eptiomics® Inc.),[197-200] caspase-9 (46 kDa, source: mouse, Stressgen Biotechnologies),[201-207] caspase-8 (57 kDa, 55 kDa, source: mouse, Stressgen Biotechnologies),[208-210] caspase-3 (35 kDa, 19 kDa, 17 kDa, source: rabbit, Stressgen Biotechnologies),[211-219] caspase-7 (35 kDa, 30 kDa, 20 kDa, source: mouse, Cell Signaling Technology®),[220-226] c-IAP1 (72 kDa, source: rabbit, R&D Systems Inc.),[227-230] XIAP (57 kDa, source: mouse, BD Biosciences Pharmingen™),[231-233] Smac (25 kDa, source: rabbit, Calbiochem®),[234] Cyt C (14 kDa, source: rabbit, Cell Signaling Technology®),[235-237] β-actin (42 kDa, source: mouse, Sigma®).[238,239] New primary antibody against c-IAP1 was kindly provided by Dr. John Silke.[193] Second antibodies against mouse IgG (H+L) (host: goat, Immuno Pure®, Thermo Scientific), rabbit IgG (H+L) (host: goat, Immuno Pure®, Thermo Scientific). Caspase-9 inhibitor I ($C_{32}H_{43}FN_6O_{10}$, 668.7 g/mol, Calbiochem®), Caspase-8 inhibitor I ($C_{21}H_{34}FN_4O_{10}$, 502.5 g/mol, Calbiochem®), Capase-3 inhibitor II ($C_{30}H_{41}FN_4O_{12}$, 690.7 g/mol, Calbiochem®).

Apoptosis Flow Cytometry: Apoptosis flow cytometry was performed with an Annexin-V and Propidium Iodide (PI) apoptosis detection kit (Annexin-V- FLUOS staining kit, Roche® Diagnostics) according to the manufacturer's instructions. After treated with Smac mimetics for the designated time, cells were harvested, washed with

ice-cold PBS (Phosphate Buffer Saline pH 7.4, 1X, GIBCO®, Invitrogen Corp.), and then stained with Annexin-V-FITC and PI for 15 minutes at room temperature in the dark. Stained cells were analyzed in a FACS caliber flow cytometer. Annexin-V positive cells were measured as apoptotic cells while Annexin-V negative and PI positive cells were analyzed as death cells.[240-246]

Trypan-blue-based Cell Death Assay: Cell viability was quantitated by a microscopic examination (model: CKX41, 10X, Olympus®) in a Trypan blue exclusion assay. After treated with Smac mimetics for a designated time, cells were harvested, and stained with an equal volume of 0.4% Trypan Blue (membrane filtered prepared in 0.85% saline, GIBCO®, Invitrogen Corp.). For the combination treatment of Smac mimetic and caspase inhibitor, cells were treated with Smac mimetic after 1 hour treatment with the designated caspase inhibitor. Both blue cells and morphological shrunk cells were scored as nonviable cells. At least 100 cells from each treatment, performed in triplicate, were counted.

WST-based Cell Growth Assay: Cells were seeded in 96-well flat bottom cell culture plates at a density of $3\text{-}4 \times 10^3$ cells/well with compounds and incubated for 4 days. The rate of cell growth inhibition after treatment with different concentrations of the inhibitors was determined by WST (2-(2-methoxy-4-nitrophenyl)-3-(4-nitrophenyl)-5-(2,4-disulfophenyl)-2H-tetrazolium monosodium salt (Dojindo Molecular Technologies Inc., Gaithersburg, Maryland). WST was added at a final concentration of 10% to each well, and then the plates were incubated at 37°C for 2-3 hrs. The absorbance of the

samples was measured at 450 nm using a TECAN ULTRA Reader. The concentration of the compounds that inhibited cell growth by 50% (IC_{50}) was calculated by comparing absorbance in the untreated and treated cells.

Western Blotting Assay: After treatment with Smac mimetics for a designated time, cells were harvested and washed with ice-cold PBS. Cell pellets were lysed in DLB (Double Lysis Buffer: 50 mmol/L Tris, 150 mmol/L Sodium Chloride, 1 mmol/EDTA [Ethylenediaminetetraacetic Acid], 0.1% SDS [Sodium Dodecyl Sulfate] and 1% NP-40 [Nonidet P 40, Igepal CA 630, BioChemika™, Fluka®, Sigma-Aldrich]) in the presence of 1 mmol/L PMSF (Phenylmethylsulphonyl Fluoride) and 2 mmol/L protease inhibitor cocktail (Complete™, Roche® Diagnostics) for 10 minutes on ice and then centrifuged at 13,000 rpm at 4ºC for 10 minutes. Protein concentrations were determined with a Bio-Rad Protein assay kit (Bio-Rad protein assay, dye reagent concentrate, Bio-Rad Laboratories® Inc.) according to manufacturer's instructions. Proteins were electrophoresed onto 4% SDS-PAGE (Polyacrylamide Gel Electrophoresis, Invitrogen™ Corp.) and then transferred to PVDF (Polyvinylidene Difluoride, Immun-Blot® PVDF membrane for protein blotting, Bio-Rad® Laboratories) membranes. Following blocking with 5% milk (blotting grade blocker non-fat dry milk, Bio-Rad® Laboratories), 0.1% Tween 20 (Fisher BioReagents®, Fisher Scientific) in 10X TBS (10X Tris-Buffered Saline, Bio-Rad® Laboratories); membranes were incubated with specific primary antibodies, washed with 10X TBS in triplicate, and incubated with linked second antibodies. The signals were visualized with the Lumi-Light Western Blotting substrate

detection kit (Lumi-Light Luminol/Enhancer solution and Sable Peroxide solution, Roche® Diagnostics).

Cell Fractionation: After treated with Smac mimetics for a designated time, cells were harvested and washed with ice-cold PBS. Cells were suspended at 3×10^7 cells/ml in MRB (Mitochondrial Resuspension Buffer: 250 mmol/L Sucrose, 10 mmol/L Potassium Chloride, 1.5 mmol/L Magnesium Dichloride, 1 mmol/L EDTA, 1 mol/L DTT [Dithiothreitol], 1 mmol/L PMSF, and 700 μg/mL of Digitonin), and 2 mmol/L protease inhibitor cocktail (Complete™, Roche® Diagnostics) for 10 minutes on ice and then centrifuged at 13,000 rpm at 4ºC for 10 minutes. The supernatants (cytosol fraction) were collected and the membrane pellets were lysed in DLB as described above, and the supernatants (mitochondrial fraction) were collected. The two fractions were subjected to Western Blotting assay.

Co-immunoprecipitation Assay: Cellular interactions of Smac mimetic SM-406, biotinylated Smac mimetic SM-222, inactive control SM-428 and c-IAP1 and XIAP were investigated by using a Biotin-Streptavidin pull-down assay. Cells were lysed in lysis buffer (20 mmol/L Tris, 150 mmol/L Sodium Chloride, and 1% NP-40) for 20 minutes. Cell lysates were precleared with Streptadvidin-Agarose beads (Upstate®, Milipore Corp.), incubated with biotinylated Smac mimetic SM-222, alone for pull down assay, or preincubated with SM-406 or SM-428 followed by co-incubation with SM-222 for competitive experiments. Complexes formed by Smac mimetics and the associated proteins were recovered by incubation with 100 μL of Streptadvidin-Agarose beads on a

124

shaker at 4ºC for 2 hours and then centrifuged at 10,000 rpm for 1 minute. The complexes were then washed three times with lysis buffer at 4ºC and eluted from the beads by boiling in 100 μL of SDS loading buffer. The eluted proteins were detected by Western Blotting assay by using the procedure described above.

CHAPTER 6

CONCLUSION

A series of monovalent and bivalent small-molecular, non-peptidic and cell-permeable Smac mimetics have been successfully developed.

For monovalent Smac mimetics, SM-245 and SM-246, in which an alkyl group is attached to the nitrogen atom in the 8-membered ring in the bicyclic system, have less potency in binding with XIAP BIR3 domain than the original lead compound SM-122. However, with the insertion of a carbonyl between the alkyl group and the nitrogen atom, SM-330 and SM-337 have improved binding potency compared with SM-245 and SM-246 against the XIAP BIR3 domain. Both SM-330 and SM-337 are 5 and 7 folds more potent than the original lead compound SM-122 in binding to the XIAP BIR3 domain respectively. These potent Smac mimetics can also bind c-IAP1/2 with high affinities as was shown in Chapter 3, with high potency in antagonizing c-IAP1/2.

Cellular studies of these monovalent Smac mimetics show that each Smac mimetic can dose- and time-dependently induce apoptosis and cell death in human breast cancer MDA-MB-231 and SK-OV-3 cells. Monovalent Smac mimetics can also efficiently inhibit tumor cell growth of MDA-MB-231, SK-OV-3 and human melanoma MALME-3M cells, as tested by using WST-based cell growth assays. The cellular

potency of these monovalent Smac mimetics is consistent with their binding potency against the XIAP BIR3 domain.

Our cell-free functional assays show that these monovalent Smac mimetics can compete off the inhibition of XIAP to recover the activity of caspase-3/7 in a dose-dependent manner, further showing their excellent potency in antagonizing XIAP. Monovalent Smac mimetics show a drug synergy effect with TRAIL in inhibiting tumor cell growth of human breast cancer MDA-MB-231 and 2LMP cells in a dose-dependent manner, as tested by using WST-based cell growth assays.

The cellular molecular events caused by our monovalent Smac mimetics were further probed by using Western blotting assays. The results show that monovalent Smac mimetics can dose-dependently induce PARP cleavage, c-IAP1 degradation, and caspase activations in MDA-MB-231 and SK-OV-3 cells.

For bivalent Smac mimetics, SAR for the bivalent linker was explored. In the five tested bivalent Smac mimetics, the linker has 2 to 10 methylene groups. The results show that the binding potency against XIAP BIR3 domain decreases as the length of the bivalent linker increases. However, all the bivalent Smac mimetics have similar binding potency against linker-BIR2-BIR3 protein as measured by our fluorescence-polarization based assay. Each bivalent Smac mimetic is 10 to 20 times more potent in binding with linker-BIR2-BIR3 protein than BIR3 only. Meanwhile, the cellular potency of bivalent Smac mimetics increases as the length of the bivalent linker increases, suggesting that bivalent Smac mimetics do not interact with XIAP BIR3 domain only.

Each bivalent Smac mimetic can efficiently inhibit tumor cell growth of MDA-MB-231, SK-OV-3 and MALME-3M cells, as tested in WST-based cell growth

assays. This tumor cell growth inhibition activity increases as the bivalent linker increases in length. However, SM-381 and SM-383, with 8 and 10 methylene groups in the bivalent linker, show the same cellular potency, suggesting that SM-381 may have already reached the optimal length for the bivalent linker.

As tested by Trypan blue cell death assays, each bivalent Smac mimetic can dose- and time-dependently induce tumor cell death in MDA-MB-231 and SK-OV-3 cells. Bivalent Smac mimetics can also induce apoptosis in MDA-MB-231 and SK-OV-3 cells in a dose-dependent manner, as tested by using Annexin V and P.I. double staining flow cytometry. Consistent with the potency trend in tumor cell growth inhibition activity as tested by WST-based cell growth assays, SM-381 and SM-383 have same potency in inducing tumor cell death and apoptosis in MDA-MB-231 cells and SK-OV3 cells, with a potency superior to that of SM-1252.

The cellular molecular events caused by our bivalent Smac mimetics were further probed by using Western blotting assays. The results show that new bivalent Smac mimetics SM-381 and SM-383 can dose-dependently induce PARP cleavage, c-IAP1 degradation, and caspase activations in MDA-MB-231 and SK-OV-3 cells, as potently as previously developed bivalent Smac mimetic SM-164. However, SM-381 and SM-383 are more synthetically accessible than SM-164.

Using potent monovalent Smac mimetic SM-337 as the template, a series of different carboxylic acids attached to the nitrogen atom of the 8-membered ring in the bicyclic system were tested. Among these new monovalent Smac mimetics, SM-406, with 3-methylbutanoic acid attached to the amine in the bicyclic system, shows much

improved pharmacokinetic properties compared with SM-337. Further cellular mechanism studies were performed by using this excellent drug candidate.

Same as the previously developed monovalent Smac mimetics, SM-406 can dose- and time-dependently induce apoptosis in MDA-MB-231, SK-OV-3 and MALME-3M cells. SM-406 can also dose- and time-dependently induce tumor cell death, PARP cleavage, c-IAP1 degradation and caspase activations in tumor cells.

Co-immunoprecipitation assays further confirm that c-IAP1 and XIAP are the cellular targets of SM-406. The biotinylated Smac mimetic SM-222 can pull down c-IAP1 and XIAP in a dose-dependent manner in both MDA-MB-231 and SK-OV-3 cell lysates, while SM-406 can dose-dependently compete off their interactions. In contrast, inactive control SM-428 cannot compete off the interaction between biotinylated Smac mimetic and IAPs.

The dependence on each caspase in the cellular activity of SM-406 was further studied by using either caspase inhibitor or siRNA. The results are interesting, because the cellular activity of SM-406 is mainly dependent on caspase-8 and caspase-3, but only partially on caspase-9. Recent studies proposed a plausible cellular molecular mechanism of Smac mimetics: the degradations of c-IAP1/2 caused by Smac mimetics lead to the release of receptor interacting protein kinase (RIPK1) from the activated TNF receptor complex to form a caspase-8-activating complex consisting of RIPK1, FADD (Fas-Associated protein with Death Domain), and caspase-8. The activated initiator caspase-8 then activates effector caspases to promote apoptosis in tumor cells.[195] Further studies of the cellular mechanism of Smac mimetics are still under investigation, and are expected to assist in elucidating the mechanism.[196]

In conclusion, a series of monovalent and bivalent small-molecular, non-peptidic and cell-permeable Smac mimetics were successfully developed. SM-406, with improved pharmacokinetic properties, is a promising drug candidate for further clinical development. We hope that our further efforts may lead to a new treatment for cancer diseases.

BIBLIOGRAPHY

1. Lowe, S.W. and Lin, A.W. (2000). Apoptosis in cancer. Carcinogenesis *21*, 485-495.

2. Fesus, L., Davies, P.J., and Piacentini, M. (1991). Apoptosis: molecular mechanisms in programmed cell death. Eur. J. Cell Biol. *56*, 170-177.

3. Williams, G.T. (1991). Programmed cell death: apoptosis and oncogenesis. Cell *65*, 1097-1098.

4. Waring, P., Kos, F.J., and Mullbacher, A. (1991). Apoptosis or programmed cell death. Med. Res. Rev. *11*, 219-236.

5. Vaux, D.L., and Strasser, A. (1996). The molecular biology of apoptosis. Proc. Nat. Acad. Sci. USA *93*, 2239-2244.

6. Hale, A.J., Smith, C.A., Sutherland, L.C., Stoneman, V.E., Longthorne, V.L., Culhane, A.C., and Williams, G.T. (1996). Apoptosis: molecular regulation of cell death. Eur. J. Biochem. *236*, 1-26.

7. Green, D.R., and Reed, J.C. (1998). Mitochondria and apoptosis. Science *281*, 1309-1312.

8. King, K.L., and Cidlowski, J.A. (1998). Cell cycle regulation and apoptosis. Annu. Rev. Physiol. *60*, 309-325.

9. O'Connor, L., Huang, D.C., O'Reilly, L.A., and Strasser, A. (2000). Apoptosis and cell division. Curr. Opin. Cell Biol. *12*, 257-263.

10. Kroemer, G. (2003). Mitochondrial control of apoptosis: an introduction. Biochem Biophys Res Commun. *304*, 433-435.

11. Martin, D.A., and Elkon, K.B. (2004). Mechanisms of apoptosis. Rheum. Dis. Clin. North Am. *30*, 441-454.

12. Modjtahedi, N., Giordanetto, F., Madeo, F., and Kroemer, G. (2006). Apoptosis-inducing factor: vital and lethal. Trends Cell Biol. *16*, 264-272.

13. Perl, M., Chung, C.S., and Ayala, A. (2005) Apoptosis. Crit. Care Med. *33*, 526-529.

14. Yan, N., and Shi, Y. (2005). Mechanisms of apoptosis through structural biology. Annu. Rev. Cell Dev. Biol. *21*, 35-56.

15. Suen, D.F., Norris, K.L., and Youle, R.J. (2008). Mitochondrial dynamics and apoptosis. Genes Dev. *22*, 1577-1590.

16. Ashkenazi, A. (2008). Targeting the extrinsic apoptosis pathway in cancer. Cytokine Growth Factor Rev. *19*, 325-331.

17. Siegel, R.M., and Lenardo, M.J. (2002). Apoptosis signaling pathways. Curr. Protoc. Immunol. Chapter *11*, Unit 11.9C.

18. Franz, S., Gaipl, U.S., Munoz, L.E., Sheriff, A., Beer, A., Kalden, J.R., and Herrmann, M. (2006). Apoptosis and autoimmunity: when apoptotic cells break their silence. Curr. Rheumatol. Rep. *8*, 245-247.

19. Meng, X.W., Lee, S.H., and Kaufmann, S.H. (2006). Apoptosis in the treatment of cancer: a promise kept? Curr. Opin. Cell Biol. 18, 668-676.

20. Ponder, B.A. (2001). Cancer genetics. Nature *411*, 336-341.

21. Nicholson, D.W. (2000). From bench to clinic with apoptosis-based therapeutic agents. Nature *407*, 810-816.

22. Reed, J.C. (1999). Mechanism of apoptosis avoidance in cancer. Curr. Opin. Oncol. *11*, 68-75.

23. Reed, J.C. (2002). Apoptosis-based therapies. Nat. Rev. Drug Discov. *1*, 111-121.

24. Desoize, B. (1994). Anticancer drug resistance and inhibition of apoptosis. Anticancer Res. *14*, 2291-2294.

25. Inoue, S., Salah-Eldin, A.E., and Omoteyama, K. (2001). Apoptosis and anticancer drug resistance. Hum Cell. *14*, 211-221.

26. Inoue, S., Salah-EldTsuruo, T., Naito, M., Tomida, A., Fujita, N., Mashima, T., Sakamoto, H., and Haga, N. (2003). Molecular targeting therapy of cancer: drug resistance, apoptosis and survival signal. Cancer Sci. *94*, 15-21.

27. Hersey, P., and Zhang, X.D. (2003). Overcoming resistance of cancer cells to apoptosis. J Cell Physiol. *196*, 9-18.

28. Hersey, P., Zhang, X.D. and Mhaidat, N. (2008). Overcoming resistance to apoptosis in cancer therapy. Adv Exp Med Biol. *615*, 105-126.

29. Hickman J.A. and Dive C. (1999). Apoptosis and cancer chemotherapy. Humana Press Inc.

30. Studziniski, G.P. (1999). Apoptosis, a practical approach. Oxford University Press.

31. Green, D.R. (1998). Apoptotic pathways: the roads to ruin. Cell *94*, 695-698.

32. Cameron R.G. and Feuer G.. (2000). Apoptosis and its modulation by drugs. Springer.

33. Evan, G.I. and Vousden, K.H. (2001). Proliferation, cell cycle and apoptosis in cancer. Nature *411*, 342-348.

34. Green, D.G. and Evan G.I. (2002). A matter of life and death. Cancer Cell *1*, 19-30.

35. Hunter, A.M., LaCasse E.C., and Korneluk R.G. (2007). The inhibitors of apoptosis (IAPs) as cancer targets. Apoptosis *12*, 1543-1568.

36. Fulda, S. (2008). Targeting inhibitor of apoptosis proteins (IAPs) for cancer therapy. Anticancer Agents Med Chem. *8*, 533-539.

37. Srinivasula, S.M., and Ashwell, J.D. (2008). IAPs: what's in a name? Mol. Cell *30*, 123-135.

38. Vucic, D. (2008). Targeting IAP (inhibitor of apoptosis) proteins for therapeutic intervention in tumors. Curr. Cancer Drug Targets *8*, 110-117.

39. Danson, S., Dean, E., Dive, C., and Ranson, M. (2007). IAPs as a target for anticancer therapy. Curr. Cancer Drug Targets *7*, 785-794.

40. Mor, G., Montagna, M.K., and Alvero, A.B. (2008). Modulation of apoptosis to reverse chemoresistance. Methods Mol. Biol. *414*, 1-12.

41. Dean, E.J., Ranson, M., Blackhall, F., and Dive, C. (2007). X-linked inhibitor of apoptosis protein as a therapeutic target. Expert Opin. Ther. Targets *11*, 1459-1471.

42. Vucic, D., and Fairbrother, W.J. (2007). The inhibitor of apoptosis proteins as therapeutic targets in cancer. Clin. Cancer Res. *13*, 5995-6000.

43. Rajapakse, H.A. (2007). Small molecule inhibitors of the XIAP protein-protein interaction. Curr. Top. Med. Chem. *7*, 966-971.

44. Kischkel F.C., Helbardt, S., Behrmann I. Germer, M., Pawlita, M., Krammer, P.H., and Peter, M.E. (1995). Cytotoxicity-dependent APO-1(Fas/CD95)-associated proteins form a death-inducing signalling complex (DISC) with the receptor. EMBO J. *14*, 5579-5588.

45. Fulda, S., and Debatin, K.M. (2006). Extrinsic versus intrinsic apoptosis pathways in anticancer chemotherapy. Oncogene *25*, 4798-4811.

46. Kang, J.J., Schaber, M.D., Srinivasula, S.M., Alnemri, E.S., Litwack, G., Hall, D.J., and Bjornsti, M.A. (1999). Cascades of Mammalian Caspase Activation in the Yeast *Saccharomyces cerevisiae*. J. Biol. Chem. *274*, 3189-3198.

47. Stennicke, H.R., Jurgensmeier, J.M., Shin, H., Deveraux, Q., Wolf, B.B., Yang, X., Zhou, Q., Ellerby, H.M., Bredesen, D., Green, D.R., Reed, J.C., Froelich, C.J., and Salvasen, G.S. (1998) Pro-casepase-3 is a major physiologic target of caspase-8. J. Biol. Chem. *273*, 27084-27090.

48. Salvesen, G.S., and Dixit, V.M. (1999). Caspase activation: the induced-proximity model. Proc. Nat. Acad. Sci. USA. *96*, 10964-10967.

49. Frisch, S.M. (2008). Caspase-8: fly or die. Cancer Res. *68*, 4491-4493.

50. Salvesen, G.S., and Riedl, S.J. (2008). Caspase mechanisms. Adv. Exp. Med. Biol. *615*, 13-23.

51. Denault, J.B., and Salvesen, G.S. (2008). Apoptotic caspase activation and activity. Methods Mol. Biol. *414*, 191-220.

52. Timmer, J.C., and Salvesen, G.S. (2007). Caspase substrates. Cell Death Differ. *14*, 66-72.

53. Kumar, S. (2007). Caspase function in programmed cell death. Cell Death Differ. *14*, 32-43.

54. Callus, B.A., and Vaux, D.L. (2007). Caspase inhibitors: viral, cellular and chemical. Cell Death Differ. *14*, 73-78.

55. Linton, S.D. (2005). Caspase inhibitors: a pharmaceutical industry perspective. Curr. Top. Med. Chem. *5*, 1697-1717.

56. Wang, Z.B., Liu, Y.Q., and Cui, Y.F. (2005). Pathways to caspase activation. Cell Biol. Int. *29*, 489-496.

57. Riedl, S.J., and Shi, Y. (2005). Molecular mechanisms of caspase regulation during apoptosis. Nat. Rev. Mol. Cell Biol. *5*, 897-907.

58. Shi, Y. (2004). Caspase activation, inhibition, and reactivation: a mechanistic view. Protein Sci. *13*, 1979-1987.

59. Shi, Y. (2004). Caspase activation: revisiting the induced proximity model. Cell *117*, 855-858.

60. Boatright, K.M., and Salvesen, G.S. (2003). Mechanisms of caspase activation. Curr. Opin. Cell Biol. *15*, 725-731.

61. Creagh, E.M., Conroy. H., and Martin, S.J. (2003). Caspase-activation pathways in apoptosis and immunity. Immunol Rev. *193*, 10-21.

62. Shi, Y. (2002). Mechanisms of caspase activation and inhibition during apoptosis. Mol. Cell *9*, 459-470.

63. Kuida, K. (2000). Caspase-9. Int. J. Biochem. Cell Biol. *32*, 121-124.

64. Takahashi, A. (1999). Caspase: executioner and undertaker of apoptosis. Int. J. Hematol. *70*, 226-232.

65. Ekert, P.G., Silke, J., and Vaux, D.L. (1999). Caspase inhibitors. Cell Death Differ. *6*, 1081-1086.

66. Kumar, S. (1999). Mechanisms mediating caspase activation in cell death. Cell Death Differ. *6*, 1060-1066.

67. Villa P, Kaufmann SH, Earnshaw WC. (1997). Caspases and caspase inhibitors. Trends Biochem. Sci. *22*, 388-393.

68. Kluck, R.M., Bossey-Wetzel E., Green, D.R., and Newmeyer D.D. (1997). The release of cytochrome *c* from mitochondria: a primary site for bcl-2 regulation of apoptosis. Science *275*, 1132-1136.

69. Ow, Y.L., Green, D.R., Hao, Z., and Mak, T.W. (2008). Cytochrome c: functions beyond respiration. Nat. Rev. Mol. Cell Biol. *9*, 532-542.

70. Hacker, G., and Weber, A. (2007). BH3-only proteins trigger cytochrome c release, but how? Arch. Biochem. Biophys. *15*, 150-155.

71. Garrido, C., Galluzzi, L., Brunet, M., Puig, P.E., Didelot, C., and Kroemer, G. (2006). Mechanisms of cytochrome c release from mitochondria. Cell Death Differ. *136*, 1423-1433.

72. Bertini I, Cavallaro G, Rosato A. (2006). Cytochrome c: occurrence and functions. Chem. Rev. *106*, 90-115.

73. Jiang, X., and Wang, X. (2004). Cytochrome C-mediated apoptosis. Annu. Rev. Biochem. *73*, 87-106.

74. Scorrano, L., and Korsmeyer, S.J. (2003). Mechanisms of cytochrome c release by proapoptotic BCL-2 family members. Biochem. Biophys. Res. Commun. 304, 437-444.

75. Saleh, A., Srinivasula, S. Acharya, S., Fishel, R., Alnemri, E.S. (1999). Cytochrome *c* and dATP-mediated oligomerization of Apaf-1 is a prerequisite for procaspase-9 activation. J. Biol. Chem. 274, 17941-17945.

76. Zou, H., Henzel, W.J., Liu, X., Lutschg, A., Wang, X. (1997). Apaf-1, a human protein homologous to C. elegans CED-4, participates in cytochrome *c*–dependent activation of caspase-3. Cell *90*, 405-413.

77. Zou, H., Li, Y., Liu, X., Wang, X. (1999). An Apaf-1 cytochrome *c* multimeric complex is a functional apoptosome that activates procaspase-9. J. Biol. Chem. *274*, 11549-11556.

78. Li, H., Zhu, H., Xu, C., amd Yuan, J. (1998). Cleavage of Bid by caspase-8 mediates the mitochondrial damage in the Fas pathway of apoptosis. Cell *94*, 491-501.

79. Luo X., Budihardjo, I., Zou, H., Slaughter, C., and Wang, X. (1998). Bid, a Bcl-2 interacting protein, mediates cytochrome *c* release from mitochondria in response to activation of cell surface death receptors. Cell *94*, 481-490.

80. Chipuk, J.E., and Green, D.R. (2008). How do BCL-2 proteins induce mitochondrial outer membrane permeabilization? Trends Cell Biol. 18, 157-164.

81. Danial, N.N. (2007). BCL-2 family proteins: critical checkpoints of apoptotic cell death. Clin. Cancer Res. *13*, 7254-7263.

82. Brooks, C., and Dong, Z. (2007). Regulation of mitochondrial morphological dynamics during apoptosis by Bcl-2 family proteins: a key in Bak? Cell Cycle *6*, 3043-3047.

83. Adams, J.M., and Cory, S. (2007). Bcl-2-regulated apoptosis: mechanism and therapeutic potential. Curr. Opin. Immunol. 19, 488-496.

84. Adams, J.M., and Cory, S. (2007). The Bcl-2 apoptotic switch in cancer development and therapy.Oncogene *26*, 1324-1337.

85. Reed, J.C. (2006). Proapoptotic multidomain Bcl-2/Bax-family proteins: mechanisms, physiological roles, and therapeutic opportunities. Cell Death Differ. 13, 1378-1386.

86. Devraux, Q.L., and Reed, J.C. (1999). IAP family proteins—suppressors of apoptosis. Genes Dev. *13*, 239-252.

87. Salvesen, G.S., and Duckett, C.S. (2002). Apoptosis: IAP proteins: blocking the road to death's door. Nat. Rev. Mol. Cell Biol. *3*, 401-410.

88. Holick, M., Gibson, H., and Korneluk, R.G. (2001). XIAP: apoptotic brake and promising therapeutic target. Apoptosis *6*, 253-261.

89. Vucic, D. (2008). Targeting IAP (inhibitor of apoptosis) proteins for therapeutic intervention in tumors.Curr. Cancer Drug Target *8*, 110-117.

90. Martin, S.J. (2002). Destabilizing influences in apoptosis: sowing the seeds of IAP destruction. Cell *109*, 793-796.

91. Verhagen, A.M., and Vaux, D.L. (2002). Cell death regulation by the mammalian IAP antagonist Diablo/Smac. Apoptosis *7*, 163-166.

92. Yang, Y.L., and Li, X.M. (2000). The IAP family: endogenous caspase inhibitors with multiple biological activities. Cell Res. *10*, 169-177.

93. Eiben, L.J., and Duckett, C.S. (1998). The IAP family of apoptotic regulators. Results Probl Cell Differ. *24*, 91-104.

94. Yang Y., Fang, S., Jensen, J.P., Weissman, A.M., and Ashwell, J.D. (2000). Ubiquitin protein ligase activity of IAPs and their degradation in proteasomes in response to apoptotic stimuli. Science *288*, 874-877.

95. Silke, J., Kratina, T., Chu, D., Ekert, P.G., Day, C.L., Pakusch, M., Huang, D.C., and Vaux, D.L. (2005). Determination of cell survival by RING-mediated regulation of inhibitor of apoptosis (IAP) protein abundance. Proc. Nat. Acad. Sci. USA 102, 16182-16187.

96. Martin, S. J. (2001). Dealing with CARDs between life and death. Trends Cell. Biol. *11*, 188-189.

97. Bouchier-Hayes, L., and Martin, S.J. (2002). CARD games in apoptosis and immunity. EMBO *3*, 616-621.

98. Verhagen, A.M., Coulson, E.J., and Vaux, D.L. (2001). IAPs and their relatives: IAPs and other BIRPs. Genome Biology *2*, 3009.1-3009.10.

99. Eckelman, B.P., Drag, M., Snipas, S.J., and Salvesen, G.S. (2008). The mechanism of peptide-binding specificity of IAP BIR domains. Cell Death Differ. *15*, 920-928.

100. Samuel, T., Welsh, K., Lober, T., Togo, S.H., Zapata, J.M., and Reed, J.C. (2006). Distinct BIR domains of cIAP1 mediate binding to and ubiquitination of tumor necrosis factor receptor-associated factor 2 and second mitochondrial activator of caspases. J. Biol. Chem. *281*, 1080-1090.

101. Shin, H., Renatus, M., Eckelman, B.P., Nunes, V.A., Sampaio, C.A., and Salvesen, G.S. (2005). The BIR domain of IAP-like protein 2 is conformationally unstable: implications for caspase inhibition.Biochem. J.385, 1-10.

102. Huang,Y., Rich, R.L., Myszka, D.G., and Wu, H. (2003). Requirement of both the second and third BIR domains for the relief of X-linked inhibitor of apoptosis protein (XIAP)-mediated caspase inhibition by Smac.J. Biol. Chem. *278*, 49517-49522

103. Miller, L.K. (1999). An exegesis of IAPs: salvation and surprises from BIR motifs.Trends Cell Biol. *9*, 323-328.

104. Lacasse, E.C., Barid, S., Korneluk, R.G., MacKenzie, A.E., (1998). The inhibitors of apoptosis (IAPs) and their emerging role in cancer. Oncogene *17*, 3247-3259.

105. Altieri, D.C. (2008). Survivin, cancer networks and pathway-directed drug discovery.Nat. Rev. Cancer. *8*, 61-70.

106. Duffy, M.J., O'Donovan, N., Brennan, D.J., Gallagher, W.M., and Ryan, B.M. (2007). Survivin: a promising tumor biomarker.Cancer Lett. *249*, 49-60.

107. Lens, S.M., Vader, G., and Medema, R.H. (2006). The case for Survivin as mitotic regulator.Curr. Opin. Cell Biol. *18*, 616-622.

108. Li, F., and Ling, X. (2006). Survivin study: an update of "what is the next wave"? J. Cell Physiol. *208*, 476-486.

109. Li, F. (2003). Survivin study: what is the next wave? J. Cell Physiol. 197, 8-29.

110. Altieri, D.C. (2003). Survivin in apoptosis control and cell cycle regulation in cancer. Prog. Cell Cycle Res. 5, 447-452.

111. Pohl, C., and Jentsch, S. (2008). Final stages of cytokinesis and midbody ring formation are controlled by BRUCE.Cell *132*, 832-845.

112. Takahashi, R., Deveraux, Q.L., Tamm, I., Welsh, K., Assa-Munt, N., Salvesen, G.S., and Reed, J.C. (1998). A single BIR domain of XIAP sufficient for inhibiting caspases. J. Biol. Chem. *273*, 7787-7790.

113. Asselin, E., Mills, G.B., and Tsang, B.K. (2001). XIAP regulates Akt activity and caspase-3-dependent cleavage during cisplatin-induced apoptosis in human ovarian epithelial cancer cells. Cancer Res. *61*, 1862-1868.

114. Deveraux, Q.L., Tahashi, R., Salvesen G.S., and Reed, J.C. (1997) X-linked IAP is a direct inhibitor of cell-death proteases. Nature *388*, 300-304.

115. Deveraux, Q.L., Leo, E., Stennicke, H.R., Welsh, K., Salvesen, G.S. and Reed, J.C. (1999). Cleavage of human inhibitor of apoptosis protein XIAP results in fragments with distinct specificities for caspases. EMBO J. *18*, 5242-5251.

116. Rajapakse, H.A. (2007). Small molecule inhibitors of the XIAP protein-protein interaction.Curr Top Med Chem. *7*, 966-971.

117. Eckelman, B.P., Salvesen, G.S., and Scott, F.L. (2007). Human inhibitor of apoptosis proteins: why XIAP is the black sheep of the family.EMBO Rep.7, 988-994.

118. Schimmer, A.D., Dalili, S., Batey, R.A., and Riedl, S.J. (2006). Targeting XIAP for the treatment of malignancy.Cell Death Differ. 13, 179-188.

119. Du, C., Fang, M., Li, Y., Li, L., and Wang, X. (2000). Smac, a mitochondrial protein that promotes cytochrome c–dependent caspase activation by eliminating IAP inhibition. Cell *102*, 33-42.

120. Verhagen, A.M., Kkert, P.G., Pakusch, M., Silke, J., Connolly, L.M., Reid, G.E., Moritz, R.L., Simpson, R.J., and Vaux, D.L. (2000). Identification of DIABLO, a mammalian protein that promotes apoptosis by binding to and antagonizing IAP proteins. Cell *102*, 43-53.

121. Ekert, P.G., Silke, J., Hawkins, C.J., Verhagen, A.M., and Vaux, D.L. (2001). DIABLO promotes apoptosis by removing MIHA/XIAP from processed caspase-9. J. Cell Biol. *152*, 483-490.

122. Liu, Z., Sun, C., Olejniczak, E.T., Meadows, R.P., Betz, S.F., Oost, T., Herrmann, J., Wu, J.C., and Feisk, S.K. (2000). Structural basis for binding of Smac/DIABLO to the XIAP BIR3 domain. Nature *408*, 1004-1008.

123. Wu, G., Chai, J. Suber, T.L., Wu, J.W., Du, C., Wang, X., and Shi, Y. (2000). Structural basis of IAP recognition by Smac/DIABLO. Nature *408*, 1008-1012.

124. Sun, C., Cai, M., Meadows, R.P., Xu, N., Gunasekera, A.H., Hermann, J., Wu, J.C., and Fesik, S.W. (2000). NMR structure and mutagenesis of the third BIR domain of the inhibitor of apoptosis protein XIAP. J. Biol. Chem. *275*, 33777-33781.

125. Sun, H., Nikolovska-Coleska, Z., Chen, J., Yang, C.-Y., Tomita, Y., Pan H., Yoshioka, Y., Krajewski, K., Roller, P.P., and Wang, S. (2005). Bioorg. Med. Chem. Lett. *15*, 793-797.

126. Nikolovska-Coleska, Z., Wang, R., Fang, X., Pan, H., Tomita, Y., Li, P., Roller, P.P., Krajewski, K., Saito, N.G., Stuckey, J.A., and Wang, S. (2004). Development and optimization of a binding assay for the XIAP BIR3 domain using fluorescence polarization. Anal. Biochem. *332*, 261-273.

127. Sun, H., Nikolovska-Coleska, Z., Yang, C.-Y., Xu, L., Liu, M., Tomita, Y., Pan, H., Yoshioka, Y., Krajewski, K., Roller, P.P., and Wang, S. (2004). Structure-based design of potent, conformationally constrained Smac mimetics. J. Am. Chem. Soc. *126*, 16686-16687.

128. Sun, H., Nikolovska-Coleska, Z., Yang, C.-Y., Xu, L., Tomita, Y., Krajewski, K., Roller, P.P., and Wang, S. (2004). Structure-based design, synthesis, and evaluation of conformationally constrained mimetics of the second mitochondria-derived activator of caspase that target the X-linked inhibitor of apoptosis protein / caspase-9 interaction site. J. Med. Chem. *47*, 4147-4150.

129. Sun, H. Nikolovska-Coleska, Z., Lu, J., Qiu, S., Yang, C.-Y., Gao, W., Meagher, J., Stuckey, J., and Wang, S. (2006). Design, synthesis, and evaluation of a potent, cell-permeable, conformationally constrained second mitochondria derived activator of caspase (Smac) mimetic. J. Med. Chem. *49*, 7916-7920.

130. Oost, T.K., Sun, C., Armstrong, R.C., Al-Assaad, A.S., Betz, S.F., Deckwerth, T.L., Ding, H., Elmore, S.W., Meadows, R.P., Olejniczak, E.T., Oleksijew, A., Oltersdorf, T., Roseberg, S.H., Shoemaker, A.R., Tomaselli, K.J., Zou, H., and Fesik, S.W. (2004). Discovery of potent antagonists of the antipoptotic protein XIAP for the treatment of cancer. J. Med. Chem. *47*, 4417-4426.

131. Shi, Y. (2001). The Mechanisms of caspase activation and inhibition during apoptosis. Mol. Cell *9*, 459-470.

132. Huang Y., Park, Y.C., Rich, R.L., Segal, D., Myszka, D.G., and Wu, H. (2001). Structure basis of caspase inhibition by XIAP: differential roles of the linker versus the BIR domain. Cell *104*, 781-790.

133. Shiozaki, E.N., and Shi, Y. (2004). Caspases, IAPs and Smac/DIABLO: mechanism from structural biology. Trends Biochem. Sci. *29*, 486-494.

134. Li, L., Thomas, R.M., Suzuki, H., Brabander, J.K.D., Wang, X., and Harran, P.G. (2004). A small molecule Smac mimic potentiates TRAIL- and TNFα-mediated cell death. Science *305*, 1471-1474.

135. Sun, H. Nikolovska-Coleska, Z., Lu, J., Meagher, J., Yang, C.-Y., Qiu, Su., Tomita, Y., Jiang, S., Krajewski, K., Roller, P.P., Stuckey, J.A., and Wang, S. (2007). Design, synthesis, and characterization of a potent, nonpeptide, cell-permeable, bivalent Smac mimetic that concurrently targets both the BIR2 and BIR3 domains in XIAP. J. Am. Chem. Soc. *129*, 15279-15294.

136. Kolb, H.C., Sharpless, K.B. (2003). The growing impact of click chemistry on drug discovery. Drug Discov Today *8*, 1128-1137.

137. Rostovstev, V.V., Green, L.G., Fokin, V.V., and Sharpless, K.B. (2002). A stepwise Huisgen cycloaddition process: copper(I)-catalyzed regioselective **l**igation of azides and terminal alkynes. Angew. Chem. Int. Ed. *41*, 2596-2599.

138. Moses, J.E., and Moorhouse, A.D. (2007). The growing applications of click chemistry. Chem. Soc. Rev. *36*, 1249-1262.

139. Tron, G.C., Pirali, T., Billington, R.A., Canonico, P.L., Sorba, G., and Genazzani, A.A. (2008). Click chemistry reactions in medicinal chemistry: applications of the 1,3-dipolar cycloaddition between azides and alkynes. Med. Res. Rev. *28*, 278-308.

140. Moorhouse, A.D., and Moses, J.E. (2008). Click chemistry and medicinal chemistry: a case of "cyclo-addiction". ChemMedChem *3*, 715-723.

141. Hein, C.D., Liu, X.M., and Wang, D. (2008). Click Chemistry, A Powerful Tool for Pharmaceutical Sciences. Pharm. Res. *25*, 2216-2230.

142. Service, R.F. (2008). Chemistry. Click chemistry clicks along. Science 320, 868-869.

143. Petersen, J.S., Fels, G., and Rapoport, H. (1984). Chirospecific syntheses of (+)- and (-)-Anatoxin α. J. Am. Chem. Soc. *106*, 4539-4547.

144. Campcell, J.A. and Rapoport, H. (1996). Chirospecific syntheses of conformationally constrained 7-azabicycloheptane amino acids by transannular alkylation. J. Org. Chem. *61*, 6313-6325.

145. Aggarwal, V.K., Astle, C.J., Christopher, J.I., Iding, H., Wirz, B., and Rogers-Evans, M. (2005). Separation of pyrrolidine allylation products by diastereoselective enzymatic ester hydrolysis. Tetrahedron Lett. *46*, 945-947.

146. Shinada, T., Hamada, M., Kawasaki, M., and Ohfune, Y. (2005). Stereoselective synthesis of 2,5-Di- and 2,2,5-trisubstituted pyrrolidines by allylation reaction of acyliminium ion. Heterocycles *66*, 511-525.

147. Colombo, L., Di Giacomo, M., Vinci, V., Colombo, M., Manzoni, L., and Scolastico, C. (2003). Synthesis of new bicyclic lactam peptidomimetics by ring-closing metathesis reactions. Tetrahedron *59*, 4501-4513.

148. Grossmith, C.E., Senia, F., and Wagner, J. (1999). Synthesis of novel unsaturated bicyclic lactams by ring-closing metathesis. Synlett *10*, 1660-1662.

149. Park, C.-M., Sun, C., Olejniczak, E.T., Wilson, A.E., Meadows, R.P., Betz, S.F., Elmore, S.W., and Fesik, S.W. (2005). Non-peptidic small molecular inhibitors of XIAP. Bioorg. Med. Chem. Lett. *15*, 771-775.

150. Peng, Y., Sun, H., and Wang, S. (2006). Design and synthesis of a 1,5-diazabicyclo[6,3,0] dodecane amino acid derivative as a novel dipeptide reverse-turn mimetic. Tetrahedron Lett. *47*, 4769-4770.

151. Chaudhary, S.K., and Hernandez, O. (1979). 4-dimethylaminopyridine: an efficient and selective catalyst for the silylation of alcohols. Tetrahedron Lett. *20*, 99-102

152. Debenham, J.S., Rodebaugh, R., and Fraser-Reid, B. (1997). TCP- and phthalimide-protected *n*-pentenyl glucosaminide precursors for the synthesis of nodulation factors as illustrated by the total synthesis of NodRf-III (C18:1, MeFuc). J. Org. Chem. *62*, 4591-4600.

153. Boger, D.L., Borzilleri, R.M., Nukui, S., Beresis, R.T. (1997). Synthesis of the Vancomycin CD and DE ring systems. J. Org. Chem. *62*, 4721-4736.

154. Scheidt, K.A., Chen, H., Follows, B.C., Chemler, S.R., Coffey, D.S., Roush, W.R. (1998). Tris(dimethylamino)sulfonium difluorotrimethylsilicate, a mild reagent for the removal of silicon protecting groups. J. Org. Chem. *63*, 6436-6437.

155. Bodanszky, M., and Bodanszky, A. (1994). The practice of peptide Synthesis 2nd edition. Springer-Verlag. Chapter 2.

156. Gibson, F.S., Bergmeier, S.C., and Rapoport, H. (1994). Selective removal of an N-Boc protecting group in the presence of a tert-butyl ester and other acid-sensitive groups. J. Org. Chem. *59*, 3216-3218.

157. Atwell, G.J., and Denny, W.A. (1984). Monoprotection of α,ω-alkanediamines with the *N*-benzyloxycarbonyl group. Synthesis *12*, 1032-1033.

158. Berkowitz, D.B., and Pedersen, M.L. (1994). Simultaneous amino and carboxyl group protection for .alpha.-branched amino acids. J. Org. Chem. *59*, 5476-5478.

159. Stahl, G.L., Walter, R., and Smith, C.W. (1978). General procedure for the synthesis of mono-N-acylated 1,6-diaminohexanes. J. Org. Chem. *43*, 2286-2286.

160. Cavelier, F. and Enjalbal, C. (1996). Studies of selective Boc removal in the presence of silyl ethers. Tetrahedron Lett. 3*7*, 5131-5134.

161. Evans, D.A., and Ellman, J.A. (1989). The total syntheses of the isodityrosine-derived cyclic tripeptides OF4949-III and K-13. Determination of the absolute configuration of K-13. J. Am. Chem. Soc. *111*, 1063-1072.

162. Sakaitani, M., Hori, K., and Ohfune Y. (1988). One-pot conversion of N-benzyloxycarbonyl group into N-tert-butoxycarbonyl group. Tetrahedron Lett. *29*, 2983-2984.

163. Mazaleyrat, J.-P., Xie, J., and Wakselman, M. (1992). Selective hydrogenolysis of the benzyloxycarbonyl protecting group of N^ε-lysine in cyclopeptides containing a benzylic phenyl ether function. Evidence for N^ε-methylated lysine side products. Tetrahedron Lett. *33*, 4301-4302.

164. Yamazaki, N., and Kibayashi, C. (1989). Asymmetric synthesis with α,β.-bis [(methoxymethyl)oxy] ketones. Enantioselective total synthesis of natural (+)-indolizidine 195B (bicyclic gephyrotoxin 195B) and (-)-pinidine and their enantiomers from a common chiral synthon. J. Am. Chem. Soc. *111*, 1396-1408.

165. Gary, B.D., and Jeffs, P.W. (1987). Alkylation and condensation reactions of N,N-dibenzylglycine esters: synthesis of α-amino acid derivatives. J. Chem. Soc. Chem. Commun. *18*, 1329-1330.

166. Peng, Y., Sun, H., Nikolovska-Coleska, Z., Yang, C.-Y., Qiu, S., Lu, J., Cai, Q., Yi, H., and Wang, S. (2008). Design, synthesis and evaluation of potent and orally bioavailable diazabicyclic Smac mimetics. Submitted to J. Med. Chem.

167. Peskin, A.V. and Winterbourn, C.C. (2000). A microtiter plate assay for superoxide dismutase using a water-soluble tetrazolium salt (WST-1). Clinnica Chimica Acta *293*, 157-166.

168. Berridge, M.V., Herst, P.M., and Tan A.S. (2005). Tetrazolium dyes as tools in cell biology: new insights into their cellular reduction. Biotechnol. Annu. Rev. *11*, 127-152.

169. Sulic, S., Panic, L., Dikic, I., and Volarevic, S. (2005). Deregulation of cell growth and malignant transformation. Croat. Med. J. *46*, 622-638.

170. Herzenberg, L.A., and DeRosa, S.C. (2000). Monoclonal antibodies and the FACS: complementary tools for immunobiology and medicine. Immunol. Today *21*, 383-390.

171. Tung, J.W., Parks, D.R., Moore, W.A., and Herzenberg, L.A. (2004). New approaches to fluorescence compensation and visualization of FACS data. Clin. Immunol. *110*, 277-283.

172. Diaz, D., Prieto, A., Reyes, E., Barcenilla, H., Monserrat, J., and Alvarez-Mon, M. (2008). Flow cytometry enumeration of apoptotic cancer cells by apoptotic rate. Methods Mol. Biol. *414*, 23-33.

173. Ibrahim, S.F., and Van Den Engh, G. (2007). Flow cytometry and cell sorting. Adv. Biochem. Eng. Biotechnol. *106*, 19-39.

174. Tung, J.W., Heydari, K., Tirouvanziam, R., Sahaf, B., Parks, D.R., and Herzenberg, L.A. (2007). Modern flow cytometry: a practical approach. Clin. Lab. Med. *27*, 453-468.

175. Sklar, L.A., Carter, M.B., and Edwards, B.S. (2007). Flow cytometry for drug discovery, receptor pharmacology and high-throughput screening. Curr. Opin. Pharmacol. *7*, 527-534.

176. Delude, R.L. (2005). Flow cytometry. Crit. Care Med. *33*, 426-428.

177. Carroll, S., and Al-Rubeai, M. (2004). The selection of high-producing cell lines using flow cytometry and cell sorting. Expert Opin. Biol. Ther. *4*, 1821-1829.

178. Givan, A.L. (2004). Flow cytometry: an introduction. Methods Mol. Biol. *263*, 1-32.

179. Cram, L.S. (2002). Flow cytometry, an overview. Methods Cell Sci. *24*, 1-9.

180. McCoy, J.P. Jr. (2002). Basic principles of flow cytometry. Hematol. Oncol. Clin. North Am. *16*, 229-243.

181. Ormerod, M.G. (2001). Using flow cytometry to follow the apoptotic cascade. Redox. Rep. *6*, 275-287.

182. Darzynkiewicz, Z., Smolewski, P., and Bedner, E. (2001). Use of flow and laser scanning cytometry to study mechanisms regulating cell cycle and controlling cell death. Clin. Lab Med. *21*, 857-873.

183. Schwartz, A., and Fernandez-Repollet, E. (2001). Quantitative flow cytometry. Clin. Lab Med. *21*, 743-761.

184. O'Connor, J.E., Callaghan, R.C., Escudero, M., Herrera, G., Martinez, A., Monteiro, M.D., and Montoliu, H. (2001). IUBMB Life *51*, 231-239.

185. Rieseberg, M., Kasper, C., Reardon, K.F., and Scheper, T. (2001). Flow cytometry in biotechnology. Appl. Microbiol. Biotechnol. *56*, 350-360.

186. Boddy, L., Wilkins, M.F., and Morris, C.W. (2001). Pattern recognition in flow cytometry. Cytometry *44*, 195-209.

187. Darzynkiewicz, Z., Bedner, E., and Smolewski, P. (2001). Flow cytometry in analysis of cell cycle and apoptosis. Semin. Hematol. *38*, 179-193.

188. Marti, G.E., Stetler-Stevenson, M., Bleesing, J.J., Fleisher, T.A. (2001). Introduction to flow cytometry. *38*, 93-99.

189. Scheffold, A., and Kern, F. (2001). Recent developments in flow cytometry. J. Clin. Immunol. 20, 400-407.

190. Givan AL. (2001). Principles of flow cytometry: an overview. Methods Cell Biol. *63*, 19-50.

191. Vermes, I., Haanen, C., and Reutelingsperger, C. (2000). Flow cytometry of apoptotic cell death. J. Immunol. Methods *21*, 167-190.

192. Varfolomeev, E., Blankenship, J.W., Wayson, S.M., Fedorava, A.V., Kayagaki, N., Garg, P., Zobel, K., Dynek, J.N., Elliott, L.O., Wallweber, H.J.A., Flygare, J.A., Fairbrother, W.J., Deshayes, K., Dixit, V.M., and Vucic, D. (2007). IAP antagonists induced autoubiquitination of c-IAPs, NF-κB activation, and TNFα-dependent apoptosis. Cell *131*, 669-681.

193. Vince, J.E., Wong, W.W.-L., Khan, N., Feltham, R., Chau, D., Ahmed, A.U., Benetatos, C.A., Chunduru, S.K., Condon, S.M., McKinlay, M., Brink, R., Leverkus, M., Tergaokar, V., Schneider, P., Callus, B.A., Koentgen, F., Vaux, D.L., and Silke J. (2007). IAP antagonists target cIAP1 to induce TNFα-dependent apoptosis. Cell *131*, 682-693.

194. Petersen, S.L., Wang, L., Yalcin-Chin, A., Li, L., Peyton, M., Minna, J., Harran, P., and Wang, X. (2007). Autocrine TNFα signaling renders human cancer cells susceptible to Smac-mimetic-induced apoptosis. Cancer Cell *12*, 445-456.

195. Wang, L., Du, F., and Wang, X. (2008). TNF-α induces two distinct caspase-8 activation pathways. Cell 133, 693-703.

196. Varfolomeev, E., Goncharov, T., Fedorova, A.V., Dynek, J.N., Zobel, K., Deshayes, K., Fairbrother, W.J., and Vucic, D. (2008). c-IAP1 and c-IAP2 are critical mediators of tumor necrosis factor alpha (TNFalpha)-induced NF-kappaB activation. J. Biol. Chem. 283, 24295-24299.

197. Ikejima, M., Noguchi, S., Yamashita, R., Ogura, T., Sugimura, T., Gill, D.M., and Miwa, M. (1990). The zinc fingers of human poly(ADP-ribose) polymerase are differentially required for the recognition of DNA breaks and nicks and the consequent enzyme activation. Other structures recognize intact DNA. J. Biol. Chem. *265*, 21907-21913.

198. Lazebnik, Y.A., Kaufmann, S.H., Desnoyers, S., Poirier, G.G., and Earnshaw, W.C. (1994). Cleavage of poly(ADP-ribose) polymerase by a proteinase with properties like ICE. Nature *371*, 346-347.

199. Tewari, M., Quan, L.T., O'Rourke, K., Desnoyers, S., Zeng, Z., Beidler, D.R., Poirier, G.G., Salvesen, G.S., and Dixit, V.M. (1995). Yama/CPP32 beta, a mammalian homolog of CED-3, is a CrmA-inhibitable protease that cleaves the death substrate poly(ADP-ribose) polymerase. Cell *81*, 801-809.

200. Kaufmann, S.H., Desnoyers, S., Ottaviano, Y., Davidson, N.E., and Poirier, G.G. (1993). Specific proteolytic cleavage of poly(ADP-ribose) polymerase: an early marker of chemotherapy-induced apoptosis. Cancer Res. *53*, 3976-3985.

201. Duan, H., Chinnaiyan, A.M., Hudson, P.L., Wing, J.P., He, W.-W. and Dixit, V.M. (1996). ICE-LAP3, a novel mammalian homologue of the *Caenorhabditis elegans* cell death protein Ced-3 is activated during Fas- and tumor necrosis factor-induced apoptosis. J. Biol. Chem. *271*, 1621-1625.

202. Srinivasula, S.M., Fernandes-Alnemri, T., Zangrilli, J., Robertson, N., Armstrong, R.C., Wang, L., Trapani, J.A., Tomaselli, K.J., Litwack, G. and Alnemri, E.S. (1996). The ced-3/interleukin 1 converting enzyme-like homolog Mch6 and the lamin-cleaving enzyme Mch2 are substrates for the apoptotic mediator CPP32. J. Biol. Chem. *271*, 27099-27106.

203. Li, P., Nijhawan, D., Budihardjo, I., Srinivasula, S.M., Ahmad, M., Alnemri, E.S., and Wang, X. (2001). Cytochrome c and dATP-dependent formation of Apaf-1/caspase-9 complex initiates an apoptotic protease cascade. Cell *91*, 479-489.

204. Liu, J.R., Opipari, A.W., Tan, L., Jiang, Y., Zhang, Y., Tang, H., and Nuñez, G. (2002). Dysfunctional apoptosome activation in ovarian cancer: implications for chemoresistance. Cancer Res. *62*, 924-931.

205. Greene, B.T., Thorburn, J., Willingham, M.C., Thorburn, A., Planalp, R.P., Brechbiel, M.W., Jennings-Gee, J., Wilkinson, J., Torti, F.M., and Torti, S.V. (2002). Activation of caspase pathways during iron chelator-mediated apoptosis. J. Biol. Chem. *277*, 25568-25575.

206. Degenhardt, K., Sundararajan, R., Lindsten, T., Thompson, C., and White, E. (2002). Bax and Bak independently promote cytochrome *c* release from mitochondria. J. Biol. Chem. *277*, 14127-14134.

207. Liu, F.T., Kelsey, S.M., Newland, A.C., and Jia, L. (2002). Liposomal encapsulation diminishes daunorubicin-induced generation of reactive oxygen species, depletion of ATP and necrotic cell death in human leukaemic cells. Br. J. Haematol. *117*, 333-342.

208. Muzio, M., Chinnaiyan, A.M., Kischkel, F.C., O'Rourke, K., Shevchenko, A., Ni, J., Scaffidi, C., Bretz, J.D., Zhang, M., Gentz, R., Mann, M., Krammer, P.H., Peter M.E., and Dixit, V.M. (1996). FLICE, a Novel FADD-homologous ICE/CED-3–like protease, is recruited to the CD95 (Fas/APO-1) death-inducing signaling complex. Cell *85*, 817-827.

209. Boldin, M.P., Goncharov, T.M., Goltseve, Y.V., and Wallach D. (1996). Involvement of MACH, a novel MORT1/FADD-interacting protease, in Fas/APO-1- and TNF receptor–induced cell death. Cell *85*, 803-815.

210. Fernandes-Alnemri, T., Armstrong, R.C., Krebs, J., Srinivasula, S.M., Wang, L., Bullrich, F., Fritz, L.C., Trapani, J.A., Tomaselli, K.J., Litwack, G., and Alnemri, E.S. (1996). *In vitro* activation of CPP32 and Mch3 by Mch4, a novel human apoptotic cysteine protease containing two FADD-like domains. Proc. Natl. Acad. Sci. USA *93*, 7464-7469.

211. Mancini, M., Nicholson, D.W., Roy, S., Thornberry, N.A., Peterson, E.P., Casciola-Rosen, L.A., and Rosen, A. (1998). The caspase-3 precursor has a cytosolic and mitochondrial distribution: implications for apoptotic signaling. J. Cell Biol. *140*, 1485-1495.

212. Samali, A., Cai, J., Zhivotovsky, B., Jones, D.P., and Orrenius, S. (1999). Presence of a pre-apoptotic complex of pro-caspase-3, Hsp60 and Hsp10 in the mitochondrial fraction of Jurkat cells. EMBO J. *18*, 2040-2048.

213. Kirsch, D.G., Doseff, A., Chau, B.N., Lim, D.-S., Souza-Pinto, N.C., Hansford, R., Kastan, M.B., Lazebnik, Y.A., and Hardwick, J.M. (1999). Caspase-3-dependent cleavage of Bcl-2 promotes release of cytochrome *c*. J. Biol. Che,. *274*, 21155-21161

214. Suria, H., Chau, L.A., Negrou, E., Kelvin D.J., and Madrenas, J. (1999). Cytoskeletal disruption induces T cell apoptosis by a caspase-3 mediated mechanism. Life Sci. *65*, 2697-2707.

215. Faleiro, L., Kobayashi, R., Fearnhead H., and Lazebnik, Y. (1997). Multiple species of CPP32 and Mch2 are the major active caspases present in apoptotic cells. EMBO J. *16*, 2271-2281.

216. Schafer, T., Scheuer, C., Roemer, K., Menger, M.D., and Vollmar, B. (2003). Inhibition of p53 protects liver tissue against endotoxin-induced apoptotic and necrotic cell death. FASEB J. *17*, 660-667.

217. Jia, L., Patwari, Y., Kelsey, S.M., Srinivasula, S.M., Agrawal, S.G, Alnemri E.S., and Newland, A.C. (2003) Role of Smac in human leukaemic cell apoptosis and proliferation. Oncogene *22*, 1589-1599.

218. Xiao, C., Yang, B.F., Asadi, N., Beguinot, F., and Hao, C. (2002). Tumor necrosis factor-related apoptosis-inducing ligand-induced death-inducing signaling complex and its modulation by c-FLIP and PED/PEA-15 in glioma cells. J. Biol. Che,. *277*, 25020-25025.

219. Hoshi, T., Sasano, H., Kato, K., Yabuki, N., Ohara, S., Konno, R., Asaki, S., Toyota, T., Tateno, H., and Nagura, H. (1998). Immunohistochemistry of Caspase3/CPP32 in human stomach and its correlation with cell proliferation and apoptosis. Anticancer Res. *18*, 4347-4353.

220. Fernandes-Alnemri, T., Takahashi, A., Armstrong, R., Krebs, J., Fritz, L., Tomaselli, K.J., Wang, L., Yu, Z., Croce, C.M., Salveson, G., Earnshaw, W.C., Litwack, G., and Alnemri, E.S. (1995). Mch3, a novel human apoptotic cysteine protease highly related to CPP32. Cancer Res. *55*, 6045-6052.

221. Lippke, J.A., Gu, Y., Sarnecki, C., Caron, P.R., and Su, M.S.-S. (1996) Identification and characterization of CPP32/*Mch2* homolog 1, a novel cysteine protease similar to CPP32. J. Biol. Chem. *271*, 1825-1828.

222. Thornberry, N.A., Rano, T.A., Peterson, E.P., Rasper, D.M., Timkey, T., Garcia-Calvo, M., Houtzager, V.M., Nordstrom, P.A., Roy, S., Vaillancourt, J.P., Chapman, K.T., and Nicholson, D.W. (1997). A combinatorial approach defines specificities of members of the caspase family and granzyme B. J. Biol. Chem. *272*, 17907-17911.

223. Chandler, J.M., Cohen, G.M., and MacFarlane, M. (1998). Different subcellular distribution of caspase-3 and caspase-7 following Fas-induced apoptosis in mouse liver. J. Biol. Chem. *273*, 10815-10818.

224. MacFarlane, M., Cain, K., Sun, X.-M., Alnemri, E.S., and Cohen, G.M. (1997). Processing/activation of at least four interleukin-1 converting enzyme-like proteases occurs during the execution phase of apoptosis in human monocytic tumor cells. J. Cell Biol. *137*, 469-479.

225. Cohen, G.M. (1997). Caspases: the executioners of apoptosis. Biochem J. *326*, 1-16.

226. Nunez, G., Benedict, M.A., Hu, Y., and Inohara, N. (1998). Caspases: the proteases of the apoptotic pathway. Oncogene *17*, 3237-3245.

227. Goyal, L. (2001). Cell death inhibition: keeping caspases in check. Cell *104*, 805-808.

228. Roy, N., Deveraux, Q.L., Takahashi, R., Salvesen, G.S., and Reed, J.C. (1997). The c-IAP-1 and c-IAP-2 proteins are direct inhibitors of specific caspases. EMBO J. *16*, 6914-6925.

229. Roy, N., Mahadevan, M.S., McLean, M., Shutler, G., Yaraghi, Z. Farahani, R., Baird, S., besner-Johnston, A., Lefebvre, C., and Kang, C. (1995). The gene for neuronal apoptosis inhibitory protein is partially deleted in individuals with spial muscular atrophy. Cell *80*, 167-178.

230. Rothe, M., Pan, M.G., Henzel, W.J., Ayres, T.M., and Goeddel, D.V. (1995). The TNFR2-TRAF signaling complex contains two novel proteins related to baculoviral inhibitor of apoptosis proteins. Cell *83*, 1243-1252.

231. Duckett, C.S., Nava, V.E., Gedrich, R.W., Clem, R.J., Van Dongen, J.L., Gilfillan, M.C., Shiels, H., Hardwick, J.M., and Thompson, C.B. (1996). A conserved family of cellular genes related to the baculovirus iap gene and encoding apoptosis inhibitors. EMBO J. *15*, 2685-2694.

232. Lee, Y.-J., and Shacter, E. (2001). Fas aggregation does not correlate with Fas-mediated apoptosis. J. Immunol. *167*, 82-89.

233. Reffey, S.B., Wurthner, J.U., Parks, W.T., Roberts, A.B., and Duckett, C.S. (2001). X-linked inhibitor of apoptosis protein functions as a cofactor in transforming growth factor-β signaling. J. Biol. Chem. *276*, 26589-26596.

234. Wang, G.-Q., Gastman, B.R., Wieckowski, E., Goldstein, L.A., Rabinovitz, A., Yin, X.-M., and Rabinowich, H. (2001). Apoptosis-resistant mitochondria in T cells selected for resistance to Fas signaling. J. Biol. Chem. *276*, 3650-3659.

235. Li, P., Nijhawan, D., Budihardjo, I., Srinivasula, S.M., Ahmad, M., Alnemri, E.S., and Wang, X. (1997). Cytochrome c and dATP-dependent formation of Apaf-1/caspase-9 complex initiates an apoptotic protease cascade. Cell *91*, 479-489.

236. Schagger, H. (2002). Respiratory chain supercomplexes of mitochondria and bacteria. Biochem. Biophys. Acta. *1555*, 154-159.

237. Liu, X., Kim, C.N., Yang, J., Jemmerson, R., and Wang, X. (1996). Induction of apoptotic program in cell-free extracts: requirement for dATP and cytochrome *c*. Cell *86*, 147-157.

238. Sawyer, C., Sturge, J., Bennett, D.C., O'Hare, M.J., Allen, W.E., Bain, J., Jones, G.E., and Vanhaesebroeck, B. (2003). Regulation of breast cancer cell chemotaxis by the phosphoinositide 3-kinase p110delta**.** Cancer Res. *63*, 1667-1675.

239. Lacor, P.N., Grayson, D.R., Auta, J., Sugaya, I., Costa, E., and Guidotti, A. (2000). Reelin secretion from glutamatergic neurons in culture is independent from neurotransmitter regulation. Proc. Natl. Acad. Sci. USA *97*, 3556-3561.

240. Andree, H.A., Reutelingsperger, C.P., Hauptmann, R., Hemker, H.C., Hermens, W.T., and Willems, G.M. (1990). Binding of vascular anticoagulant alpha (VAC alpha) to planar phospholipid bilayers. J. Biol. Chem. *265*, 4923-4928.

241. Fadok, V.A., Savill, J.S., Haslett, C., Bratton, D.L., Doherty, D.E., Campbell, P.A., and Henson, P.M. (1992). Different populations of macrophages use either the vitronectin receptor or the phosphatidylserine receptor to recognize and remove apoptotic cells. J. Immunol. *149*, 4029-4035.

242. Creutz, C.E. (1992). The annexins and exocytosis. Science *258*, 924-931.

243. Vermes, I., Haanen, C., Steffens-Nakken, H., and Reutelingsperger, C. (1995). A novel assay for apoptosis. Flow cytometric detection of phosphatidylserine expression on early apoptotic cells using fluorescein labelled Annexin V. J. Immunol. Methods *184*, 39-51.

244. Koopman, G., Reutelingsperger, C.P., Kuijten, G.A., Keehnen, R.M., Pals, S.T., van Oers, M.H. (1994). Annexin V for flow cytometric detection of phosphatidylserine expression on B cells undergoing apoptosis. Blood *84*, 1415-1420.

245. Homburg, C.H., de Haas, M., von dem Borne, A.E., Verhoeven, A.J., Reutelingsperger, C.P., and Roos, D. (1995). Human neutrophils lose their surface Fc gamma RIII and acquire Annexin V binding sites during apoptosis in vitro. Blood *85*, 532-540.

246. Verhoven, B., Schlegel, R.A., and Williamson, P. (1995). Mechanisms of phosphatidylserine exposure, a phagocyte recognition signal, on apoptotic T lymphocytes. J. Exp. Med. 182, 1597-1601.